TRANSPARENT AND CONDUCTIVE POLYMER LAYERS BY GAS PLASMA TECHNIQUES

PROEFSCHRIFT

ter verkrijging van
de graad van doctor aan de Universiteit Twente,
op gezag van de rector magnificus,
prof.dr. F.A. van Vught,
volgens besluit van het College voor Promoties
in het openbaar te verdedigen
op vrijdag 10 november 2000 te 15.00 uur.

door

Lucas Marinus Hendrikus Groenewoud

geboren op 20 april 1972
te Heeten

Dit proefschrift is goedgekeurd door:

Promotor:	Prof.dr. J. Feijen
Assistent-promotor:	Dr.ir. G.H.M. Engbers
Referent:	Dr.ir. J.G.A. Terlingen

“Ik wil wel eerlijk zijn in alles, maar niet eenzaam zijn”

Acda en de Munnik, *Wacht op mij*

Transparent and conductive polymer layers by gas plasma techniques / L.M.H. Groenewoud
Thesis University of Twente, Enschede, the Netherlands
With references – With summary in English and Dutch

ISBN 90 365 15165

The research described in this thesis was sponsored by the Dutch Ministry of Economic Affairs (Senter): grant number IOT 95001

Printed by SONODRUK, Drukkerij SONO BV, Heino, the Netherlands

Contents

1

General introduction

Introduction

Polymers are widely used in a great number of applications because of their many advantageous, general properties such as low density and cost, and processability. For applications requiring electrical conductivity, the choice of a suitable polymer is limited to polymers with a conjugated chemical structure such as polyacetylene, polypyrrole, and polythiophene. In a number of applications, both conductivity and transparency are required (e.g., antistatic layers on photographic films and paper), for which metals, inorganic conductors (e.g., ITO)[1-5] and ion-conducting polymers[6-9] can be used. However, these materials suffer from several drawbacks. Metals are expensive, posses a high density, and are rather brittle, as are the inorganic conductors. Ion conductors need water to be conductive, which makes their conductive properties highly dependable on humidity. In the strive for reduction in size, costs and weight of electronic equipment, the combination of polymeric properties and conductivity would be highly advantageous. This has long been recognised by the scientific and industrial community and has resulted in extensive research in this field that is summarised in several books.[10-13]

As already mentioned, for polymers to be conductive a conjugated structure is required. Along the conjugated structures, charge (i.e., electricity) is transported by charge carriers. The obtained conductivity ranges from the antistatic (10^{-11} – 10^{-6} S/cm, S = Ω^{-1}) to the metallic (> 10^{2} S/cm) regime. However, the stability of the conductive properties is rather low due to the high reactivity of the conjugated structure. Furthermore, the conjugated structure of conductive polymers inherently results in a non-transparent, intractable polymer that has lost some of the aforementioned advantages over the alternative conductors. Improving the transparency and flexibility of inherently conductive polymers can be done in a number of ways. Some researchers have tried to tune the optical and conductive properties by tideous multistep chemistry, which makes those polymers only suitable for specific high added-value applications.[14,15] A more simple method is the dilution of the conductive phase with a transparent phase. Usually, this will also result in a decrease in conductivity, but some

of the applications where transparency is needed require only a relatively low conductivity (e.g., antistatic layers on photographic films). Several methods have been applied to achieve this, among which are the coating of transparent particles with a conductive layer[16,17] and blending[18-21]/copolymerization[22,23] of a conductive polymer with a transparent non-conductive phase. These methods also need solvent and multistep chemistry is involved.

A very attractive alternative would be the plasma technique. With this technique it is possible to modify the surface properties of a substrate, while retaining the transparency and bulk properties of the substrate material. Furthermore, it is a solvent-free, fast and versatile process. However, a plasma consists of a variety of reactive species (electrons, ions, radicals etc.)[24-28] and therefore many different reactions can occur.[29-32] As a consequence, the exact chemical structure of the surface after exposure to a plasma is not precisely predictable, which necessitates detailed investigation.[30]

Aim

The aim of this study is to obtain transparent and conductive polymers using the plasma technique. In view of this objective, plasma can be used to actually modify the surface top-layer (plasma treatment) of or to deposit a thin conductive layer (plasma polymerisation) on a transparent substrate. For both methods, complicated relations between substrate material, gas composition, plasma conditions, and the characteristics of the resulting surface exist. A better understanding of these relations might result in plasma generated transparent and conductive polymeric layers.

Structure of this thesis

A literature survey on conductive polymers and the plasma technique is presented in Chapter 2. In Chapter 3, vinyl polymers (polyacryclic acid and polyvinylchloride) are treated with an argon plasma in order to selectively remove the pendant group, thereby creating unsaturated bonds in the surface layer. Characterisation is carried out using analysis techniques such as X-ray induced photoelectron spectroscopy (XPS), Fourier transform infrared spectroscopy (FTIR), and solid-state nuclear magnetic resonance (SSNMR).

Plasma polymerisation (PP) is used to deposit a thin conductive layer from a thiophene plasma, thereby keeping the loss in transparency low (Chapter 4). The influence of deposition conditions such as pressure and power on the characteristics of the plasma and the resulting

PP thiophene (PPT) layer (e.g., chemical structure, transparency, and conductivity) has been investigated in detail.

Next to the process parameters, the monomer structure may also be used to gain better control over the chemistry of the deposition process. Therefore, the effect of substituent(s) on thiophene, varying in nature, position and number, on the fragmentation during deposition (Chapter 5) and the mechanism of deposition (Chapter 6) has been studied. The plasma phase was characterised with optical emission spectroscopy (OES) and mass spectroscopy (MS), while for the characterisation of the resulting PP layers XPS, FTIR, NMR, and ellipsometry were used.

In the last two chapters, the doping process of PPT layers is addressed. Iodine is frequently used as dopant because of the ease of the doping procedure, and therefore it is also used in Chapter 7. The effect of doping time, thickness and chemical structure of the PP layer, and exposure time to air before and after doping on the conductivity and chemical structure of PPT layers has been evaluated using XPS, FTIR, and conductivity measurements. Iodine is obviously not a suitable dopant for industrial applications. Therefore, two alternative dopants systems ($ThClO_4$ and $NOPF_6$ in CH_2Cl_2) have been used in Chapter 8. The transparency, the conductivity (including the stability thereof), and the distribution of the dopant in the PP layer are measured with UV-Vis, conductivity measurements, and XPS and Auger electron spectroscopy (AES) sputter profiles, respectively.

References

[1] Martins, R.; Maçarico, A.; Ferreira, I.; Nunes, R.; Bicho, A.; Fortunato, E. *Thin Solid Films* **1997**, *303*, 47-52.

[2] Wu, X.; Coutts, T. J.; Mulligan, W. P. *J. Vac. Sci. Technol. A* **1997**, *15*, 1057-1062.

[3] Wang, R.; King, L. L. H.; Sleight, A. W. *J. Mater. Res.* **1996**, *11*, 1659-1664.

[4] Sernelius, B. E. *Thin Solid Films* **1996**, *278*, 104-107.

[5] Nishio, K.; Miyake, S.; Sei, T.; Watanabe, Y.; Tsuchiya, T. *J. Mater. Sci.* **1996**, *31*, 3651-3656.

[6] Lindford, R. G. In *Applications of electroactive polymers;* Scrosati, B., Ed.; Chapman and Hall: London, **1993**, pp 1-28.

[7] Inoue, K.; Takiue, K.; Tanigaki, T. *J. Polym. Sci. Part A: Polym. Chem.* **1996**, *34*, 1331-1336.

[8] Sun, J.; MacFarlane, D. R.; Forsyth, M. *J. Polym. Sci. Part A: Polym. Chem.* **1996**, *34*, 3465-3470.

[9] Zhou, P.; Samuelson, L.; Alva, K. S.; Chen, C.-C.; Blumstein, R. B.; Blumstein, A. *Macromolecules* **1997**, *30*, 1577-1581.

[10] *Handbook of conducting polymers*; Skotheim, T. A., Ed.; Marcel Dekker: New York, **1986**; Vol. 1 and 2.

[11] Reynolds, J. R.; Baker, C. K.; Jolly, C. A.; Poropatic, P. A.; Ruiz, J. P. In C*onductive polymers and plastics*; Margolis, J. M., Ed.; Chapmann and Hall: New York, **1989**, pp 1-40.

[12] Sethi, R. S.; Goosey, M. T. In *Special polymers for electronics and optoelectronics*; Chilton, J. A. and Goosey, M. T., Ed.; Chapman and Hall: London, **1995**.

[13] Frommer, J. E.; Chance, R. R. In *Encycl. Polym. Sci. Eng.*; Mark, H. F. and Kroschwitz, J. I., Ed., **1986**; Vol. 5, pp 462-507.

[14] McCullough, R. D.; Williams, S. P. *J. Am. Chem. Soc.* **1993**, *115*, 11608-11609.

[15] Brédas, J. L. *Synth. Met.* **1997**, *84*, 3-10.

[16] Huijs, F. Thin transparent conducting films based on core-shell latexes; University of Groningen: Groningen, **2000**.

[17] Khan, M. A.; Armes, S. P. *Adv. Mater.* **2000**, *12*, 671-674.

[18] Yin, W.; Li, J.; Gu, T.; Wu, J. *J. Appl. Polym. Sci.* **1997**, *63*, 13-16.

[19] Isotalo, H.; Ahlskog, M.; Stubb, H.; Laakso, J.; Karna, T.; Jussila, M.; Osterholm, J. E. *Synth. Met.* **1993**, *57*, 3581-3586.

[20] Laakso, J.; Osterholm, J. E.; Nyholm, P. *Synth. Met.* **1989**, *28*, C467-C471.

[21] Laakso, J.; Osterholm, J. E.; Nyholm, P.; Stubb, H.; Punkka, E. *Synth. Met.* **1990**, *37*, 145-150.

[22] Dai, L.; White, J. W. *Polymer* **1997**, *38*, 775-783.

[23] Park, Y. H.; Jeon, Y. J.; Lee, Y.; Baik, D. H.; Son, Y. *Mol. Cryst. Liq. Cryst.* **1996**, *280*, 193-198.

[24] Boenig, H. V. In *Encycl. Polym. Sci. Eng.*; Mark, H. F. and Kroschwitz, J. I., Ed., **1986**; Vol. 11, pp 248-261.

[25] Yasuda, H. *Plasma polymerization*; Academic Press: Orlando, **1985**.

[26] d'Agostino, R. *Plasma deposition, treatment, and etching of polymers*; Academic Press: Boston, **1990**.

[27] *Techniques and applications of plasma chemistry*; Hollahan, J. R.; Bell, A. T., Ed., John Wiley & Sons: New York, **1974**.

[28] Polak, L. S.; Lebedev, Y. A. *Plasma Chemistry*; Cambridge International Sci. Publ.: Cambridge, **1998**.

[29] Terlingen, J. G. A. *Introduction of functional groups at polymer surfaces by glow discharge techniques*; University of Twente: Enschede, **1993**.

[30] Suhr, H. In *Techniques and applications of plasma chemistry*; Hollahan, J. and Bell, A. T., Ed.; John Wiley & Sons: New York, **1974**, pp 57-111.

[31] Coburn, J. W.; Chen, M. *J. Appl. Phys.* **1980**, *51*, 3134-3136.

[32] Gazicki, M.; Yasuda, H. *J. Appl. Pol. Sci., Appl. Pol. Symp.* **1984**, *38*, 35-44.

2

Conductive polymers by plasma techniques: A literature survey

Conductive polymers

Conduction mechanism in polymers. The combination of conductivity and polymeric properties such as flexibility, processability, and a reduction in weight and costs would be advantageous for a number of applications. Therefore, conductive polymers have been the subject of much research since the observation that the conductivity of polyacetylene (PA) increased 12 orders when oxidised with iodine.[1]

Conduction is the transport of charge from one point to the other and is governed by charge carriers that move through a specimen. In general, the conductivity (σ) can be described by the following equation:

Equation 2.1. $$s = |q| \,.\, n \,.\, m \quad [\text{S/cm}]$$

where q is the charge carried by the carrier [A.s], n is the number of charge carriers [cm^{-3}], and m the mobility of the charge carriers [$cm^2.V^{-1}.s^{-1}$].

Conduction in solids can be described with the widely accepted band model.[1-5] In this model two new molecular orbitals arise when two atoms, both with half filled orbitals, are brought close enough to each other for the orbitals to overlap (cf. molecular orbital theory). The energy-difference (E_g) between the newly formed orbitals is determined by the degree of overlap between the constituting orbitals. As the degree of overlap is different for every pair of orbitals, a low-energy band (valence band, VB) and a high-energy band (conduction band, CB) are formed (Figure 2.1).

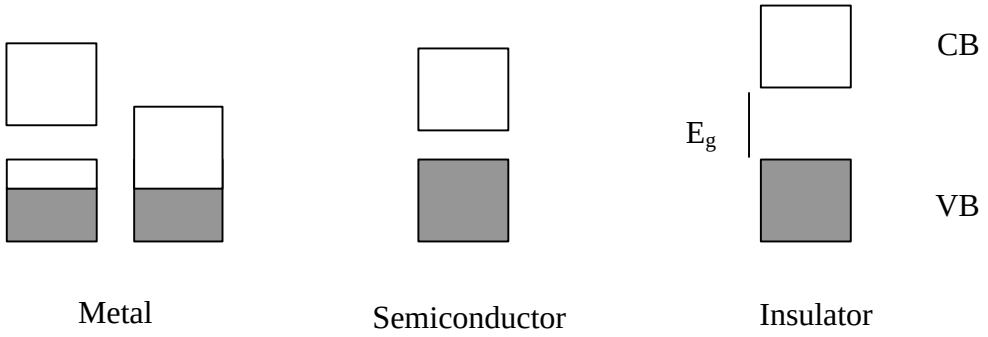

Figure 2.1. Schematic representation of the band structure of a metal, a semiconductor, and an insulator. (E_g is the energy gap between the valence band (VB) and the conduction band (CB)).

The extent of occupation of the energy bands and the energy gap between them determine the conductivity of a material. Metals are characterised by either a partially filled VB or an overlap between the VB and the CB. This implies a complete freedom of movement for the charge carriers under the influence of an applied field (Equation 2.1, $\mu \rightarrow \infty$). In semiconductors and insulators the VB is completely filled (Equation 2.1, $\mu = 0$) and the CB is empty (Equation 2.1, $n = 0$). Therefore, conduction can only take place when charge carriers are promoted from the VB to the CB. In insulators the energy gap is too large for charge carriers to be thermally excited, whereas for semiconductors excitation is possible.

The basic concepts of the band model also apply to conductive polymers. A characteristic that all conductive polymers have in common is their conjugated structure (Figure 2.2).[6,7] The conjugation length is an important parameter influencing the conductivity.[8-12] For instance, Garnier *et al.* found that relatively short oligomers of thiophene show a conductivity that is comparable to that of the polymer. The carrier mobility (and consequently the conductivity) increases with increasing conjugation length up to the hexamer of thiophene.[9]

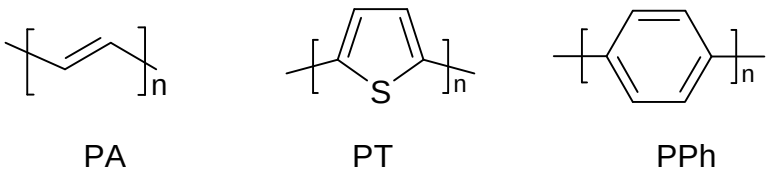

Figure 2.2. Chemical structure of polyacetylene (PA), polythiophene (PT), and polyphenylene (PPh).

Because polymer molecules do not extend over the full specimen, charge carriers have to move along the extended π-system of the conjugated backbone (int**ra**chain conductivity) as well as between the individual molecules (int**er**chain conductivity). The measured macroscopic conductivity is a superposition of these microscopic conduction mechanisms. Several models have been proposed for the intra- and interchain conductivity. [4-6,13-21] However, none of the proposed mechanisms applies to all conductive polymers and, what is more important, all proposed models have not been fully validated.

The majority of theoretical considerations are based on polyacetylene (Figure 2.2), being the simplest conjugated polymer.[3-6,13-18,21-23] In *trans*-polyacetylene two energetically equivalent resonance structures are possible (two-fold degeneration). At the conversion points of these structures unpaired electrons are present, which are called solitons (see Figure 2.3). This conversion point is actually spread out over several (2-10) bonds.[1,10-12]

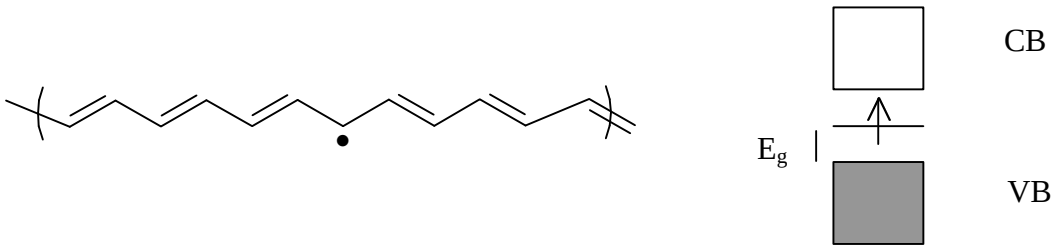

Figure 2.3. Soliton in trans-polyacetylene (left) and electronic state induced between the VB and CB by the soliton (right).

Solitons introduce a localised electronic state in the middle of the energy gap between the VB and the CB of polyacetylene (Figure 2.3). As this reduces the energy gap for charge carriers, conductivity is facilitated. Solitons are chargeless, but spin carrying (i.e., neutral radicals). An interesting feature of solitons in *trans*-polyacetylene is that, because of the degenerate ground state, they can move along the chain without the need to overcome an energy barrier. In fact, this is why they are called solitons: they have the same properties as a solitary wave. For *cis*-polyacetylene the two resonance structures are non-degenerate and therefore the movement of charge carriers along the backbone is energy consuming. This is shown by the lower conductivity of *cis*-polyacetylene compared to *trans*-polyacetylene (10^{-11} and 10^{-6} S/cm, respectively).[24,25]

Other conjugated polymers such as polythiophene (PT) also do not have a degenerate ground state. Still, different resonance structures can be present (cf. benzoid and quinoid

structures of PPh) and unpaired electrons are formed at the conversion points. These electrons polarise the local environment, which then relaxes into a new equilibrium position. This induces two electronic states in the band gap, again facilitating conductivity. The combination of a charge carrier and its distorted environment is called a polaron. The chemical equivalent is a charged radical.[5]

Doping. The number of naturally occurring solitons and polarons in conducting polymers is not sufficient to render them highly conducting (e.g., 10^{-6} S/cm for *trans*-polyacetylene). Charge carriers can be generated by oxidation or reduction of the polymer. This process is called doping, after the similar treatment of metals. The mechanism of doping in polymers however is different from that in metals. In doped metals, non-equivalent dopant atoms replace the metal atoms. Depending on the valence of the dopant, either holes (lower valence) or electrons (higher valence) are generated, which can act as charge carrier. Upon doping of polymers, charge is transferred from the dopant to the polymer.[6] Oxidation of the polymer (electrons from polymer to dopant) results in a hole-conducting polymer (p-type), whereas an electron-conducting polymer (n-type) is formed upon reduction. In order to maintain charge neutrality, counter-ions are also incorporated. Confusingly, these counter-ions are sometimes called dopant ions.[26-28] Counter-ions lower the mobility of the charge carriers by their interaction with the charge carriers on the conjugated polymer (pinning effect).[24] This pinning effect is less when the size and the degree of charge delocalisation on the counter-ion is larger. Furthermore, the stability of the conductivity shows a positive relation with the size of the counter-ion,[29] whereas the diffusion rate of the counter-ion into the doped layer shows a negative relation with size.[28]

Doping of polyacetylene results in the formation of new, neutral solitons and the charging of both newly formed and already existing solitons. The chemical equivalents are carbocations or -anions, radical cations or anions (polarons), and carbodianions or -dications (bipolarons).[4,5] Doping of conductive polymers other than polyacetylene results in the formation of polarons and further oxidation/reduction of newly formed and already existing polarons. The presence of solitons, polarons, and bipolarons in conjugated polymers has been observed in several studies.[10-12,30-35] The increase in conductivity upon doping can be as high as 14 orders of magnitude for different polymer-dopant combinations.[25,36,37] Upon doping with n-type dopants, organic anions are formed that are highly unstable towards air and water. Consequently, the conductivity generated by n-type doping is less stable than by

p-type doping.[38] Therefore, p-type dopants are more frequently used. Some examples are I_2, AsF_5, $FeCl_3$, nitrosonium salts (e.g., $NOPF_6$) and acids (e.g., H_2SO_4, $HClO_4$).[25,29,30,39-43]

Applications. Due to their conjugated structure, conducting polymers are intractable, insoluble and black in their conducting state. As a consequence, most of the mentioned advantages (e.g., flexibility, processability) are lost and the number of applications already marketed is therefore limited.[4,13,44,45] However, expectations are huge and in several reviews many foreseen applications are summarised.[44-49] Applications include light-emitting cells and diodes,[50-52] rechargeable batteries,[53] sensors,[54-63] and polymeric electronics[2,38] such as transistors.[50,64-68]

Transparency. In some applications, besides conductivity, transparency is also vital (e.g., photographic film) or desirable for aesthetic reasons (e.g., antistatic packaging, photographic paper). Some of the applications where transparency is needed require only a low conductivity. For instance, the surface conductivity of antistatic coatings should be in the range of 10^{-6} - 10^{-11} S. The transparency can be enhanced by dilution of the conductive phase with a transparent phase. This will also result in a decrease in conductivity but, considering the high conductivity of conductive polymers, this will not be a problem for applications requiring a low conductivity. Several methods are available for the dilution of conductive polymers, for example the grafting of alkyl side chains onto the conjugated backbone,[69-74] block-copolymerisation,[75-77] or blending with a transparent polymer,[78,79] and polymerising a thin layer of a conductive polymer on a transparent particle.[80,81] All these methods require the use of solvent and/or time consuming, multistep chemistry. This also holds for thin film production by electrochemical methods.[40,69,82-87]

With glow discharge techniques it is possible to modify polymer surfaces in one step without the use of solvent.[83,88-94] Due to the shallow modification depth, the transparency and the bulk mechanical properties of the substrate material remain intact.[90,91,94-98] A glow discharge is generated by applying either a strong electric field or a high temperature to a gas at low pressure. The high temperature method is not suitable for polymeric substrates and will therefore not be discussed further. When a strong electric field is applied to a gas at low pressure, the gas partly ionises and a plasma consisting of a variety of reactive species (electrons, ions, radiation etc.) is generated (see Figure 2.4). When a surface is exposed to a plasma, the interaction of plasma species results in either modification/etching (plasma

treatment) of or deposition (plasma polymerisation) on the substrate surface. Due to the multiple interactions the exact chemical structure of the surface layer after exposure to a plasma is not precisely predictable.[91-93,99-101]

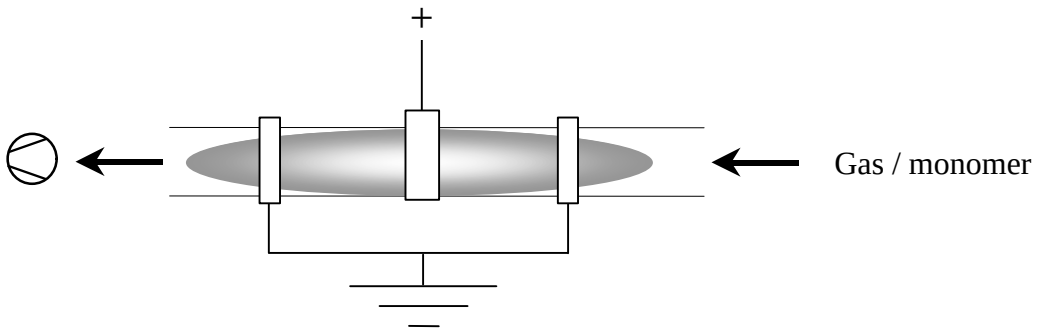

Figure 2.4. Schematic drawing of a plasma in a 3-electrode reactor.

In view of the objective to obtain transparent and conductive surfaces, the plasma technique can be used to either transform the surface top-layer of a transparent polymer into a conductive structure (plasma treatment) or to deposit a very thin layer of a conductive polymer on top of a transparent polymer (plasma polymerisation). Both techniques will be described in the following section in more detail.

Plasma techniques

Plasma treatment. Although in several studies plasma treatment was used to increase and/or stabilise the conductivity of conjugated polymers,[102-104] the amount of reports on plasma treatment of polymers with the objective to obtain conductive surfaces is rather limited. When conjugated polymers are used, the aforementioned disadvantages of conjugated polymers are not circumvented. When plasma treatment is used as a means to transfer a polymer surface into a conductive surface layer, these disadvantages may be overcome. A prerequisite is that the substrate material has all the desired properties for a specific application, but only lacks conductivity.

Drachev *et al.* treated polyimide (PI) films with an air plasma at 50 MHz, which resulted in the formation of a negative charge on the surface by the injection of electrons.[105] An increase of the conductivity was mentioned, but no exact figures were given. In a similar approach, Wu *et al.* used a N_2 plasma as an ion source for ion implantation in PI.[106] An increase in surface conductivity of 6 orders of magnitude up to 10^{-11} S was observed, while

the volume conductivity remained more or less constant (≈ 10^{15} S/cm). This indicated the formation of a conductive surface layer. Based on Fourier transform infrared spectroscopy (FTIR) and X-ray photoelectron spectroscopy (XPS) measurements, it could be concluded that the surface PI layer was converted into a carbon-rich layer by the ion bombardment.

Polypropylene (PP) was treated with different plasmas (He, Ar, Ne, H_2, N_2, and O_2) and the effect on the conductance was investigated.[107] Treatment with noble gases (He, Ne, Ar) resulted in an increase in conductance. XPS measurements showed that a graphite layer was formed at the surface when noble gases were used. A bulk conductivity of 10 S/cm was calculated, but the ion penetration depth was wrongly assumed to be the thickness of the conductive layer. The increase in conductance increased with increasing negative potential on the substrate. Helium appeared to be the most effective in decreasing the conductance. This was explained by a more effective energy transfer from impinging ions to the surface when the ions are lighter. No effect on the resistance was found for treatment with plasmas of reactive gases (H_2, N_2, O_2). Due to the incorporation of new chemical species the formation of a graphite layer was prevented in these cases.

Plasma polymerisation. In literature a vast amount of articles on plasma polymerisation can be found. The main reason for applying plasma polymerisation is that thin, stable, and pinhole-free films are obtained, which show good adherence to many substrates. A disadvantage is the poor predictability of the chemical structure of the resulting plasma polymerised (PP) layer. Several monomers have been plasma polymerised with the objective to obtain conductive surfaces, with varying success. Unfortunately, the transparency of the PP-layers is seldomly addressed.

Acrylonitrile (ACN) has often been used as a monomer in plasma polymerisation.[108-114] As polyacrylonitrile is known to become conductive upon pyrolysis, the PPACN layers were deposited on various substrates (glass, platinum, and glassy carbon) and either pyrolysed during deposition[108,112,114] or afterwards.[109-111] The pyrolysed PPACN layers showed interesting properties such as good adherence to the substrate, high mechanical stability, a conductivity of 10^{-7} – 10^{-9} S/cm and a high transparency (> 90% for PPACN films of 100 nm).[112] Grünwald *et al.* used 2-chloro-ACN as a monomer for plasma polymerisation on heated glass substrates (150 °C).[115,116] When the layers were deposited in the presence of iodine an increase in conductivity of 4 orders of magnitude was found (10^{-5} S/cm) compared

to PPACN layers. Unfortunately, the temperatures used in the studies on ACN and ACN derivatives (150 - 400°C) exclude most polymers to be used as substrates.

Plasma polymerisations were also carried out with xylenes.[117-120] Current densities up to 10^{-8} A/cm^2 were measured under high field conditions for *p*-xylene. An AC conductivity of 3.10^{-9} S/cm was found for PP-*m*-xylene.[118] FTIR measurements showed that in the PP-*p*-xylene layers the monomer structure was retained to a higher extent than in the PP-*m*-xylene layers. This indicates that the monomer structure has an effect on the degree of fragmentation during deposition, either in the plasma phase or via the interaction of plasma species with the deposited layer.

Aniline (An) and aniline derivatives were plasma polymerised by several authors.[121-125] Based on FTIR and XPS measurements it was concluded that the aromatic monomer structure was retained to some extent in the PPAn layers.[121,123,124] When aniline was plasma polymerised in the presence of iodine (10% w/w), the conductivity was enhanced by seven orders of magnitude up to 2.3×10^{-5} S/cm at RT.[123] Tong *et al.* irradiated PPAn layers with Ar^+ ions (100 keV) or I^+ ions (24 keV) after deposition and observed an increase in conductivity from 10^{-16} to 10^{-4} S/cm.[124] The penetration depth of the ions was taken as the thickness of the conductive layer. A carbon-rich phase was formed upon bombardment with Ar^+ ions, whereas a charge transfer (CT) complex (I_3^-) was responsible for the decrease in resistivity of I^+ irradiated layers.

Because heterocyclic polymers such as polypyrrole[84,126-132] and polythiophene[86,133-136] are known for their high and relatively stable conductivity, many studies are reported on the plasma polymerisation of these monomers. An idealised scheme of the deposition is given in Scheme 2.1.

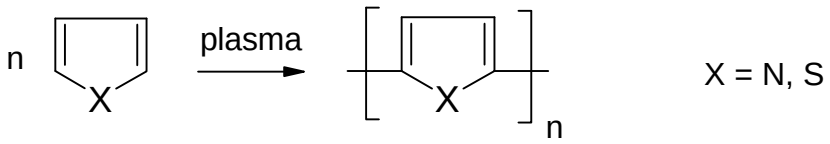

Scheme 2.1. Idealised scheme of plasma polymerisation of heterocyclic compounds.

Lee *et al.* deposited PP-pyrrole (PPPy) layers in a capacitively coupled bell jar configuration at 13.56 MHz.[137] After deposition, the PPPy layers were heat-treated (300 ºC) in a nitrogen atmosphere, which resulted in an increase of the unsaturation in the PPPy layers. An increase in p-type conductivity from 10^{-9} to 10^{-5} S/cm was observed. Van Ooij *et al.* deposited PPPy layers in a DC type plasma reactor.[138] FTIR measurements showed that no pyrrole rings were retained in the PPPy layers, which indicates a total destruction of the monomer by the plasma. Without additional doping, still conductivities of 10^{-3} to 10^{-4} S/cm were determined by the rarely used Franklin test. Zhang *et al.* were able to retain the pyrrole ring (determined with FTIR and XPS) to a certain extent during plasma polymerisation in a capacitively coupled coil (RF) configuration, but the conductivity was not determined.[139] Recently, Cruz *et al.* deposited PP layers from plasmas of pyrrole and of pyrrole and iodine.[140] In both cases, absorption bands characteristic for pyrrole rings were observed in the FTIR spectra of the PPPy layers. The conductivity of the PPPy films increased gradually from 10^{-11} to 10^{-9} S/cm with increasing (30 - 90%) relative humidity (RH) of the environment. This was explained by an increase in the mobility of the PPPy chains due to the interaction with water. For the PPPy/I films, a sharp increase from to 10^{-9} S/cm at 10 - 75% RH to 10^{-3} S/cm at RH > 90% was observed. The authors state that a second conductivity mechanism dominates in this latter region, which is reinforced by the presence of iodine. Another explanation would be that the sharp increase is due to water with dissolved iodine ions. At high values of the RH a continuous “path” of the water phase through the layer might be obtained, resulting in a sharp increase in the conductivity.

Plasma polymerisation was carried out for thiophene[58,141-146] and some of its derivatives.[147-150] Sadhir *et al.* prepared plasma polymerised thiophene (PPT) layers using argon as an initiator (4 W, 0.1 mbar, coil electrode configuration). After overnight doping with iodine, conductivities ranging from 10^{-6} to 10^{-4} S/cm were obtained.[141-143] Tanaka *et al.* investigated the effect of plasma frequency (AF (7.3 kHz) vs. RF (13.56 MHz), bell jar configuration) on the conductivity of argon initiated PPT layers. Although FTIR measurements did not indicate the presence of thiophene rings in the layers, conductivities ranging from 10^{-3} (AF, 100 W) to 10^{-4} S/cm (RF, 25 W) were found after 5 hrs doping with iodine.[145] In situ doping was carried out by Giungato *et al.*, using a mixture of argon (15 sccm), thiophene (5 sccm) and iodine (0.2 sccm) for plasma polymerisation (5 W, 0.67 mbar, two internal electrodes).[58] Based on FTIR measurements it was concluded that, although fragmentation had taken place during deposition, the thiophene ring was preserved

to some extent in the PPT layer. A conductivity of 10^{-5} S/cm was obtained for the PPT layers, without additional doping. Depositions of thiophene at atmospheric pressure were carried out by Tanaka *et al.* using helium as diluent.[146] The effect of the addition of argon to the diluent, substrate temperature (20 - 140 °C), and discharge current (0.5 - 3 mA) on the conjugation length (determined by FTIR) and the conductivity was investigated. A higher conductivity (maximum 10^{-8} S/cm) was observed for PPT layers containing more conjugation.

Benzo-[b]-thiophene was plasma polymerised under various conditions (RF and AF plasmas initiated by argon (Ar) or nitrogen (N_2)).[149] FTIR measurements showed that the aromaticy in the PP benzo-[b]-thiophene layer was higher than for PPT layers, but no effect on the conductivity was observed. In order to achieve a homogeneous doping Kruse *et al.* used 2-iodothiophene as a monomer for plasma polymerisation.[148] Besides covalently bound iodine, homogeneously distributed iodine ions were present in the PP film. A maximum conductivity of $2{,}6.10^{-1}$ S/cm was obtained.

Deposition conditions. As mentioned before, the conductivity of thiophene oligomers increases with increasing conjugation length.[9] The same relation between conductivity and conjugation length was found for a number of different PP layers.[109,121,137,146,151,152] Consequently, the conjugated structure of the monomer should be retained in the deposited layer to obtain PP layers with a high conductivity (see also Scheme 2.1). The effect of process parameters such as field strength (power), pressure, and flow on the plasma characteristics has been described in general terms in several books.[91,98,99] For instance, at higher field strengths the electrons pick up more energy between collisions, which raises the electron energy. An opposite effect on the electron energy is predicted for an increase in pressure. Since it is not possible to predict the optimal working conditions for a specific combination of a plasma system and a monomer up-front,[99] the influence of process parameters on the plasma characteristics has been investigated in many studies.

The effect of the deposition conditions (excitation frequency (125-375 kHz), power input (10 and 50 W), pressure (40-80 Pa), and deposition time (1-5 min)) on the chemical structure of the resulting PPAn layers was studied by Gong *et al.*[121] FTIR analysis showed an increase in the amount of quinoid and aliphatic structures relative to the amount of benzoid structures with increasing power input and deposition time, whereas a maximum in the relative amount of these structures was observed with increasing pressure. In the range studied no effect of the frequency was observed. Tanaka *et al.* also found a minor effect of the frequency (AF and

RF) on the conductivity of argon initiated PPT layers.[145] In another study, the observed conductivity of PP-2-iodothiophene layers was found to increase by 3 orders of magnitude in the order: RF< AF< MW (2.45 GHz).[148] For *p*-xylene it was found that the resulting plasma polymers resembled poly-*p*-phenylene the most when low powers and high frequencies were used.[119,120]

O'Toole *et al.* used various carboxylic acid and alcohol containing monomers and found an inverse relation between the power supplied to the plasma and the retention of the carboxylic acid and alcohol functionality in the deposited layers.[153,154] In the plasma polymerisation of styrene a higher degree of fragmentation was observed with decreasing pressure and increasing discharge power.[155] Brumlik *et al.* found an increase in sulfonate content when the partial pressure of the sulphonate containing monomer was increased.[156] PPPy layers deposited at low deposition pressure had a high carbon content, whereas at high pressure they were hydrogenated to a higher extent.[138]

An influence of the position of the substrate in the plasma reactor on the morphology, the deposition rate and the conductivity of the resulting PPT films was observed by Sadhir *et al.*[141-143] The morphology gradually changed from a platelet structure close to the high flux region to a spherulite structure further away from this region. Films deposited close to the monomer inlet did resemble polythiophene in morphology. The deposition rate showed a maximum, indicating a competition between ablation and polymerisation (CAP).[157] Films deposited at positions away from the high RF-flux region (i.e., away from the coil) showed a higher conductivity than films deposited near the coil.

Lowering the substrate temperature increased the amount of monomer that was incorporated in the film without substantial fragmentation.[158,159] This was explained by an increase of the monomer concentration at the surface at lower temperatures.

For various monomers it has been observed that pulsation of the plasma results in a decrease in fragmentation during deposition.[99,160-162] This has been explained by flushing of products out of the discharge zone between two pulses, thereby minimising fragmentation.[99] Ryan *et al*. state that during the plasma "on" time radicals are produced in the growing film surface and the vapour phase, which can subsequently act as initiation centres for radical chain-growth polymerisation during the "off" time.[160] However, the deposition of saturated fluorocarbons was also explained by this mechanism, which is obviously impossible.[162] Furthermore, no experimental results (e.g., thickness as a function of duty cycle) were given to support this explanation. Wang *et al.* state that the mechanism proposed by Ryan *et al.*[160]

can explain their results, but that other aspects (e.g., increased substrate temperature during CW plasma deposition) also influence the overall film chemistry. The results obtained by Uchida *et al.*, who showed that acetylene exclusively deposits during the plasma "on" time,[163,164] are also not consistent with the mechanism proposed by Ryan *et al*.

Summarising the literature on plasma polymerisation, it can be hypothesised that retention of the monomer structure in the PP layer will be high if deposition is carried out on cooled substrates away from the high flux region, using a pulsed plasma at low power input, high frequency, and high pressure. Due to the complexity of the plasma deposition process, results obtained from a specific deposition system (i.e., reactor, electrode configuration etc.) cannot be directly applied to other systems. Consequently, a series of optimisation experiments of the deposition conditions is needed for every combination of monomer and deposition system.

Monomer structure. Next to the deposition conditions, the monomer structure is sometimes used to gain control over the deposition process. Substituents are used to be preferentially removed or to stabilise the parent monomer structure, thereby increasing the amount of unfragmented monomer structures in the PP layer. PP-2-chloro-ACN layers were deposited by Grünwald *et al.* with the objective to create extended double bond systems via HCl elimination.[115,116] XPS measurements showed that about 50% of the chlorine was removed. According to the authors, this resulted in the formation of extensive conjugated structures in the PP-2-ClACN layers. However, this was based on, as the authors state, "noisy" XPS spectra. Furthermore, the layers were deposited on heated substrates (150 °C), which could have induced HCl elimination.[165]

Several cyano-containing compounds were used as monomers for plasma polymerisation.[166] Deposition was found to proceed via a preferential opening of the unsaturated cyano substituent, resulting in preservation of the structure of the parent molecule.

Perylene, 3,4,9,10-perylenetetracarboxylic-dianhydride (PTCDA) and – diimide (PTCDI) were polymerised with the use of a plasma. [167-169] It was concluded that at low power input the anhydride or imide groups are preferentially destroyed, thereby protecting the condensed ring structure. At high power the ring structure was also lost.

Benzo-[b]-thiophene was plasma polymerised under various conditions (RF and AF Ar, RF and AF N_2).[149] It was thought that the benzene ring would protect the thiophene ring structure during plasma polymerisation. Based on FTIR measurements it could indeed be concluded that the aromatic skeleton of the monomer was retained in the deposited layers to a higher extent than for PPT layers. However, it was not clear whether this was due to retention of the thiophene or the benzene ring.

Mechanism. Although plasma polymerisations have been observed and studied for a long time, the mechanism of deposition is not clear at all.[90,97,98] Obviously, the mechanism depends on the species present during deposition, of which the type (e.g., radicals, ions) and amount are influenced by the process parameters.[170] Mechanisms involving ions[153,154] and radicals have been described to explain the experimental data.[90] At the present time, many investigators believe that the polymerisation mechanism as proposed by Yasuda *et al.*[88,98,101,157] is the most reasonable concept.[90] In this stepwise initiation-recombination sequence, radicals are formed upon generation of the discharge (most probably by electron impact). These primary radicals recombine to a species that again is radical initiated and so on. Polymer formation can occur at the surface and/or in the plasma phase,[171] both of which can be explained by this mechanism.

Because of the multiple species present in a plasma, many reactions may result in the formation of radicals. For instance, in the DC plasma polymerisation of pyrrole no effect of the sign of the charge on the electrode was found, showing that a radical growth mechanism should apply.[172] The authors postulated that the growth is initiated by radicals present in the film surface, which are generated by impinging H^+ ions on the cathode and by electrons on the anode.

Uchida *et al.* explain the plasma polymerisation of acetylene by a radical mechanism.[163,164] Radicals are generated at the surface by neutralisation of impinging positive ions on which acetylene molecules have absorbed.

Due to the complex relation between deposition conditions, reactive species, and polymerisation mechanism, several mechanisms can explain the results of one experiment.[97] For instance, according to Chen *et al.* a variety of reactive species (excited species, radicals, and ions) was generated by electron impact on monomer molecules in a plasma of styrene.[155]

The relative amount of these species was different in different regions of the reactor and varied with deposition conditions as mentioned before. In a follow-up study, Chen *et al.* tried to obtain more control over the deposition process by extracting electrons or positive ions from the deposition region.[173] A maximum in deposition rate was observed both at positive and negative potential of the extraction grid. It was concluded that positive ions play an active role in the film formation, whereas electrons generate reactive species by collisions with other particles. These reactive particles are also responsible for the deposition.

A nice example of the complexity of the plasma polymerisation process is given by Fujita *et al.* They found an effect of the position in the reactor on the polymerisation mechanism for a methane plasma.[174,175] Graphite-like carbon layers were deposited by ionic reactions in the centre of the tube, whereas polymer-like carbonaceous films were formed on the reactor wall by radical reactions.

This again shows that a detailed study is necessary for every combination of monomer and deposition system to be able to deduce a reasonable polymerisation mechanism.

Strategy

In view of the objective to obtain transparent and conductive polymeric systems, the plasma technique can be used to obtain thin conductive polymer layers on transparent polymeric substrates. This can be done both by plasma treatment and plasma polymerisation as depicted in Figure 2.5.

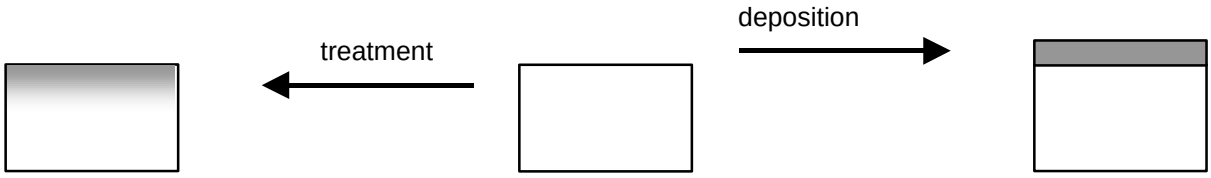

Figure 2.5. Schematic drawing of the effect of plasma techniques (treatment and deposition) on transparent, nonconducting polymeric substrates in order to obtain transparent and conductive polymeric systems (gray colour indicates conductivity).

For plasma treatment, the transparent substrate material should be chosen such that upon plasma treatment a conjugated structure is created in the surface layer. In the aforementioned studies on plasma treatment, the substrate material was not given a specific function in the treatment process. A carbon-layer was formed by destruction of the surface layer by the plasma treatment, irrespective of the substrate material. In principle, the preferential removal of pendant groups from vinyl polymers may lead to the formation of a conjugated structure at

the surface, which can be used for the transport of electricity. For instance, it has been shown by optical emission spectroscopy (OES) measurements that the vacuum UV light (wavelength < 150 nm) emitted by an argon plasma induced decarboxylation in PAAc.[176,177] Furthermore, unsaturated carbon bonds were observed in PVC after treatment by a number of surface treatments (e.g., γ-radiation,[178-183] UV irradiation,[184,185] ion beam,[186,187] and electron beam[188]).

A disadvantage of this strategy is that it limits the number of possibly usable substrate materials drastically. Plasma polymerisation does not suffer from this disadvantage as PP layers can be deposited on almost any transparent substrate.

Plasma polymerisation has been frequently used to obtain conductive polymer layers using conjugated monomers that by conventional chemistry also result in conjugated and conductive polymers. For instance, polythiophene is known for its high and stable conductivity and therefore, thiophene is often used as monomer for plasma polymerisation.[58,141-146] To obtain PP layers with a high conductivity, the conjugated structure of the monomer should be retained in the PP layers. The deposition conditions and the monomer structure can be used as variables to achieve this. Because of the complex relationships between monomer structure, deposition conditions, reactive species, together with the uncertainty of the deposition mechanism, a detailed study is necessary for every monomer and deposition system.[99]

References

[1] *Handbook of conducting polymers*; Skotheim, T. A., Ed.; Marcel Dekker: New York, **1986**; Vol. 1 and 2.

[2] Bloor, D. *Nature* **1988**, *335*, 115-117.

[3] Bhaumik, D.; Mark, J. E. *Polym. Prepr.* **1984**, *25*, 266-267.

[4] Przyluski, J. *Conducting polymers*; Sci-Tech Publications: Liechtenstein, **1991**.

[5] Lyons, M. E. G. In *Electroactive polymers*; Lyons, M. E. G., Ed.; Plenum Press: New York, **1994**, pp 1-65.

[6] Bott, D. C. In *Handbook of conducting polymers*; Skotheim, T. A., Ed.; Marcel Dekker: New York, **1986**, pp 1191-1232.

[7] Baughman, R. H.; Brédas, J. L.; Chance, R. R.; Elsenbaumer, R. L.; Shacklette, L. W. *Chem. Rev.* **1982**, *82*, 209-222.

[8] ten Hoeve, W.; Wynberg, H.; Havinga, E. E.; Meijer, E. W. *J. Am. Chem. Soc.* **1991**, *113*, 5887-5889.

[9] Garnier, F.; Deloffre, F.; Horowitz, G.; Hajlaoui, R. *Synth. Met.* **1993**, *57*, 4747-4754.

[10] Fichou, D.; Horowitz, G.; Garnier, F. *Synth. Met.* **1990**, *39*, 125-131.

[11] Fichou, D.; Horowitz, G.; Garnier, F. *Synth. Met.* **1990**, *39*, 243-259.

[12] Fichou, D.; Xu, B.; Horowitz, G.; Garnier, F. *Synth. Met.* **1991**, *41-43*, 463-469.

[13] Sethi, R. S.; Goosey, M. T. In *Special polymers for electronics and optoelectronics*; Chilton, J. A. and Goosey, M. T., Ed.; Chapman and Hall: London, **1995**.

[14] Brédas, J. In *Handbook of conducting polymers*; Skotheim, T. A., Ed.; Marcel Dekker: New York, **1986**; Vol. 2, pp 859-914.

[15] Reynolds, J. R.; Baker, C. K.; Jolly, C. A.; Poropatic, P. A.; Ruiz, J. P. In *Conductive polymers and plastics*; Margolis, J. M., Ed.; Chapmann and Hall: New York, **1989**, pp 1-40.

[16] Naarmann, H.; Theophilou, N. In *Handbook of conducting polymers*; Skotheim, T. A., Ed.; Marcel Dekker: New York, **1988**, pp 1-39.

[17] Kane, P. F.; Larrabee, G. B. *Characterization of semiconductor materials*; McGraw-Hill Book Company: New York, **1970**.

[18] Baker, G. L. In *Electronic and photonic applications of polymers*; Bowden, M. J. and Turner, S. R., Ed.; Am. Chem. Soc.: Washington, **1988**, pp 271-296.

[19] Gorman, C. B.; Grubbs, R. H. In *Conjugated polymers*; Brédas, J. and Silbey, R., Ed.; Kluwer academic publishers: Dordrecht, **1991**, pp 1-49.

[20] Menon, R. In *Handbook of organic conductive molecules and polymers*; Nalwa, H. S., Ed.; John Wiley & Sons: Chichester, **1997**; Vol. 4, pp 55-75.

[21] Metzger, K. C.; Welsh, W. J. *Polym. Prepr.* **1984**, *25*, 270-271.

[22] Yaniger, S. I.; Kletter, M. J.; Dairmid, A. G. M. *Polym. Prepr.* **1984**, *25*, 264-265.

[23] Metzger, K. C.; Welsh, W. J. *Polym. Prepr.* **1984**, *25*, 268-269.

[24] Chien, J. C. W. *Polym. Prepr.* **1984**, *25*, 262-263.

[25] Diarmid, A. G. M.; Heeger, A. J. *Synth. Met.* **1979**, *1*, 101-118.

[26] Masubuchi, S.; Kazama, S. *Synth. Met.* **1995**, *74*, 151-158.

[27] Mizoguchi, K.; Honda, M.; Masubuchi, S.-I.; Kazama, S.; Kume, K. *Jpn. J. Appl. Phys.* **1994**, *33*, L1239-1241.

[28] Mohammed, F. *Synth. Met.* **1999**, *99*, 149-154.

[29] Djellab, H.; Armand, M.; Delabouglise, D. *Synth. Met.* **1995**, *74*, 223-226.

[30] Friend, R. H.; Giles, J. R. M. *J. Chem. Soc., Chem. Comm.* **1984**, 1101-1103.

[31] Sersen, F.; Cik, G.; Szabo, L.; Dlhan, L. *Synth. Met.* **1996**, *80*, 297-300.

[32] Matsuura, Y.; Oshima, Y.; Misaki, Y.; Fujiwara, H.; Tanaka, K.; Yamabe, T.; Hotta, S. *Synth. Met.* **1996**, *82*, 155-158.

[33] Kuwabara, M.; Abe, S.; Ono, Y. *Synth. Met.* **1997**, *85*, 1109-1110.

[34] Haare, J. A. E. H. v.; Groenendaal, L.; Havinga, E. E.; Meijer, E. W.; Janssen, R. A. J. *Synth. Met.* **1997**, *85*, 1091-1092.

[35] Chance, R. R.; Boudreaux, D. S.; Bredas, J. L.; Silbey, R. In *Handbook of conducting polymers*; Skotheim, T. A., Ed.; Marcel Dekker: New York, **1986**; Vol. 2, pp 825-857.

[36] Ivory, D. M.; Miller, G. G.; Sowa, J. M.; Shacklette, L. W.; Chance, R. R.; Baughman, R. H. *J. Chem. Phys.* **1979**, *71*, 1506-1507.

[37] Tour, J. M. *Adv. Mater.* **1994**, *6*, 190-198.

[38] Leeuw, D. M. d.; Simenon, M. M. J.; Brown, A. R.; Einerhand, R. E. F. *Synth. Met.* **1997**, *87*, 53-59.

[39] Kobmehl; Chatzitheodorou, G. *Macrmol. Chem., Rapid Commun.* **1983**, *4*, 639-643.

[40] Tourillon, G.; Garnier, F. *J. Electroanal. Chem.* **1982**, *135*, 173-178.

[41] Wellinghoff, S. T.; Deng, Z.; Reed, J.; Racchini, J. *Polym. Prepr.* **1984**, *25*, 238-239.

[42] Kim, O. K. *J. Polym. Sci., Pol. Lett. Ed.* **1982**, *20*, 663-666.

[43] Gagnon, D. R.; Capistran, J. D.; Karasz, F. E.; Lenz, R. W. *Polym. Prepr.* **1984**, *25*, 284-285.

[44] Ellis, J. R. In *Handbook of conducting polymers*; Skotheim, T. A., Ed.; Marcel Dekker: New York, **1986**; Vol. 1, pp 489-500.

[45] Bäuerle, P. *Adv. Mater.* **1993**, *5*, 879-885.

[46] Sillion, B. *High Performance Polymers* **1999**, *11*, 417-436.

[47] Miller, J. S. *Adv. Mater.* **1990**, *2*, 98-99.

[48] Miller, J. S. *Adv. Mater.* **1993**, *5*, 587-589.

[49] Bloor, D. *Nature* **1991**, *349*, 738-740.

[50] Burroughes, J. H.; Jones, C. A.; Friend, R. H. *Nature* **1988**, *335*, 137-141.

[51] Greenham, N. C.; Moratti, S. C.; Bradley, D. D. C.; Friend, R. H.; Holmes, A. B. *Nature* **1993**, *365*, 628-630.

[52] Pei, Q.; Yang, Y.; Yu, G.; Zhang, C.; Heeger, A. J. *J. Am. Chem. Soc.* **1996**, *118*, 3922-3929.

[53] Caja, J.; Kaner, R. B.; MacDiarmid, A. G. *J. Electrochem. Soc.* **1984**, 2744-2750.

[54] Josowicz, M.; Janata, J. In *Applications of electroactive polymers*; Scrosati, B., Ed.; Chapman and Hall: London, **1993**, pp 310-343.

[55] Yue, J.; Epstein, A. J. *J. Chem. Soc., Chem. Comm.* **1992**, 1540-1542.

[56] Bidan, G.; Niel, M.-A. *Synth. Met.* **1997**, *85*, 1387-1388.

[57] Collins, G. E.; Buckley, L. J. *Synth. Met.* **1996**, *78*, 93-101.

[58] Giungato, P.; Ferrara, M. C.; Musio, F.; d'Agostino, R. *Plasmas Polym.* **1996**, *1*, 283-297.

[59] Kim, J. M.; Yoo, S. Y.; Shin, H. K.; Kwon, Y. S. *Synth. Met.* **1997**, *85*, 1423-1424.

[60] MacDiarmid, A. G.; Zhang, W. J.; Huang, Z.; Wang, P.-C.; Huang, F.; Xie, S. *Polym. Prepr.* **1997**, *38*, 333-334.

[61] Ogura, K.; Kokura, M.; Nakayama, M. *J. Electrochem. Soc.* **1995**, *142*, L152-L153.

[62] Talaie, A. *Polymer* **1997**, *38*, 1145-1150.

[63] Barisci, J. N.; Conn, C.; Wallace, G. G. *TRIP* **1996**, *4*, 307-311.

[64] Brown, A. R.; Pomp, A.; Hart, C. M.; Leeuw, D. M. d. *Science* **1995**, *270*, 972-974.

[65] Horowitz, G. *Adv. Mater.* **1998**, *10*, 365-377.

[66] Tsumura, A.; Koezuka, H.; Ando, T. *Synth. Met.* **1988**, *25*, 11-23.

[67] White, H. S.; Kittlesen, G. P.; Wrighton, M. S. *J. Am. Chem. Soc.* **1984**, *106*, 5375-5377.

[68] Yang, Y.; Heeger, A. J. *Nature* **1994**, *372*, 344-346.

[69] Glenis, S.; Benz, M.; LeGoff, E.; Kanatzidis, M. G.; Groot, D. C. d.; Schindler, J. L.; Kannewurf, C. R. *Synth. Met.* **1995**, *75*, 213-221.

[70] Zotti, G.; Salmaso, R.; Gallazzi, M. C.; Marin, R. A. *Chem. Mater.* **1997**, *9*, 791-795.

[71] McCullough, R. D.; Williams, S. P. *J. Am. Chem. Soc.* **1993**, *115*, 11608-11609.

[72] Laakso, J.; Osterholm, J. E.; Nyholm, P.; Stubb, H.; Punkka, E. *Synth. Met.* **1990**, *37*, 145-150.

[73] Andreani, F.; Salatelli, E.; Lanzi, M.; Bertinelli, F.; Fichera, A. M.; Gazzano, M. *Polymer* **2000**, *41*, 3147-3157.

[74] Taka, T.; Loponen, M. T.; Laakso, J.; Suuronen, K.; Valkeinen, P.; Osterholm, J. E. *Synth. Met.* **1991**, *41*, 567-570.

[75] Dai, L.; White, J. W. *Polymer* **1997**, *38*, 775-783.

[76] Park, Y. H.; Jeon, Y. J.; Lee, Y.; Baik, D. H.; Son, Y. *Mol. Cryst. Liq. Cryst.* **1996**, *280*, 193-198.

[77] Yin, W.; Li, J.; Gu, T.; Wu, J. *J. Appl. Polym. Sci.* **1997**, *63*, 13-16.

[78] Laakso, J.; Osterholm, J. E.; Nyholm, P. *Synth. Met.* **1989**, *28*, C467-C471.

[79] Isotalo, H.; Ahlskog, M.; Stubb, H.; Laakso, J.; Karna, T.; Jussila, M.; Osterholm, J. E. *Synth. Met.* **1993**, *57*, 3581-3586.

[80] Khan, M. A.; Armes, S. P. *Adv. Mater.* **2000**, *12*, 671-674.

[81] Huijs, F. *Thin transparent conducting films based on core-shell latexes*; University of Groningen: Groningen, **2000**.

[82] Bhattacharya, A.; De, A.; Das, S. *Polymer* **1996**, *37*, 4375-4382.

[83] Dai, L.; Mau, A. W. H.; Gong, X.; Griesser, H. J. *Synth. Met.* **1997**, *85*, 1379-1380.

[84] Diaz, A. F.; Kanazawa, K. K. *J. Chem. Soc., Chem. Comm.* **1979**, 635-636.

[85] Diaz, A. F.; Bargon, J. In *Handbook of conducting polymers*; Skotheim, T. A., Ed.; Marcel Dekker: New York, **1986**, pp 81-116.

[86] Kaneto, K.; Kohno, Y.; Yoshino, K.; Inuishi, Y. *J. Chem. Soc., Chem. Comm.* **1983**, 382-383.

[87] Niwa, T.; Tamamura, T. *J. Chem. Soc., Chem. Comm.* **1984**, 817-818.

[88] Yasuda, H. *J. Macromol. Sci.* **1976**, *A10*, 383-420.

[89] Oktem, T.; Ayhan, H.; Seventekin, N.; Piskin, E. *J. Soc. Dyers Colour.* **1999**, *115*, 274-279.

[90] Inagaki, N. *Plasma Surface Modification and Plasma Polymerization*; Technomic Publishing: Lancaster, **1996**.

[91] d'Agostino, R. *Plasma deposition, treatment, and etching of polymers*; Academic Press: Boston, **1990**.

[92] *Techniques and applications of plasma chemistry*; Hollahan, J. R.; Bell, A. T., Ed.; John Wiley & Sons: New York, **1974**.

[93] Terlingen, J. G. A. *Introduction of functional groups at polymer surfaces by glow discharge techniques*; University of Twente: Enschede, **1993**.

[94] Collaud, M.; Groening, P.; Nowak, S.; Schlapbach, L. In *Polymer surface modification: relevance to adhesion*; Mittal, K. L., Ed.; VSP: Utrecht, **1996**, pp 87-99.

[95] Boenig, H. V. In *Encycl. Polym. Sci. Eng.*; Mark, H. F. and Kroschwitz, J. I., Ed.; **1986**; Vol. 11, pp 248-261.

[96] Roth, J. R. *Industrial plasma engineering*; Institute of Physics Publishing: Bristol, **1995**.

[97] Polak, L. S.; Lebedev, Y. A. *Plasma Chemistry*; 1st ed.; Cambridge International Sci. Publ.: Cambridge, **1998**.

[98] Yasuda, H. *Plasma polymerization*; Academic Press: Orlando, **1985**.

[99] Suhr, H. In *Techniques and applications of plasma chemistry*; Hollahan, J. and Bell, A. T., Ed.; John Wiley & Sons: New York, **1974**, pp 57-111.

[100] Coburn, J. W.; Chen, M. *J. Appl. Phys.* **1980**, *51*, 3134-3136.

[101] Gazicki, M.; Yasuda, H. *J. Appl. Pol. Sci., Appl. Pol. Symp.* **1984**, *38*, 35-44.

[102] Nguyen, T. P.; Rendu, P. L.; Amgaad, K.; Cailler, M.; Tran, V. H. *Synth. Met.* **1995**, *72*, 35-39.

[103] Mizutani, T.; Mori, T.; Takai, Y.; Ieda, M. *Conf. Rec. IEEE Int. Symp. Elec. Insul.* **1988**, 154-157.

[104] Tu, D. M.; Zhuang, G. P.; Kao, K. C. *J. Appl. Polym. Sci.* **1991**, *43*, 1625-1632.

[105] Drachev, A. I.; Gil'man, A. B.; Tuzov, L. S.; Potapov, V. K. *High Energy Chem.* **1995**, *29*, 295-296.

[106] Wu, Z. F.; Shi, Y. C.; Chen, H. M.; Chen, Y. F. *Chin. Sci. Bull.* **1993**, *38*, 510-513.

[107] Coen, M. C.; Groening, P.; Dietler, G.; Schlapbach, L. *J. Appl. Phys.* **1995**, *77*, 5695-5701.

[108] Suleimanov, B. A.; Akhmedov, M. M.; Suleimanova, Y. I.; Kerimov, M. K. *Thin Solid Silms* **1991**, *197*, 319-326.

[109] Bhuiyan, A. H.; Bhoraskar, S. V. *J. Mat. Sci.* **1989**, *24*, 3091-3095.

[110] Bhuiyan, A. H.; Bhraskar, S. V. *Ind. J. Pure Appl. Phys.* **1989**, *27*, 819-821.

[111] Bhuiyan, A. H.; Bhoraskar, S. V. *Thin Solid Films* **1993**, *235*, 43-46.

[112] Doblhofer, K.; Nölte, D.; Ulstrup, J. *Ber. Bunsen-Ges. Phys. Chem.* **1978**, *83*, 403-408.

[113] Dake, S. B.; Bhoraskar, S. V. *Pramana* **1985**, *24*, 895-903.

[114] Munro, H. S.; Grünwald, H. *J. Polym. Sci. Polym. Chem. Ed.* **1985**, *23*, 479-488.

[115] Grünwald, H.; Munro, H. S.; Wilhelm, T. *Mater. Sci. Eng.* **1991**, *A 139*, 356-358.

[116] Grünwald, H.; Munro, H. S.; Wilhelm, T. *Synth. Met.* **1991**, *41*, 1465-1469.

[117] Ieda, M.; Takai, Y.; Hayase, Y.; Mizutani, T. *Conf. Rec. IEEE Int. Symp. Elec. Insul.* **1984**, 178-181.

[118] Islam, O.; Bhuiyan, A. H.; Ahmed, S. *Thin Solid Films* **1994**, *238*, 191-194.

[119] Takai, Y.; Hayase, T.; Mizutani, T.; Ieda, M. *J. Phys. D: Appl. Phys.* **1984**, *17*, 399-406.

[120] Takai, Y.; Mizutani, T.; Ieda, M. *Jpn. J. Appl. Phys.* **1987**, *26*, 812-817.

[121] Gong, X.; Dai, L.; Mau, A. W. H.; Griesser, H. J. *J. Polym. Sci. Part A: Polym. Chem.* **1998**, *36*, 633-643.

[122] Cruz, G. J.; Morales, J.; Castillo-Ortega, M. M.; Olayo, R. *Synth. Met.* **1997**, *88*, 213-218.

[123] Bhat, N. V.; Joshi, N. V. *Plasma Chem. Plasma Process.* **1994**, *14*, 151-161.

[124] Tong, Z. S.; Wu, M. Z.; Pu, T. S.; Zhou, F.; Liu, H. Z. *Synth. Met.* **1995**, *68*, 125-131.

[125] Samal, S.; Mohanty, B. C.; Nayak, B. B. *Polym. Sci.* **1994**, *1*, 222-226.

[126] Chen, X.; Devaux, J.; Issi, J. P.; Billaud, D. *Polym. Eng. Sci.* **1995**, *35*, 642-647.

[127] Jasne, S. In *Encycl. Polym. Sci. Eng*, Mark, H. F. and Kroschwitz, J. I., Ed., **1986**; Vol. 13, pp 42-55.

[128] Kanazawa, K. K.; Diaz, A. F.; Geiss, R. H.; Gill, W. D.; Kwak, J. F.; Logan, J. A.; Rabolt, J. F.; Street, G. B. *J. Chem. Soc., Chem. Comm.* **1979**, 854-855.

[129] Kunugi, T.; Okuzaki, H. *J. Polym. Sci. Part B: Polym. Phys.* **1996**, *34*, 1269-1275.

[130] MacDiarmid, A. G. *Synth. Met.* **1997**, *84*, 27-34.

[131] Thieblemont, J. C.; Planche, M. F.; Petrescu, C.; Bouvier, J. M.; Bidan, G. *Synth. Met.* **1993**, *59*, 81-96.

[132] Satoh, M.; Ishikawa, H.; Amano, K.; Hasegawa, E.; Yoshino, K. *Synth. Met.* **1994**, *65*, 39-44.

[133] Tourillon, G. In *Handbook of conducting polymers*; Skotheim, T. A., Ed.; Marcel Dekker: New York, **1986**; Vol. 1, pp 293-350.

[134] Schopf, G.; Kossmehl, G. *Adv. Polym. Sci.* **1997**, *129*.

[135] McCullough, R. D. *Adv. Mater.* **1998**, *10*, 93-116.

[136] Bjornholm, T.; Hassenkam, T.; Greve, D. R.; McCullough, R. D.; Jayaraman, M.; Savoy, S. M.; Jones, C. E.; McDevitt, J. T. *Adv. Mater.* **1999**, *11*, 1218-1221.

[137] Lee, K. P.; Park, S. Y.; Kim, N.; Song, S. K. *Mol. Cryst. Liq. Cryst.* **1993**, *224*, 53-59.

[138] Ooij, W. J. v.; Eufinger, S.; Ridgway, T. H. *Plasmas and polym.* **1996**, *1*, 229-260.

[139] Zhang, J.; Wu, M. Z.; Pu, T. S.; Zhang, Z. Y.; Jin, R. P.; Tong, Z. S.; Zhu, D. Z.; Cao, D. X.; Zhu, F. Y.; Cao, J. Q. *Thin Solid Films* **1997**, *307*, 14-20.

[140] Cruz, G. J.; Morales, J.; Olayo, R. *Thin Solid Films* **1999**, *342*, 119-126.

[141] Sadhir, R.; K.F. Schoch, J. *Thin Solid Films* **1993**, *223*, 154-160.

[142] Sadhir, R. K.; K.F. Schoch, J. *Polym. Prepr.* **1992**, *33*, 412-413.

[143] Sadhir, R.; K.F. Schoch, J. *Polym. Prepr.* **1995**, *34*, 679-680.

[144] Thomas, B.; Pillai, M. G. K.; Jayalekshmi, S. *J. Phys. D.: Appl. Phys.* **1988**, *21*, 503-508.

[145] Tanaka, K.; Yoshizawa, K.; Takeuchi, T.; Yamabe, T.; Yamauchi, J. *Synth. Met.* **1990**, *38*, 107-116.

[146] Tanaka, K.; Okazaki, S.; Inomata, T.; Kogoma, M. *8th Symp. Plasma Sci. Mater.*, **1995**, 33-37.

[147] Ryan, M. E.; Hynes, A. M.; Wheale, S. H.; Badyal, J. P. S.; Hardacre, C.; Ormerod, R. M. *Chem. Mater.* **1996**, *8*, 916-921.

[148] Kruse, A.; Schlett, V.; Baalmann, A.; Hennecke, M. *Fresenius' J. Anal. Chem.* **1993**, *346*, 284-289.

[149] Tanaka, K.; Yamabe, T.; Takeuchi, T.; Yoshizawa, K.; Nishio, S. *J. Appl. Phys.* **1991**, *70*, 5653-5660.

[150] Nishio, S.; Takeuchi, T.; Matsuura, Y.; Yoshizawa, K.; Tanaka, K.; Yamabe, T. *Synth. Met.* **1992**, *46*, 243-250.

[151] Xie, X.; Thiele, J. U.; Steiner, R.; Oelhafen, P. *Synth. Met.* **1994**, *63*, 221-224.

[152] Osada, Y.; Yasunaga, H.; Wang, F. S.; Chen, J. *J. Appl. Phys.* **1988**, *4*, 1476-1483.

[153] O'Toole, L.; Beck, A. J.; Ameen, A. P.; Jones, F. R.; Short, R. D. *J. Chem. Soc. Faraday Trans.* **1995**, *91*, 3907-3912.

[154] O'Toole, L.; Short, R. D. *J. Chem. Soc. Faraday Trans.* **1997**, *93*, 1141-1145.

[155] Chen, M.; Yang, T.-S.; Zhou, X. *J. Polym. Sci.* **1996**, *34*, 113-120.

[156] Brumlik, C. J.; Parthasarathy, A.; Chen, W.; Martin, C. R. *J. Electrochem. Soc.* **1994**, *141*, 2273-2279.

[157] Yasuda, H.; Yasuda, T. *J. Polym. Sci. Part A: Polym. Chem.* **2000**, *38*, 943-953.

[158] Lopèz, G. P.; Ratner, B. D. *J. Polym. Sci. Part A: Polym. Chem.* **1992**, *30*, 2415-2425.

[159] Lopèz, G. P.; Chilkoti, A.; Briggs, D.; Ratner, B. D. *J. Polym. Sci. Part A: Pol. Chem.* **1992**, *30*, 2427-2441.

[160] Ryan, M. E.; Hynes, A. M.; Badyal, J. P. S. *Chem. Mater.* **1996**, *8*, 37-42.

[161] Wang, J.-H.; Chen, X.; Chen, J.-J.; Calderon, J. G.; Timmons, R. B. *Plasmas Polym.* **1997**, *2*, 245-260.

[162] Mackie, N. M.; Fisher, E. R. *Polym. Prepr.* **1997**, *38*, 1059-1060.

[163] Uchida, T.; Senda, K.; Vinogradov, G. K.; Morita, S. *Thin Solid Films* **1996**, *281-282*, 536-538.

[164] Uchida, T.; Vinogradov, G. K.; Morita, S. *J. Electrochem. Soc.* **1997**, *144*, 1434-1439.

[165] Chuvyrov, A. N.; Kuvatov, Z. K.; Kogarmanov, S. M. *Carbon* **1994**, *32*, 181-182.

[166] Osada, Y.; Yu, Q. S.; Yasunaga, H.; Kagami, Y. *J. Polym. Sci. Part A: Pol. Chem.* **1989**, *27*, 3799-3809.

[167] Tanaka, K.; Nishio, S.; Matsuura, Y.; Yamabe, T. *J. Appl. Phys.* **1993**, *73*, 5017-5022.

[168] Tanaka, K.; Nishio, S.; Matsuura, Y.; Yamabe, T. *Synth. Met.* **1993**, *55*, 896-901.

[169] Tanaka, K.; Nishio, S.; Matsuura, Y.; Yamabe, T. *Synth. Met.* **1994**, *64*, 209-215.

[170] Hallil, A.; Despax, B. *Thin Solid Films* **2000**, *358*, 30-39.

[171] Bartnik, J.; Zurakowska-Orszagh, J. *Int. Polym. Sci. Technol.* **1993**, *21*, T67-T72.

[172] Eufinger, S.; Ooij, W. J. v.; Ridgway, T. H. *J. Appl. Polym. Sci.* **1996**, *61*, 1503-1514.

[173] Chen, M.; Yang, T.-C.; Ma, Z.-G. *J. Polym. Sci. Part A: Pol. Chem.* **1998**, *36*, 1265-1270.

[174] Fujita, T.; Matsumoto, O. *J. Electrochem. Soc.* **1989**, *136*, 2624-2629.

[175] Fujita, T.; Inagaki, C.; Uyama, H.; Matsumoto, O. *J. Electrochem. Soc.* **1990**, *137*, 1645-1647.

[176] Terlingen, J. G. A.; Hoffman, A. S.; Feijen, J. *J. Appl. Polym. Sci.* **1993**, *50*, 1529-1539.

[177] Terlingen, J. G. A.; Takens, G. A. J.; Gaag, F. J. v. d.; Hoffman, A. S.; Feijen, J. *J. Appl. Polym. Sci.* **1994**, *52*, 39-53.

[178] Zahran, A. H.; Hegazy, E. A.; Eldin, F. M. E. *Radiat. Phys. Chem.* **1985**, *26*, 25-32.

[179] Arakawa, K.; Seguchi, T.; Yoshida, K. *Radiat. Phys. Chem.* **1986**, *27*, 157-163.

[180] Dakin, V. I.; Egorova, Z. S.; Karpov, V. L. *Khim. Vys. Energ. (transl.)* **1977**, *11*, 378-379.

[181] Dakin, V. I.; Dachenko, A. V.; Karpov, V. L. *Polym. Sci. USSR* **1984**, *26*, 2473-2479.

[182] Shaban, A. M. *Mater. Letters* **1995**, *22*, 309-312.

[183] Burillo, G.; Ogawa, T. *Radiat. Phys. Chem.* **1985**, *25*, 383-388.

[184] Kwei, K. S. *J. Appl. Polym. Sci.* **1968**, *12*, 1543-1550.

[185] Sobue, H.; Tabata, Y.; Tajima, Y. *J. Polym. Sci.* **1958**, *27*, 596-597.

[186] Davenas, J.; Tran, V. H.; Boiteux, G. *Synth. Met.* **1995**, *69*, 583-584.

[187] Venkatesan, T.; Forrest, S. R.; Kaplan, M. L.; Murray, C. A.; Schmidt, P. H.; Wilkens, B. J. *J. Appl. Phys.* **1983**, *54*, 3150-3153.

[188] Lindberg, K. A. H.; Vesely, D.; Bertilsson, H. E. *J. Mater. Sci.* **1985**, *20*, 2225-2232.

3

Removal of pendant groups of vinyl polymers by argon plasma treatment*

Poly(acrylic acid) (PAAc) and poly(vinyl chloride) (PVC) were treated with an argon plasma to create unsaturated bonds at the surface. By use of Fourier transform infrared measurements and X-ray photoelectron spectroscopy it was shown that the pendant groups of these polymers are removed by the argon plasma treatment. This resulted in the formation of unsaturated bonds and cross-links in the modified layer. It was found that the removal of the pendant groups is induced by UV light emitted by the argon plasma. During treatment of PAAc decarboxylation took place, which made the argon plasma more oxidative in character. The modified layer was reoxidised and eventually the PAAc surface was ablated with time. The removal of chlorine from PVC was found to be preferential and a highly cross-linked layer, containing at least 15% unsaturated bonds was obtained. The outermost top-layer of this modified layer became oxidised after exposure to air due to a reaction between long-living radicals and oxygen.

Introduction

Glow discharge processes (e.g., corona and low pressure plasma treatments) are frequently used to modify the surface properties of engineering plastics.[1-8] These processes have certain advantages over other surface modifying techniques such as flame treatment, ultraviolet (UV)[9-12]- and γ-irradiation,[13] and wet chemical treatments.[14-16] For instance, the modification depth is small and complex geometries can be treated in one step without the use of solvent.[3,7,17-23] Furthermore, a broad range of surface properties can be obtained, although the specificity toward the type of functional groups introduced at the surface is considered to be low.[1,24,25] Some improvements have been made by preadsorbing surfactants on polymeric substrates followed by a gas-plasma treatment.[23,26,27]

In earlier studies it was shown by optical emission spectroscopy (OES) measurements that, upon argon plasma treatment of PAAc, decarboxylation took place.[28,29] This resulted in the presence of CO, CO_2, and water in the plasma phase. It was found that decarboxylation was induced by the vacuum UV (wavelength < 150 nm) emitted by the argon plasma. In principle, the preferential removal of pendant groups from vinyl polymers may lead to the formation of unsaturated bonds. After the plasma treatment, these could be used for example in grafting or the transport of electrons. In the case of PAAc, removal of the polymer layer was also observed (i.e., etching). From literature it is known that oxidation processes can result in etching of the treated polymer.[9,24] The observed ablation of PAAc may therefore be due to

* The work described in this chapter has been published in Groenewoud *et al.*, *Langmuir*, **1999**, *15*, 5396-5402.

the oxidative environment caused by the release of oxygen-containing species in the plasma phase. This oxidation can be minimised by a pulsed plasma treatment based on the assumption that the oxygen-containing species are removed from the reactor by the argon flow during the "off" time between two pulses.

The pendant group in a vinyl polymer (e.g., polyvinylalcohol (PVA), -chloride (PVC), -fluoride (PVF), and polystyrene (PS)) can also be selected to obtain a highly unsaturated surface and to minimise reoxidation or ablation or both. Considering the results found for PAAc, oxygen-containing pendant groups as in PVA are not interesting alternatives. A disadvantage of PS is the stability of the pendant phenyl group, which makes selective removal of this group difficult. To obtain selective removal of the pendant group, volatile compounds should be formed. From PVF and PVC, volatile compounds such as HF and HCl can easily be formed. Of these two polymers, PVC seems to be the most promising substrate as the carbon-chlorine has a lower bond energy compared with the carbon-fluorine bond.

In literature, several studies on the effect of γ-radiation,[13,30-34] UV-irradiation,[35,36] ion beam,[37,38] and electron beam[39] treatment on the surface properties of PVC have been published. It was found that the carbon-chlorine bond in PVC is readily cleaved. Furthermore, unsaturated structures were observed after treatment. Most of the species used for treatment in the cited studies are also present in an argon plasma (e.g., electrons, ions, and UV). Although the energy of these species in a plasma may be different, a similar effect of an argon plasma treatment on PVC might be expected.[40] Furthermore, the plasma technique is relatively simple, only modifies the surface and offers the possibility to treat large surface areas in one step.

The aim of the present study was to introduce unsaturated bonds at the surface of vinyl polymers by an argon plasma treatment. To investigate this, argon plasma treated PAAc and PVC samples were characterised with X-ray induced photoelectron spectroscopy (XPS) and Fourier transform infrared (FTIR) spectroscopy. Furthermore, the argon plasma treated samples were extracted with the appropriate solvents, and the residual insoluble layer was analysed with FTIR and solid-state NMR (SSNMR).

Experimental

Materials. PAAc (M_w 250000) and PVC (M_w 97000, M_n 55000) were purchased from Aldrich Chemie (Brussels, Belgium). All solvents were of analytical grade purity and were purchased from Merck (Darmstadt, Germany). Bromine was of synthetic grade purity (99%) and also obtained from Merck (Darmstadt, Germany). Argon (purity ≥ 99.999%) was obtained from Hoekloos (Schiedam, the Netherlands). Water used was doubly deionised. All chemicals were used as received. Glass discs (∅ 2.5 cm, used for FTIR analysis) with a sputtered chromium and gold layer were supplied by the FFW division (Department of Applied Physics and Electrical Engineering, University of Twente, Enschede, the Netherlands). Glass discs (∅ 1.5 cm, used for XPS analysis) were purchased from Knittel Waldemar (Braunschweig, Germany).

Cleaning. All glassware, substrates, and tools were cleaned ultrasonically, consecutively three times in toluene, acetone, water, and acetone and subsequently dried *in vacuo* at room temperature (RT).

Spin coating. PAAc and PVC were dissolved to a concentration of 2 % w/w in methanol and THF, respectively. Spin coating was carried out at 2000 rpm using a Teflon sample holder mounted on an IKA RW 20 DZM mechanical stirrer (Janke & Kunkel, Staufen, Germany). A volume of 0.025 ml of the polymer-containing solution was dropped on rotating glass discs with a diameter of 1.5 cm. For discs with a diameter of 2.5 cm, a volume of 0.05 ml was used. After rotating for 1 min, the spin-coated glass discs were taken out of the sample holder and dried over night *in vacuo* at RT.

Casting. PAAc films were made by casting 250 ml of a 2% w/v solution of PAAc in methanol in a Petri dish (∅ 19 cm). PVC films were made by casting a 30% w/w solution in THF on a glass plate with a casting knife (0.075 mm). After evaporation of the solvent at RT, the films were dried *in vacuo* at RT under a metal plate to keep the samples flat. Finally the films were rinsed three times with hexane and dried *in vacuo* at RT.

Thickness measurement. The thickness of spin-coated layers was determined with a Dektak IIA (Sloan Technology Co., Santa Barbara, USA). After removing the spin-coated layer from part of the substrate, the needle was moved over the boundary between the bare and the covered substrate. The height difference was taken as the thickness of the spin-coated layer. For the determination of the thickness of the cast films, an ID-C112B thickness meter (Mitutoyo, Japan) was used.

Plasma treatment. The plasma apparatus has been described in detail in literature.[28,29] In short, it consists of a tubular reactor (internal diameter 6.5 cm, length 80 cm) with three externally placed, capacitively coupled electrodes. The two grounded (cold) electrodes were placed at a distance of 10 cm on either side of the powered (hot) electrode, which was placed in the centre of the reactor. Typically, the procedure for an argon plasma treatment was as follows. The samples were placed on two glass plates, which were placed in the centre between the hot and the cold electrodes. After pumping the reactor to a pressure < 3×10^{-6} mbar, it was flushed with an argon flow (10 sccm/min, 0.08 mbar) for 15 min. The samples were then treated with either a continuous or a pulsed (0.1 s on; 8.5 s off) plasma (13.56 MHz, 50 W, 10 sccm/min, 0.08 mbar) for a predetermined time. After the plasma treatment, the argon flow was maintained for 2 min, after which the reactor was brought to atmospheric pressure with air. All treated samples were stored at -18°C.

Extraction of plasma treated films. The insoluble fractions of argon plasma treated films (300 s) of PAAc and PVC were obtained by extracting the films (± 10 PAAc films; 2.5 cm x 2.5 cm or 10-15 PVC films; 4 cm x 10 cm) at RT in 5 ml/film of methanol (PAAc) or THF (PVC). After gentle stirring and sedimentation of the insoluble fraction, the solvent was removed with a pipette and refreshed. This was repeated five times, after which the insoluble fraction was filtered off (glass filter no. 5). After thorough washing with solvent (± 500 ml) the insoluble fraction was dried *in vacuo* at 35°C. The thickness of the insoluble layer can be calculated by

Equation 3.1. $$d = M/(A\times r)$$

where M is the mass of the insoluble fraction [kg], A is the total surface area of the films used for extraction [m^2], r refers to the density of the polymer [kg/m^3],[41] and d is the thickness of the insoluble

layer [m]. In Equation 3.1, it is assumed that the insoluble layer has the same density throughout, equal to that of the pristine polymer, and that this layer is totally insoluble.

Reaction of unsaturated bonds with bromine. Unsaturated bonds at the surface were reacted with Br_2 vapour. A polymeric sample was placed on glass beads in a glass vial. Subsequently, a drop of Br_2 was injected under the sample between the glass beads. The vial was closed and the reaction was allowed to proceed in the dark for 1 min at RT. After evaporation of adsorbed Br_2, the sample was stored at -18°C and subsequently analysed with XPS. Because an extra element is taken into account in the calculation of the atom concentrations, the concentrations of the other elements should decrease proportionally.

Characterisation. XPS measurements were carried out on either spin-coated glass discs (∅ 1.5 cm) or cast films using a Kratos XSAM 800 (Manchester, UK) equipped with a Mg K_α source (1253.6 eV). The analyser was placed perpendicular to the sample surface. The input power was 150 W (10 mA, 15 kV). The analysed spot size was 3 mm x 6 mm. Survey scans (1100 - 0 eV binding energy (BE) window) were recorded with a pass energy (PE) of 100 eV and a dwell of 0.1 s. Relative peak areas for the different elements were calculated by numerical integration of the detail scans (20 eV BE window, 50 eV PE) using sensitivity factors given in literature.[42] After normalisation, the concentrations of the various elements were obtained.

FTIR spectra were recorded from spin-coated glass discs (∅ 2.5 cm) using a BioRad FTS-60 (Cambridge, UK) in the reflectance mode. Background spectra were recorded using a clean substrate.

^{13}C CP-Mass SSNMR studies were performed on a Bruker MSL-400 NMR spectrometer (Bruker Canada Ltd., Milton, Canada), working at a 100.627 MHz ^{13}C frequency, and equipped with a 4 mm cross-polarisation magic angle spinning (CP-MAS) probe. The spinning speed was 10 kHz. Cross-polarisation experiments were performed under Hartman-Hahn conditions with a contact time of 2 ms and a recycle delay of 2 s. The $\pi/2$ proton pulse was 4.7 μs.

Results & Discussion

The results of the spin coating and casting of PAAc and PVC are summarised in Table 3.1 together with the results of the XPS measurements on untreated samples. The thickness of spin-coated layers on substrates used for XPS measurements (glass discs, ∅ 1.5 cm) was around 0.20 μm. This means that no signals of the underlying substrate will be detected by XPS (measuring depth XPS is ± 10 nm). Considering the error in the XPS measurement, the oxygen content of PAAc and the chlorine content of PVC are equal to the theoretical value (40.0% and 33.3%, respectively). Furthermore, PVC is slightly oxidised at the surface. Together with the absence of other signals in the XPS spectra, this shows that the samples do not contain any impurities.

The thickness of the spin-coated layers on substrates used for FTIR measurements (glass discs with a sputtered gold layer, ∅ 2.5 cm) was around 0.25 μm which is below the measuring depth of the technique (± 1 μm).

Table 3.1. Thickness of spin-coated layers and cast films of PAAc and PVC and chemical composition (determined with XPS, no other signals were detected) of PAAc and PVC samples.

Substrate	**PAAc**	**PVC**
discs ∅ 1.5 cm	0.17 ± 0.03 μm	0.24 ± 0.01 μm
discs ∅ 2.5 cm	0.23 ± 0.02 μm	0.28 ± 0.01 μm
Casting	374 ± 93 μm	61 ± 7 μm
C (%)	60.4 ± 0.6	69.8 ± 0.8
O (%)	39.6 ± 0.6	1.1 ± 0.5
Cl (%)	-	29.1 ± 1.1

The PAAc and PVC samples were treated with an argon plasma for different times. To study the effect of the argon plasma treatment time on PAAc and PVC, the chemical composition of the surface of untreated and argon plasma treated samples was determined with XPS (Figure 3.1). For PAAc, a decrease in oxygen content with increasing treatment time is found. At longer treatment times, the oxygen content seems to level off to around 20 % for continuously plasma treated samples. These values are in good agreement with those found earlier.[29] For pulsed plasma treated samples, a decrease to around 15% is found. For both treatments, no nitrogen was incorporated.

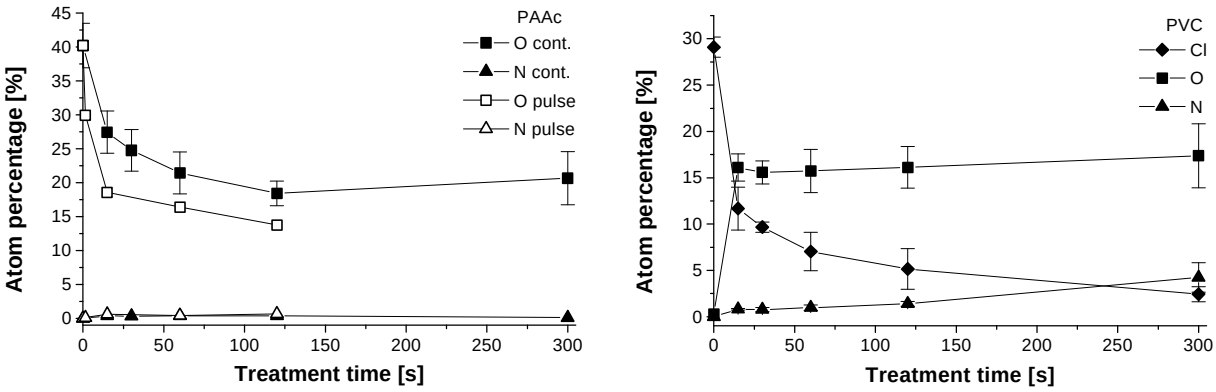

Figure 3.1. Left: Oxygen and nitrogen concentration (determined with XPS) at the surface of continuously (solid symbols, n = 3 ± sd) and pulsed (open symbols, t_{on} = 0.1 s; t_{off} = 8.5 s, n = 1) argon plasma treated PAAc samples as a function of treatment time. Right: Concentration of chlorine, oxygen, and nitrogen (determined with XPS) at the surface of continuously argon plasma treated PVC samples as a function of treatment time (n = 3 ± sd). Treatment time refers to the total plasma "on" time.

The C_{1s} spectra (Figure 3.2) give additional insight into the chemical structure of the surface of the treated samples.[42] Taking charging effects into account, the peaks at 287.1 eV and at 291.2 eV in the C_{1s} spectrum of untreated PAAc can be assigned to carbon atoms in the polymer backbone and to carbon atoms in carboxylic acid groups, respectively.[43] The C_{1s} spectra of the argon plasma treated samples clearly show that the decrease in oxygen content is due to the removal of pendant carboxylic acid groups. Furthermore, for continuously plasma treated PAAc samples, the main peak shows a small broadening on the high BE side at longer treatment times, indicating the formation of other oxygen-containing groups.[43] This reoxidation may be caused by oxygen-containing species that are released from the PAAc surface by the argon plasma treatment. Terlingen *et al.* already showed that CO, CO_2, and H_2O are present in the plasma phase when PAAc is treated with an argon plasma.[28,29]

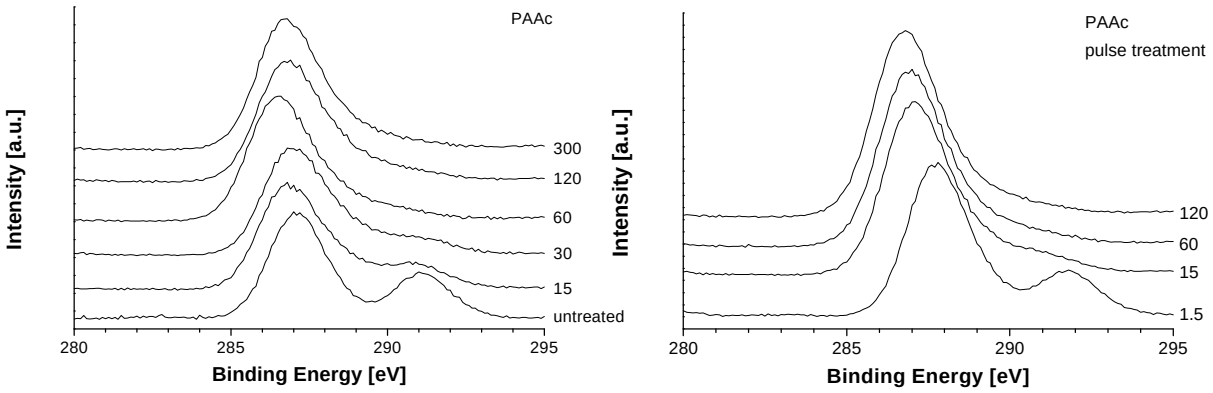

Figure 3.2. XPS C_{1s} spectra of untreated and continuously argon plasma treated PAAc (left) and pulsed (t_{on} = 0.1 s; t_{off} = 8.5 s) argon plasma treated PAAc (right) samples. The numbers refer to the total plasma "on" time (s).

Due to the presence of these oxygen-containing species the argon plasma becomes more oxidative in character, probably resulting in the observed reoxidation of the surface. This suggestion is substantiated by the lower oxygen content found for the pulsed plasma treated samples (Figure 3.1). When a pulsed plasma is applied, the carboxylic acid peak disappears faster (cf. C_{1s} spectra of 15 s pulsed and continuously argon plasma treated samples). The oxygen-containing species in the plasma phase are removed between two pulses. Therefore, the argon plasma is not much altered, resulting in less reoxidation. An additional cause for the reoxidation might be the possible presence of adsorbed water on the reactor walls and/or on the PAAc films.

The chlorine content of the surface of argon plasma treated PVC decreases with increasing treatment time to about 3% after 300 s (Figure 3.1). In Figure 3.3, the charge corrected C_{1s} spectra are depicted. Interestingly, the pristine polymer showed a charge shift, which was 1.2 eV higher than the plasma treated samples. This indicates that the surface conductivity of the plasma treated samples is higher, which might be due to the introduction of unsaturated carbon bonds. The C_{1s} peak of PVC is built up from signals of carbon atoms only attached to carbon and carbon atoms directly attached to chlorine.[43] Due to the low resolution, only one C_{1s} peak is visible in Figure 3.3 (left). The C_{1s} spectra show that the main peak is shifted to lower BE by the argon plasma treatment, probably due to the removal of chlorine.

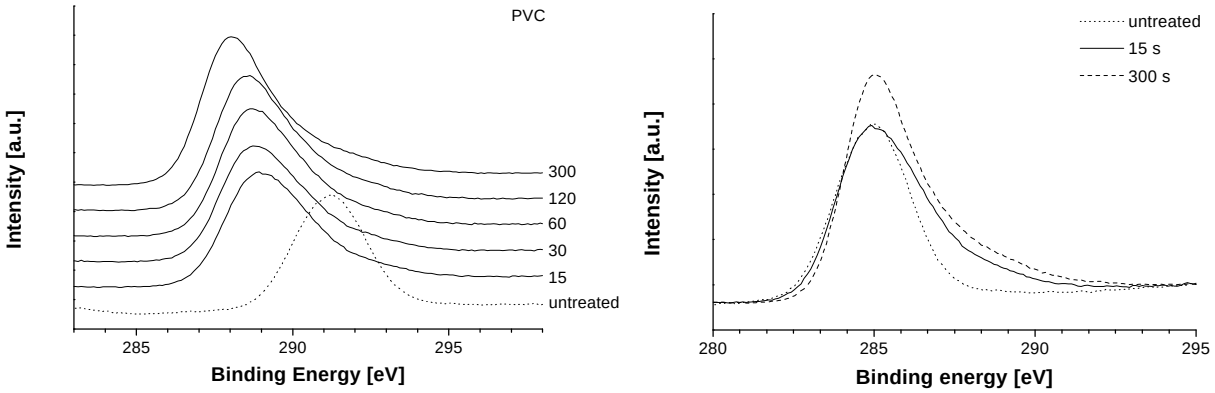

Figure 3.3. Left: XPS C_{1s} spectra of untreated (dotted line) and continuously argon plasma treated PVC samples. Charging effects were corrected by setting the Cl_{2p} peak at 202 eV. The numbers refer to the treatment time (s). Right: XPS C_{1s} spectra of untreated (dotted line), 15 s argon plasma treated (solid line) and 300 s argon plasma treated (dashed line) PVC samples. The maximum of the C_{1s} peaks was set at 285 eV.

The removal of the chlorine groups affects the position of the C_{1s} peak in two ways. First, due to the presence of chlorine, the carbon atoms only attached to carbon in PVC already show a shift of 0.7 eV compared to carbon atoms in, for example, polyethylene.[43] This gives rise to a shift when chlorine is removed. Furthermore, when chlorine is removed from the surface, the contribution to the (combined) C_{1s} peak of carbon atoms attached to chlorine will diminish and the maximum of the C_{1s} peak will shift to lower BE. Broadening of the C_{1s} peak upon longer plasma treatment times is illustrated by setting the maximum of the C_{1s} peaks at 285 eV (Figure 3.3, right).

On the argon plasma treated PVC samples, an oxygen content of 15-17% is found, almost independent of treatment time. The nitrogen content increases with treatment time (0% - 4%). Several processes may result in the observed oxygen and nitrogen contents. Most probably, oxygen is incorporated by a post-treatment reaction between air and long living radicals in

the PVC films.[9,10] Nitrogen probably originates from contaminations in the reactor that react with nitrogen (and oxygen) during the air plasma cleaning of the reactor. Upon subsequent argon plasma treatment, nitrogen is liberated and becomes an active plasma species. Other possibilities are that the incorporation of oxygen and nitrogen results from an air leak in the system or that the oxygen incorporation results from adsorbed water being desorbed during the argon plasma treatment. However, the C_{1s} peak (Figure 3.3, right) is only slightly broadened by the argon plasma treatment, indicating the formation of C-OH groups that are expected from a post-treatment reaction between radicals and air.[43] Higher degrees of oxidation (e.g., carbonyl and carboxylic acid groups) and a corresponding broader C_{1s} peak would be expected when water or air was present during the argon plasma treatment. Thus, the post-treatment oxidation reaction seems to be the major cause for the observed oxygen incorporation.

Table 3.2. Chemical composition (determined with XPS) of untreated and continuously argon plasma treated PAAc and PVC films after derivatisation with Br_2 (n = 1).

Sample	**O (%)**	**Cl (%)**	**Br (%)**
PAAc, untreated	37.6	-	0.2
PVC, untreated	0.6	27.8	0.8
PAAc, 5 min Ar	17.1	-	5.9
PVC, 5 min Ar	18.7	1.5	7.3

Both untreated and argon plasma treated PAAc and PVC films were derivatised with Br_2 in order to detect unsaturated bonds. The results are summarised in Table 3.2. For both polymers, a significant increase in bromine content is observed after argon plasma treatment. From the amount of incorporated bromine, it can be calculated that for argon plasma treated PAAc about 7.7% of the carbon atoms is present in unsaturated C=C bonds, assuming that no side reactions have taken place. For argon plasma treated PVC this amount is about 10%. The slightly lower oxygen and chlorine contents after plasma treatment and derivatisation compared to those found without derivatisation (see Figure 3.1) can be explained by the fact that an extra element is taken into account in the calculations of the atomic concentrations.

The measuring depth of the XPS technique is about 100 Å. Therefore, only information about the chemical composition of the uppermost surface is obtained. Reflectance FTIR was used to investigate the chemical structure of the whole layer. A FTIR spectrum was taken before and after argon plasma treatment. The absorption spectrum of the untreated sample was subtracted from the absorption spectrum of the plasma treated sample. In this way, the net effect of the argon plasma treatment is made visible. These "difference" FTIR spectra of argon plasma treated PAAc are depicted in Figure 3.4 together with the spectrum of the untreated polymer. The absorption bands visible in the FTIR spectrum of untreated PAAc (Figure 3.4, left) can be assigned to aliphatic CH_2 groups (2930, 2850, 1450, and 780 cm^{-1}) and COOH groups (3200-3000, 1740, and 1250 cm^{-1}). In the difference spectra of argon plasma treated PAAc (Figure 3.4, right) these absorption bands are also visible as negative absorption bands. The intensity of all absorption bands in the spectrum decreases with increasing treatment time. Furthermore, no new absorption bands develop upon argon plasma treatment. Since the thickness of the spin-coated PAAc layer is below the measuring depth, this means that the PAAc layer is removed (i.e., etched) by the argon plasma treatment. The etching of PAAc was shown to be caused by the UV light generated by the argon plasma.[28,29] Oxidative chain scission processes, induced by the liberated oxygen-containing species in the plasma phase may also cause etching.[24,25]

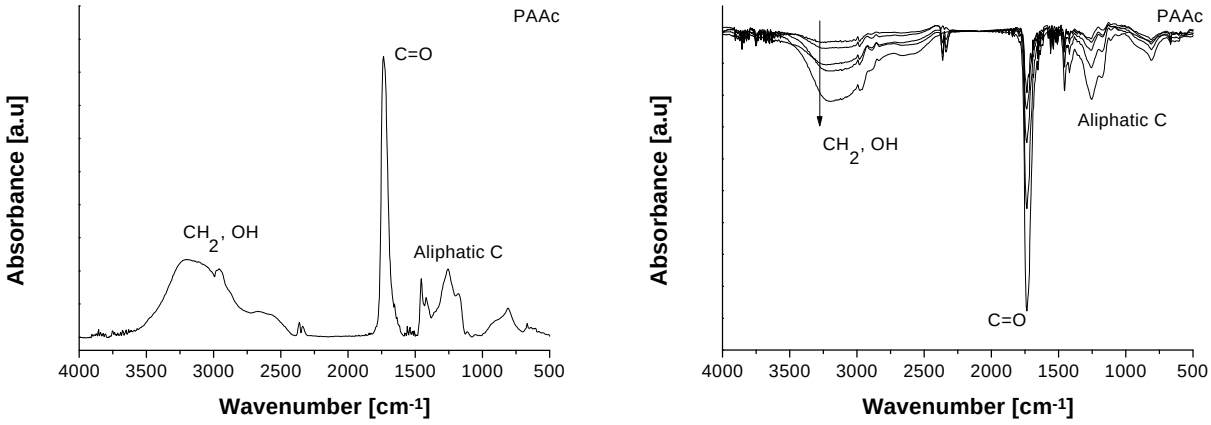

Figure 3.4. Left: Absorption FTIR spectrum of untreated PAAc. Right: Difference FTIR spectra of argon plasma treated PAAc samples, calculated by subtracting the absorption spectrum of the untreated sample from that of the treated sample. The arrow indicates the direction of increasing treatment time (15, 30, 60, 120, and 300 s).

The absorption bands in the FTIR spectrum of untreated PVC (Figure 3.5, left) can be assigned to aliphatic CH_2 groups (2975, 2910, 1430, and 970 cm^{-1}) and C-Cl groups (695 and 617 cm^{-1}). For the argon plasma treated PVC samples some details of the difference FTIR spectra are pointed out (Figure 3.5, right). With increasing treatment time, the absorption bands at 2975 and 2910 cm^{-1} and at 695, 667, and 617 cm^{-1} decrease in intensity. These correspond to CH_2 groups next to C-Cl groups and C-Cl groups, respectively. Furthermore, some new absorption bands develop at 3020 cm^{-1} and at 2930, 2890, and 2860 cm^{-1}. These can be assigned to C=C-H and aliphatic CH_2 groups, respectively. From the FTIR spectra, it can be calculated that after 300s about 80% of the chlorine is removed. In combination with the XPS results (90% removed after 300 s, see Figure 3.1), it can be concluded that chlorine is removed evenly throughout a layer of at least 0.25 μm. At this depth, only the UV light emitted by the argon plasma can be responsible for the removal of chlorine. Other plasma species (e.g., ions, electrons) do not have sufficient energy to penetrate that far into the polymer.

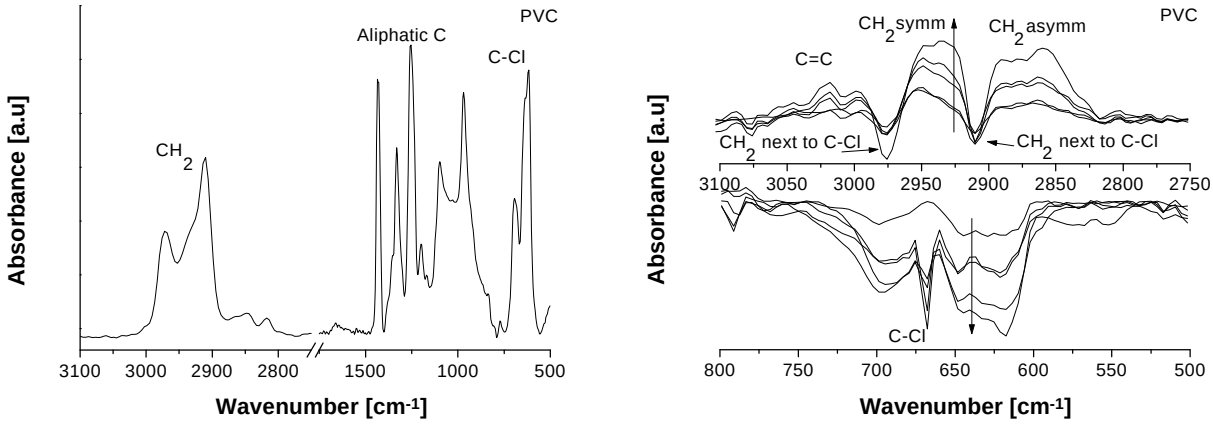

Figure 3.5. Left: Absorption FTIR spectrum of untreated PVC. Right: Details in the C-H and C-Cl absorption region of difference FTIR spectra of argon plasma treated PVC samples, calculated by subtracting the absorption spectrum of the untreated sample from that of the treated sample. The arrows indicate the direction of increasing treatment time (15, 30, 60, 120, and 300 s).

In Figure 3.6, the intensities of absorption bands corresponding to some characteristic groups of PAAc (CH_2 and C=O) and PVC (CH_2 and C-Cl) after argon plasma treatment are plotted relative to the intensities of the same absorption bands before argon plasma treatment. Figure 3.6 clearly shows that both backbone CH_2 and pendant carboxylic acid groups are removed from PAAc by the argon plasma treatment (i.e., etching). In the case of PVC, the

removal of chlorine is more preferential. Only chlorine is removed while the concentration of backbone CH_2 groups is almost constant.

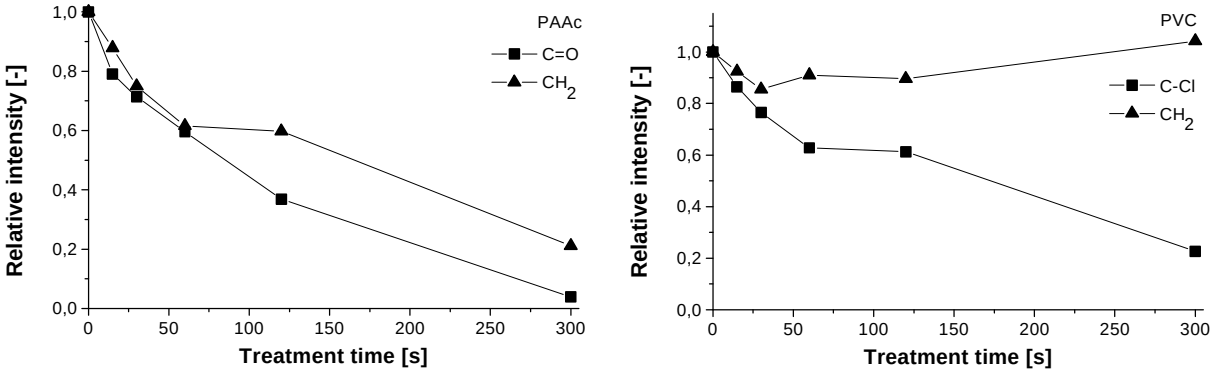

Figure 3.6. FTIR absorption band intensities of carbonyl (C=O, 1740 cm^{-1}), methylene (CH_2, 2910 cm^{-1}) and chlorine (C-Cl, 617 cm^{-1}) groups of argon plasma treated PAAc (left) and PVC (right) samples, relative to the intensities of the corresponding absorption bands of the untreated samples, as a function of treatment time.

From literature, it is known that upon (argon) plasma treatment of polymers cross-linking may occur.[3,24,44] The cross-linked layer is usually not soluble in the solvent for the unmodified polymer. To get an indication of the thickness of the modified layer, the argon plasma treated PAAc and PVC films were extracted with methanol and THF, respectively. The thicknesses of the insoluble layers were calculated from the obtained masses of the residual insoluble fractions using Equation 3.1 and are depicted in Figure 3.7 as a function of treatment time.

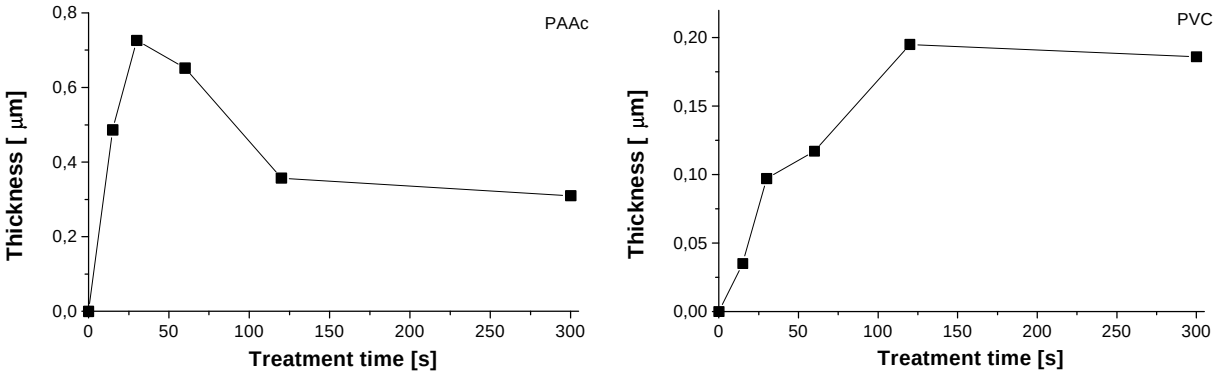

Figure 3.7. Thicknesses (calculated by Equation 3.1) of the insoluble layers (obtained by extraction) of continuously argon plasma treated PAAc (left) and PVC (right) films as a function of treatment time (n = 1).

For PAAc, the thickness of the insoluble layer reaches a maximum after which it decreases again. For longer treatment times, it seems to level off to 0.3 μm. The insolubility of the layer is most probably caused by cross-linking, although the formation of unsaturated bonds, as observed with derivatisation XPS, may also lower the solubility. The course of the thickness of the insoluble layer with plasma treatment time indicates that in the early stages of the plasma treatment mainly modification is taking place. The results of the pulsed treatments (Figure 3.1) suggest that the pendant carboxylic acid groups are removed in the early stages of the treatment. This results in the formation of unsaturated bonds and cross-links. However, upon prolonged continuous treatment, the released oxygen-containing species cause ablation of this modified layer. Eventually, an equilibrium between modification and ablation (i.e., a surface renewal) seems to be reached. The thickness of the insoluble layer of argon plasma treated PVC initially increases with treatment time and levels off to 0.19 μm at longer treatment times. This again shows that UV light emitted by the argon plasma is the main cause for the modification.

Information about the chemical structure of the insoluble fractions of the argon plasma treated samples is obtained with FTIR. In Figure 3.8, the spectra of the insoluble fractions of argon plasma treated PAAc and PVC are compared with the spectra of the untreated polymers. The spectrum of the insoluble fraction of argon plasma treated PAAc is similar to that of the untreated polymer. The absorption band at 1740 cm^{-1} (C=O) is somewhat decreased in intensity. Furthermore, a broad absorption band around 3250 cm^{-1} is observed, which can be ascribed to both OH groups and water absorbed by the KBr. The possible formation of OH groups is in good agreement with the broadening of the main peak in the C_{1s} spectra (Figure 3.2, left). In literature, an oxidation sequence for polyethylene is proposed[1,24,25] in which, first, alcohol groups are formed that oxidise further to carbonyl and carboxylic acid groups. Eventually, these carboxylic acid groups are etched off of the surface. Therefore, the formation of OH groups, together with the resemblance of the FTIR spectra of pristine PAAc and the insoluble fraction of argon plasma treated PAAc, is also consistent with the proposed equilibrium between modification and ablation.

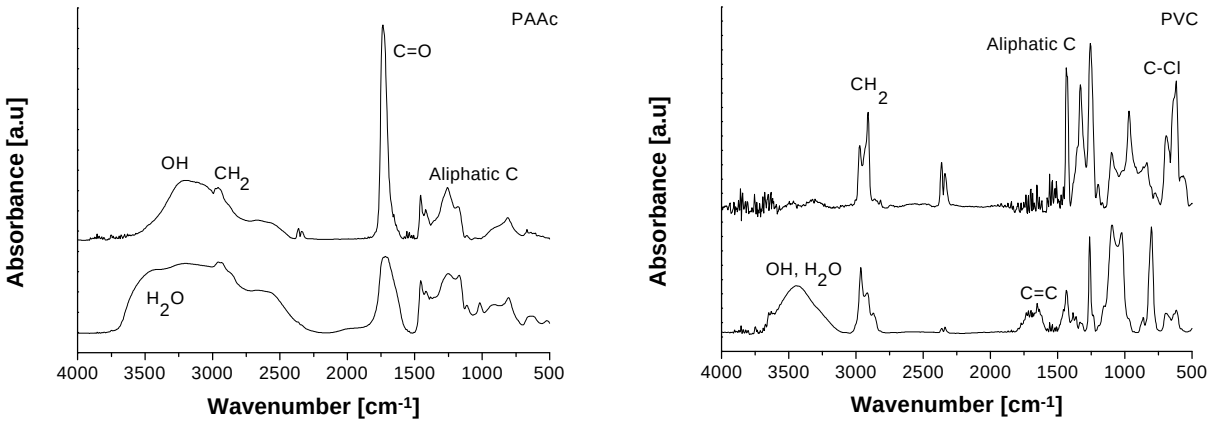

Figure 3.8. FTIR spectra of untreated (upper curve) and the insoluble fraction (lower curve, obtained by extraction, KBr pellet) of continuously argon plasma treated (300 s) PAAc (left) and PVC (right) samples.

The spectrum of the insoluble fraction of argon plasma treated PVC is markedly different from the spectrum of the untreated polymer. The chlorine absorption bands at 617 and 695 cm^{-1} have disappeared, and a new absorption band appears at 1600 cm^{-1}, which can be assigned to unsaturated bonds. Around 3400 cm^{-1}, a broad absorption band is observed, which is probably due to water absorbed by KBr. The changes in the 3000-2750 cm^{-1} region are the same as in Figure 3.5. The small absorption band around 1700 cm^{-1} indicates that the insoluble fraction is only slightly oxidised. Considering the high oxygen content measured with XPS (Figure 3.1, right), this implies that oxidation only takes place at the outermost top-layer. This is in good agreement with the proposed cause for the observed oxidation.

^{13}C SSNMR is a valuable technique to detect unsaturated and aliphatic bonds. Therefore, the insoluble fraction of argon plasma treated PVC was characterised with SSNMR (Figure 3.9). In Figure 3.9, the signals of untreated PVC (46.8 and 57.1 ppm) are also visible in the spectrum of the insoluble fraction. Furthermore, two additional peaks can be observed. The peak around 130 ppm can be assigned to main-chain unsaturation. The peak at 30.7 ppm originates from either carbon atoms incorporated in cross-links or from carbon atoms next to unsaturated C=C bonds. The oxidation found with XPS (cf. Figure 3.1, right) is not visible in the SSNMR spectra of the insoluble fraction of argon plasma treated PVC (absence of peaks between 200 and 250 ppm). It can therefore be concluded that only the outermost layer is oxidised. This is consistent with the proposed mechanism of oxidation.

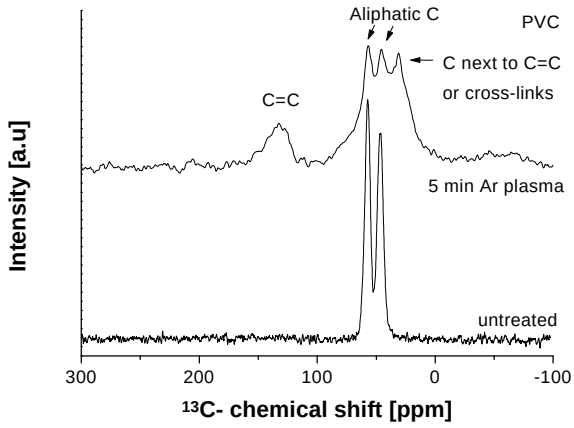

Figure 3.9. ^{13}C SSNMR spectra of untreated (lower curve) and the insoluble fraction (upper curve, obtained by extraction) of continuously argon plasma treated (300 s) PVC films.

The used NMR technique (CP-MAS) does not allow the calculation of absolute concentrations from the peak intensities. The low mobility of the system increases the intensity of signals coming from carbon atoms close to cross-links, whereas the reduced number of hydrogen atoms decreases the intensity of these signals because these structures have fewer protons than PVC. The latter effect is the most important. Taking these effects into account, the percentage of carbon atoms incorporated in unsaturated bonds was estimated to be at least 15%. This is higher than was found with derivatisation XPS and is probably due to the oxidation of the outermost top-layer that has a more pronounced effect on the XPS results than on the SSNMR results.

Conclusions

Argon plasma treatment of vinyl polymers results in the introduction of unsaturated carbon-carbon bonds in combination with the formation of cross-links. A prerequisite for the introduction of unsaturated carbon-carbon bonds is that the pendant group is easily removed from the backbone and is nonetching as a plasma component.

Acknowledgements

The authors thank R. Winters from University of Leiden (Leiden, the Netherlands) for performing and evaluating the SSNMR measurements and A. v.d. Berg from the MESA Institute (Enschede, the Netherlands) for useful discussions about and the support with the XPS measurements.

References

[1] Kang, E. T.; Kato, K.; Uyama, Y.; Ikada, Y. *J. Mater. Res.* **1996**, *11*, 1570-1573.

[2] Yun, H. K.; Cho, K.; Kim, J. K.; Park, C. E.; Sim, S. M.; Oh, S. Y.; Park, J. M. *J. Adhes. Sci. Technol.* **1997**, *11*, 95-104.

[3] Nihlstrand, A.; Hjertberg, T.; Johansson, K. *Polymer* **1997**, *38*, 3581-3589.

[4] Nihlstrand, A.; Hjertberg, T.; Johansson, K. *Polymer* **1997**, *38*, 3591-3599.

[5] Gheorghui, M.; Arefi, F.; Amouroux, J.; Placinta, G.; Popa, G.; Tatoulian, M. *Plasma Sources Sci. Technol.* **1997**, *6*, 8-19.

[6] Iriyama, Y.; Ikeda, S. *Polym. J.* **1994**, *26*, 109-111.

[7] Dewez, J. L.; Humbeek, E.; Evereart, E.; Doren, A.; Rouxhet, P. G. *Polym. Surf. Interf.* **1991**, 463-474.

[8] Baalmann, A.; Vissing, K. D.; Born, E.; Gross, A. *J. Adhes.* **1994**, *46*, 57-66.

[9] Fozza, A.; Roch, J.; Klemberg-Sapieha, J. E.; Kruse, A.; Holländer, A.; Wertheimer, M. R. *Polym. Prepr.* **1997**, *38*, 1097-1098.

[10] Holländer, A.; Klemberg-Sapieha, J. E.; Wertheimer, M. R. *Surf. Coat. Technol.* **1995**, *74-75*, 55-58.

[11] Holländer, A.; Klemberg-Sapieha, J. E.; Wertheimer, M. R. *J. Polym. Sci. Part A: Polym. Chem.* **1996**, *34*, 1511-1516.

[12] Holländer, A.; Behnisch, J. *Polym. Prepr.* **1997**, *38*, 1051-1052.

[13] Shaban, A. M. *Mater. Letters* **1995**, *22*, 309-312.

[14] Park, Y. H.; Jeon, Y. J.; Lee, Y.; Baik, D. H.; Son, Y. *Mol. Cryst. Liq. Cryst.* **1996**, *280*, 193-198.

[15] Doblhofer, K.; Nölte, D.; Ulstrup, J. *Ber. Bunsen-Ges. Phys. Chem.* **1978**, *83*, 403-408.

[16] Dai, L.; Mau, A. W. H.; Gong, X.; Griesser, H. J. *Synth. Met.* **1997**, *85*, 1379-1380.

[17] Collaud, M.; Groening, P.; Nowak, S.; Schlapbach, L. In *Polymer surface modification: relevance to adhesion*; Mittal, K. L., Ed.; VSP: Utrecht, **1996**, pp 87-99.

[18] d'Agostino, R. Plasma deposition, treatment, and etching of polymers; Academic Press: Boston, **1990**.

[19] Darque-Ceretti, E.; Puydt, Y. d.; Repoux, M.; Pascal, J. *Surf. Modif. Technol.* **1995**, *8*, 240-244.

[20] *Techniques and applications of plasma chemistry*; Hollahan, J. R.; Bell, A. T., Ed.; John Wiley & Sons: New York, **1974**.

[21] Yasuda, H. *Plasma polymerization*; Academic Press: Orlando, **1985**.

[22] Kampfrath, G.; Duschl, D.; Hamann, C.; Finster, J. *Proc. Annu. Int. Conf. Plasma Chem. Technol.* **1986**, 81-89.

[23] Terlingen, J. G. A. Introduction of functional groups at polymer surfaces by glow discharge techniques; University of Twente: Enschede, **1993**.

[24] Takens, G. A. J. Functionalization of polymeric surfaces by oxidative gas plasma treatment; University of Twente: Enschede, **1997**.

[25] Takens, G. A. J.; Terlingen, J. G. A.; Engbers, G. H. M.; Feijen, J. *12th Intern. Symp. Plasma Chem.*; Herberlein, J. V., Ernie, D. W. and Roberts, J. F., Ed.: Minneapolis, Minnesota, **1995**; Vol. 1, pp 33-38.

[26] Lens, J. P. Gas plasma immobilization of surfactants to improve the blood compatibility of polymeric surfaces; University of Twente: Enschede, **1996**.

[27] Lens, J. P.; Terlingen, J. G. A.; Engbers, G. H. M.; Feijen, J. *J. Polym. Sci. Part A: Polym. Chem.* **1998**, *36*, 1829-1846.

[28] Terlingen, J. G. A.; Hoffman, A. S.; Feijen, J. *J. Appl. Polym. Sci.* **1993**, *50*, 1529-1539.

[29] Terlingen, J. G. A.; Takens, G. A. J.; Gaag, F. J. v. d.; Hoffman, A. S.; Feijen, J. *J. Appl. Polym. Sci.* **1994**, *52*, 39-53.

[30] Zahran, A. H.; Hegazy, E. A.; Eldin, F. M. E. *Radiat. Phys. Chem.* **1985**, *26*, 25-32.

[31] Arakawa, K.; Seguchi, T.; Yoshida, K. *Radiat. Phys. Chem.* **1986**, *27*, 157-163.

[32] Dakin, V. I.; Egorova, Z. S.; Karpov, V. L. *Khim. Vys. Energ. (transl.)* **1977**, *11*, 378-379.

[33] Dakin, V. I.; Dachenko, A. V.; Karpov, V. L. *Polym. Sci. USSR* **1984**, *26*, 2473-2479.

[34] Burillo, G.; Ogawa, T. *Radiat. Phys. Chem.* **1985**, *25*, 383-388.

[35] Kwei, K. S. *J. Appl. Polym. Sci.* **1968**, *12*, 1543-1550.

[36] Sobue, H.; Tabata, Y.; Tajima, Y. *J. Polym. Sci.* **1958**, *27*, 596-597.

[37] Davenas, J.; Tran, V. H.; Boiteux, G. *Synth. Met.* **1995**, *69*, 583-584.

[38] Venkatesan, T.; Forrest, S. R.; Kaplan, M. L.; Murray, C. A.; Schmidt, P. H.; Wilkens, B. J. *J. Appl. Phys.* **1983**, *54*, 3150-3153.

[39] Lindberg, K. A. H.; Vesely, D.; Bertilsson, H. E. *J. Mater. Sci.* **1985**, *20*, 2225-2232.

[40] Golub, M. A. *Langmuir* **1996**, *12*, 3360-3361.

[41] *Polymer Handbook*; Brandup, J.; Immergut, E. H., Ed.; John Wiley & Sons: New York, **1991**.

[42] Briggs, D.; Seah, M. P. *Practical surface analysis*; 2nd ed.; John Wiley & Sons: New York, **1986**; Vol. 1.

[43] Beamson, G.; Briggs, D. *High resolution XPS of organic polymers*; John Wiley & Sons: New York, **1992**.

[44] Poncin-Epaillard, F.; Vallon, S.; Drévillon, B. *Macromol. Chem. Phys.* **1997**, *198*, 2439-2456.

4

Pulsed plasma polymerisation of thiophene*

Highly transparent (> 80%) and conductive layers (10^{-6} S/cm) were obtained by pulsed plasma polymerisation of thiophene. The influence of power, pressure, pulse time, duty cycle, and position in the reactor on the conductivity of the resulting plasma polymerised thiophene layers was evaluated. In the used ranges, only pressure had a significant influence on the conductivity of the deposited layer. The results could be correlated to the effect of the deposition parameters on the fragmentation of the thiophene monomer. At high pressure there was less fragmentation of thiophene, resulting in a higher conductivity of the layer. It was shown that the use of a pulsed plasma as a means to minimise fragmentation is most efficient when the off time is chosen such that the reactor is replenished with new monomer during the off period.

Introduction

Materials that combine conductivity with polymeric properties such as flexibility and processability can be used in a number of applications, e.g., polymeric batteries, flexible LCD's, and antistatic coatings.[1-6] For a polymer to be conductive, a conjugated system is required. For example, polythiophene is known for its high (10^3 S/cm) and stable conductivity.[7-10] Due to the nature of the conjugated system, conductive polymers are nontransparent and intractable, which is also the case for polythiophene.[11] Several authors investigated the effect of the length of the conjugated sequences in polythiophene on conductivity. For instance, ten Hoeve *et al.* found that an oligomer with 11 thiophene units has the same conductivity as polythiophene with a higher molecular weight.[12] Garnier *et al.* found that relatively short oligomers of thiophene show many of the properties of the polymer.[13] The carrier mobility and the conductivity increase with increasing conjugation length up to the hexamer of thiophene.

For certain applications where conductivity is necessary, the transparency is of major importance (e.g., antistatic coatings on photographic films, LCD's) and should generally be higher than 90%. By 'dilution' of the conductive polymer with a transparent phase the transparency can be increased, but usually this will also result in a decrease in conductivity. Some of the applications where transparency is needed require only a low conductivity. For instance, antistatic coatings should have a surface conductivity of 10^{-6} - 10^{-11} S. Several methods are available for the dilution of polythiophene, for example grafting of alkyl side

* The work described in this chapter has been published in Groenewoud *et al., Langmuir*, **2000**, *16*, 6278-6286.

chains onto the conjugated backbone,[14,15] block-copolymerisation[16] or blending with a transparent polymer,[17,18] and making composites by polymerisation of thiophene absorbed in an insulating polymer.[19] Furthermore, very thin layers of polythiophene can be deposited by electrochemical procedures[14] and plasma polymerisation.[20-26] The latter technique offers the possibility to obtain very thin, pinhole-free layers that adhere tightly to almost any substrate, without the use of solvent.[27,28] Sadhir *et al.* prepared plasma polymerised thiophene (PPT) layers using argon as an initiator (4 W, 0.1 mbar, coil configuration). After overnight doping with iodine, conductivities ranging from 10^{-6} to 10^{-4} S/cm were obtained. Films deposited at positions away from the high RF-flux region (i.e., away from the coil) showed a higher conductivity than films deposited near the coil.[21-23] Tanaka *et al.* investigated the effect of plasma frequency (AF vs. RF, bell jar configuration) on the conductivity of argon-initiated PPT layers. Although Fourier transform infrared (FTIR) measurements did not indicate the presence of thiophene rings in the layers, conductivities ranging from 10^{-3} S/cm (AF, 100 W) to 10^{-4} S/cm (RF, 25 W) were found after 5 hrs doping with iodine.[20] In situ doping was carried out by Giungato *et al.*, using a mixture of argon, thiophene, and iodine (5 W, 0.67 mbar, two internal electrodes). On the basis of FTIR measurements it was concluded that, although fragmentation had taken place during deposition, the thiophene ring was preserved to some extent in the PPT layer. A conductivity of 10^{-5} S/cm was obtained for the PPT layers, without additional doping.[25] Depositions at atmospheric pressure were carried out by Tanaka *et al.* using helium as diluent.[24] A higher conductivity was observed for PPT layers containing more conjugation.

In the studies cited above, noble gases were used as initiators to prepare PPT layers with an enhanced preservation of the monomer structure. The authors hypothesised that this improves the conductivity of the resulting PPT layer. From literature it is known that pulsed plasma polymerisation in general results in a higher retention of the monomer structure than continuous wave (CW) plasma polymerisation.[29-33] Therefore, an alternative method to preserve the monomer structure in the PPT layer may be the application of a pulsed plasma. To our knowledge, no pulsed plasma polymerisation of thiophene has been reported until now. Furthermore, the transparency of the PPT layers and the effect of plasma deposition parameters on the preservation of the monomer structure in the PPT layers have not been studied in detail.

In the present study, a pulsed plasma is used to obtain transparent and conductive PPT layers. The effect of different deposition parameters (power, pressure, pulse time (t_{on}), duty

cycle ($t_{on}/(t_{on} + t_{off})$), and substrate position in the reactor) on the electrical properties of the PPT layers after iodine doping is evaluated. X-ray induced photoelectron spectroscopy (XPS) and FTIR are used to get insight into the relation between chemical composition/structure and the electrical properties of the PPT layers. The plasma phase is characterised using mass spectrometry (MS) and optical emission spectroscopy (OES). The transparency of the deposited PPT layers is determined with ellipsometry.

Experimental

Materials. Thiophene (99.5 % purity) was purchased from Merck (Darmstadt, Germany). All solvents were of analytical grade purity and were also purchased from Merck. Water used was doubly deionised. All chemicals were used as received. Glass slides (∅ 2.5 cm, used for FTIR analysis) with a sputtered chromium and gold layer were obtained from the FFW division (University of Twente, Enschede, the Netherlands). Glass slides (∅ 1.5 cm, used for XPS analysis) were purchased from Knittel (Braunschweig, Germany). The samples used for the conductivity measurements (glass slides with four electrodes with extensions to contact areas for the measurement leads) were supplied by the MESA Institute (University of Twente, Enschede, the Netherlands). 2,2',5',2"-terthiophene (T_3) was synthesised according to literature and had the characteristics reported therein (mp 92.3-93.5 °C, ^{13}C NMR ($CDCl_3$) after recrystallisation from n-heptane: 137.1 (2,2"), 136.2 (2',5'), 127.9 (4,4"), 124.5 (5,5"), 124.3 (3',4'), 123.7 (3,3") ppm).[34,35]

Cleaning. All glassware, substrates, and tools were cleaned ultrasonically consecutively three times in toluene, hexane, acetone, water, and acetone and subsequently dried *in vacuo* at room temperature (RT).

Plasma polymerisation. A schematic picture of the plasma apparatus is shown in Figure 4.1. In short, it consists of a tubular glass reactor (length 1.5 m, internal diameter 10 cm) with three externally placed, capacitively coupled electrodes. The powered (hot) electrode was placed in the centre of the reactor. The grounded (cold) electrodes were placed at 30 cm on either side of the hot electrode. The flow of monomer vapour through the reactor was calculated from the rate of the pressure increase in the reactor, once pumping of the reactor was stopped, assuming ideal gas behaviour. Mass flow controllers (MKS Instruments, Andover, USA) controlled the flow of noncondensing gases.

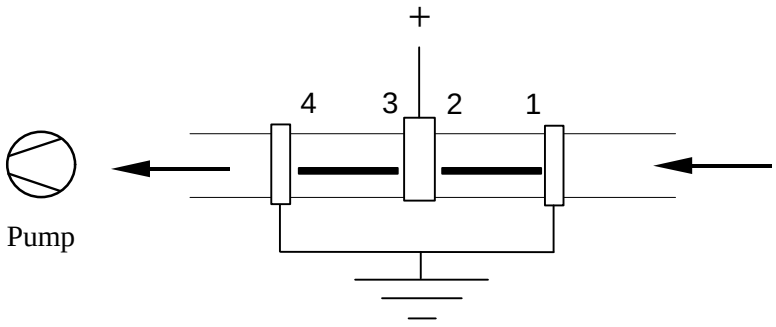

Figure 4.1. Schematic drawing of the plasma apparatus. The arrows indicate the direction of the gas flow. The thick lines represent the glass plates on which the samples are located. The numbers refer to the position of samples in the reactor.

The system (without the substrates) was first cleaned by applying an air plasma (5 sccm/min, 85 W, 0.12 mbar) for 60 min. The substrates were placed on two glass plates (see Figure 4.1 for positions), which were placed in the centre between the hot and cold electrodes, and the reactor was evacuated to < 5.10^{-3} mbar. The substrates were cleaned with an air plasma (5 sccm/min, 85 W,

0.12 mbar) for 5 min, after which the reactor was again evacuated to < 5.10^{-3} mbar. Subsequently, a monomer flow was established through the reactor, and after 2 min, pulsed plasma depositions were carried out varying in power, pressure, pulse time (t_{on}), and duty cycle ($t_{on}/(t_{on}+ t_{off})$). The total plasma "on" time was always 100 s. The pressure in the reactor was controlled by the temperature of the monomer. After deposition, the monomer flow was sustained for another 2 min and the reactor was brought to atmospheric pressure with air. The samples were stored at –18 ºC.

Characterisation of plasma phase. MS was carried out to analyse the gas composition at the outlet of the reactor. The spectrometer was a differentially pumped QMS 421 mass spectrometer (Balzers, Utrecht, the Netherlands). The pressure in the mass spectrometer was kept at 5.10^{-6} mbar using a leak valve.

OES analysis was carried out using an MCPD-1000 spectrophotometer (Otsuka, Osaka, Japan) with a slit width of 0.2 mm. The measuring probe was placed at the reactor entrance in line of sight of the plasma. Spectra were recorded from 180 to 875 nm with a step width of 2 nm.

Characterisation of PPT layers. On the samples used for the conductivity measurements the thickness of the deposited PPT layers (*d*) was determined with a profilometer (Dektak IIA, Sloan Technology Corporation, Santa Barbara, USA). During plasma deposition, the contact areas were covered with glass slides to locally prevent deposition. The needle was moved over the boundary between areas of the substrate that were covered and not covered during plasma deposition. The height difference was taken as the thickness of the deposited layer.

The conductivity of the PPT layers was determined using specially designed electrodes as substrates for deposition (configuration in accordance with ASTM D257, see Figure 4.2.A).

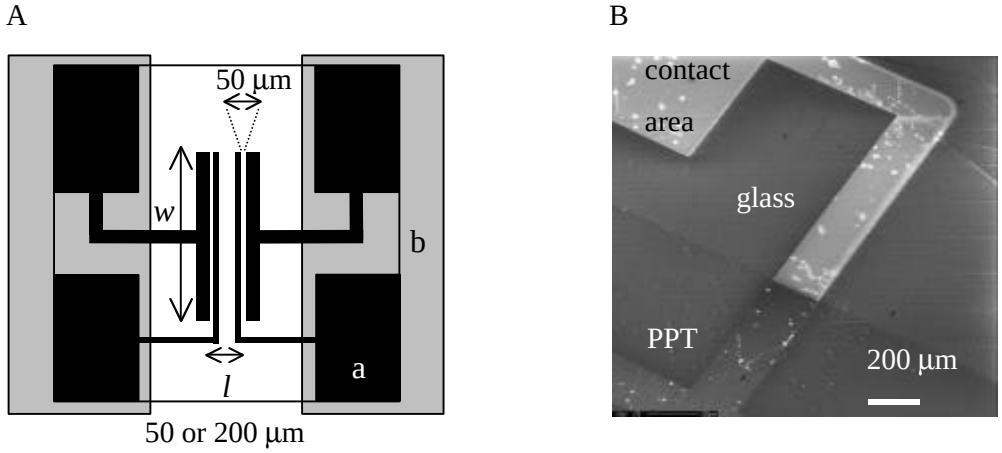

Figure 4.2. A. Schematic drawing of samples with the pre-deposited electrodes and extensions to contact areas (a) used for the conductivity measurements. During deposition the samples are partially covered by glass slides (b). B. SEM picture of a detail of a sample used for conductivity measurements, partly covered by a PPT layer.

The samples were doped by placing them in iodine vapour for 5 min. A current was applied via the outer electrodes and after 1 min the voltage drop was measured over the inner electrodes, using Keithley 617 electrometers (Keithley Instruments, Cleveland, USA).The volume and surface conductivities of the deposited layers were calculated with the following formulas:

Equation 4.1. $s_{vol} = (I/U) \cdot (l/wd)$ [S/cm]

Equation 4.2. $s_{surf} = (I/U) \cdot (l/w)$ [S]

in which s = conductivity
U = measured voltage [V]
I = applied current [A]
w = length of the electrodes [cm]
d = thickness of the PPT layer [cm]
l = distance between electrodes [cm]

For FTIR analysis, PPT layers were deposited on gold-coated glass discs (∅ 2.5 cm) and spectra were recorded using a BioRad FTS-60 (Biorad, Cambridge, UK) in the reflectance mode. A background spectrum was recorded using a clean substrate. For the FTIR analysis of T_3, this compound was mixed into a KBr pellet, and spectra were recorded in the transmission mode.

XPS analysis of PPT layers was carried out on layers deposited on glass discs (∅ 1.5 cm) using a Kratos XSAM 800 (Manchester, UK) equipped with a Mg K_α source (1253.6 eV). The analyser was placed perpendicular to the sample surface. The input power was 150 W (10 mA, 15 kV). The analysed spot size was 3 mm x 6 mm. Survey scans (1100-0 eV binding energy (BE) window) were recorded with a pass energy (PE) of 100 eV and a dwell of 0.1 s. Relative peak areas for the different elements were calculated by numerical integration of the detail scans (20 eV BE window, 50 eV PE) using empirically determined sensitivity factors. After normalisation, the concentrations of the various elements were obtained.

The transparency and the thickness of PPT layers deposited on silicon wafers were determined with ellipsometry. The instrument used was a home-built rotating polariser type (frequency 67 Hz),[36] equipped with a 75W Xe lamp and a photomultiplier. The instrument was calibrated using the residue method. An energy scan (1.5 - 4.2 eV) was made recording the ellipsometric parameters (Ψ and Δ) at an angle of incidence of 70 º. From these values the refractive index and optical absorption of the layers were calculated, which were used to derive the effective penetration depth of the incident light in the layer (d_{eff}). At d_{eff} two thirds of the incident light has been absorbed. The transparency of a deposited layer can then be calculated from the intensity of the reflected light (I) and d_{eff} via:

Equation 4.3. $$T = I/ I_0 = exp(-d/ d_{eff})$$

With T = transparency
I = intensity of reflected light at a certain wavelength
I_0 = intensity of incident light at a certain wavelength
d = thickness of the layer
d_{eff} = effective optical thickness

The surface morphology of the PPT layers was studied by Scanning Electron Microscopy (SEM) analysis using a Hitachi S-800 Field Emission SEM (6 kV, 20° tilt).

Results & Discussion

Plasma polymerisation of thiophene resulted in homogeneous and pinhole-free PPT layers, as can be seen in Figure 4.3. The thickness of the PPT layers as a function of the number of pulses was determined from the ellipsometric measurements and is shown in Figure 4.4. The optical properties of the PPT layer were modelled with a Lorentzian absorption profile. The parameters, i.e., the PPT layer thickness and the characteristic parameters for the Lorentzian profile were optimised in a non-linear fit. A linear increase with plasma “on” time is found (irrespective of the plasma “off” time), indicating that deposition only takes place during the plasma on time. Similar results were found by Uchida *et al.* for PP-acetylene layers.[37,38]

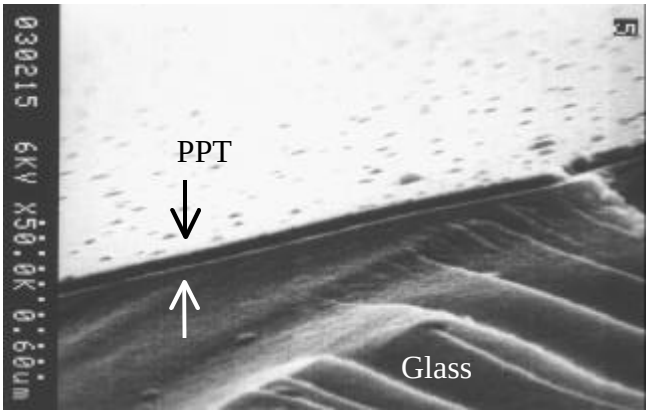

Figure 4.3. SEM picture of a 30 nm thick PPT layer deposited on glass. The small dots on the PPT layer are due to the gold sputtering used for sample preparation.

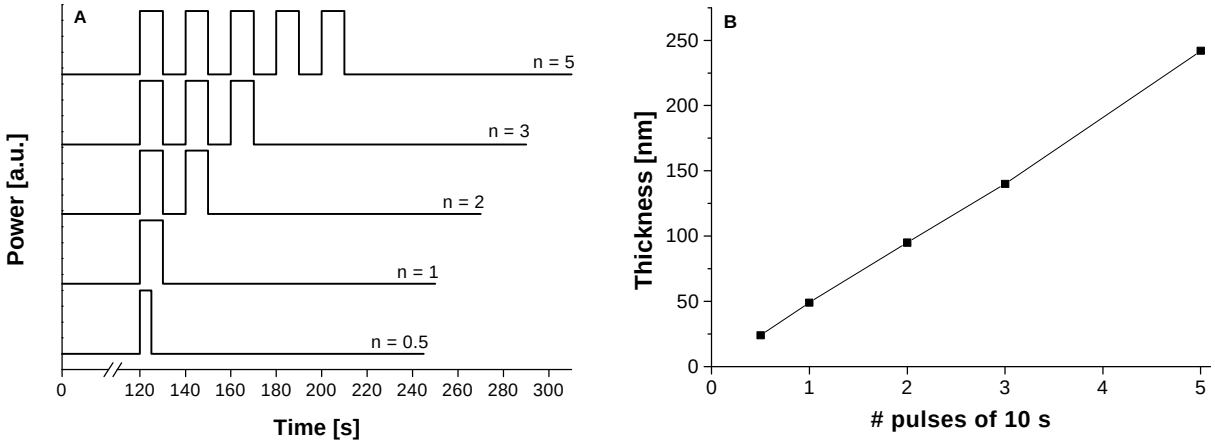

Figure 4.4. Thickness (determined by ellipsometry) of PPT layers (0.06 mbar, 115 W) as a function of the number of pulses (n) of 10 s (B). Power input as a function of time (A) for the pulsed plasma deposition of the layers used in Figure 4.4.B. Step height is 115 W.

In Figure 4.5 the course of the pressure during plasma polymerisation is depicted for different starting pressures and power inputs. In all cases, the pressure increases when a plasma is generated. The increase in pressure is larger at high power input and low starting pressure than at low power input and high starting pressure, respectively. Furthermore, the pressure is almost instantly constant at a high starting pressure, whereas at low starting pressure the pressure increases continuously during the plasma pulse.

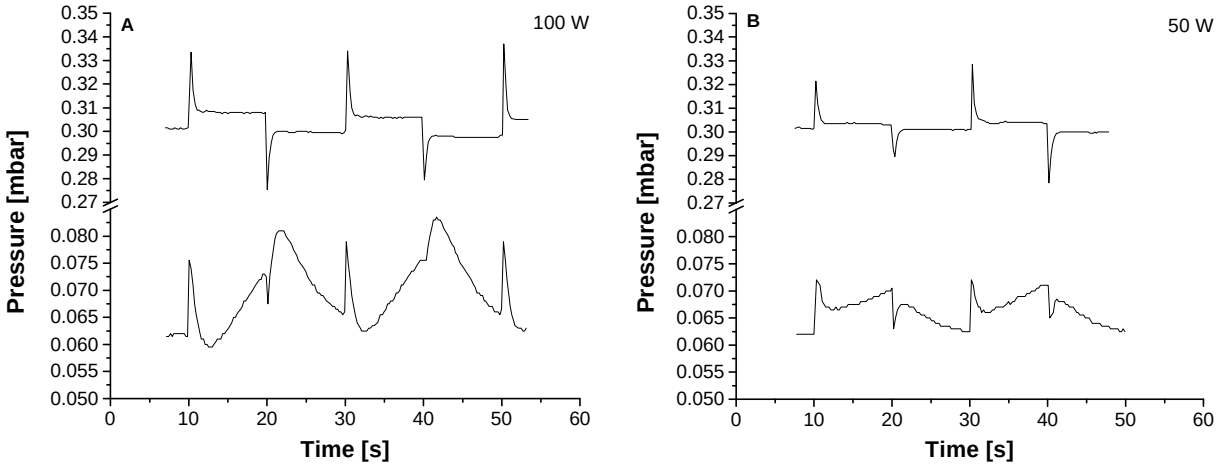

Figure 4.5. Course of the pressure in the reactor during plasma polymerisation (10 s on, duty cycle 0.5) at different initial pressures (0.3 and 0.06 mbar) at 100 W (A) and 50 W (B). The spikes in the spectra are due to turning on/shutting off the plasma.

Table 4.1 gives the increase in the number of species during the plasma on time as calculated from the pressure increase during a pulse of 10 s. It was assumed that the ideal gas law holds and that the temperature does not change during deposition. Other measurements showed that for air, CF_4, and CO_2 plasmas the temperature increase in the plasma phase is less than 10 °C for pulse times < 10 s.[39] From Table 4.1 it is clear that at high power input and low starting pressure both the relative and absolute increase in the number of species is much larger than at low power input and high starting pressure.

Table 4.1. Increase in the number of plasma species (in µmol and between brackets in % of the initial number of species, calculated from the pressure increase during the plasma pulse (Figure 4.5)) during pulsed plasma deposition (10 s on, 10 s off) at different initial pressures and power inputs.

Pressure	**100 W**	**50 W**
0.06 mbar	102 (33.6%)	41.3 (13.6%)
0.3 mbar	34.0 (2.5%)	12.1 (0.8%)

A balance over the reactor with respect to the number of species gives insight into the cause for the increase in pressure during the plasma on time. During plasma polymerisation, plasma species are brought in by flow (monomer) and are generated by fragmentation, whereas they are removed by flow, deposition, and recombination. Assuming that the flow of species in and out of the reactor is the same at a given pressure, a pressure increase means

that more species are generated by fragmentation than removed by recombination and/or deposition ("netto" fragmentation). The deposition rate increases with increasing power input and decreasing starting pressure (data not shown). Based on the fact that oligomers of thiophene are much less volatile (for instance, T_3 only sublimates and no peaks appear in the MS) it might be assumed that there is a positive relation between recombination and deposition. The larger pressure increase at high power and low starting pressure then indicates that more fragmentation takes place at high power input and low starting pressure. Furthermore, at low pressure, "netto" fragmentation is taking place continuously, whereas at high pressure an equilibrium between fragmentation and deposition/recombination is reached.

The effect of power input on the fragmentation is explained by the fact that in a RF system an increase in power input results in an increase in electron density.[40] As these electrons have sufficient energy (about 0-20 eV) to cause cleavage of covalent bonds (bond energy 3-8 eV), more electrons cause the fragmentation of more molecules. Pressure affects the plasma in several ways. First, the mean free path of plasma species will be less at higher pressure. This results in a lower average energy of the collisions (i.e., lesser degree of fragmentation). Secondly, in our case a higher pressure inherently results in a higher flow rate. This means that the residence time of the species in the plasma is decreased at higher pressure. The species are thus subjected to the plasma for a shorter time. Both effects result in a lesser degree of fragmentation.

Characterisation of the plasma phase. OES and MS were used to determine the nature of the species present in the plasma phase. In the OES spectra depicted in Figure 4.6.A, two new peaks at 257 and 265 nm respectively, appear when a plasma is applied. According to literature, light of these wavelengths is emitted by decaying excited CS species,[41] indicating that fragmentation of at least part of the thiophene molecules is taking place.

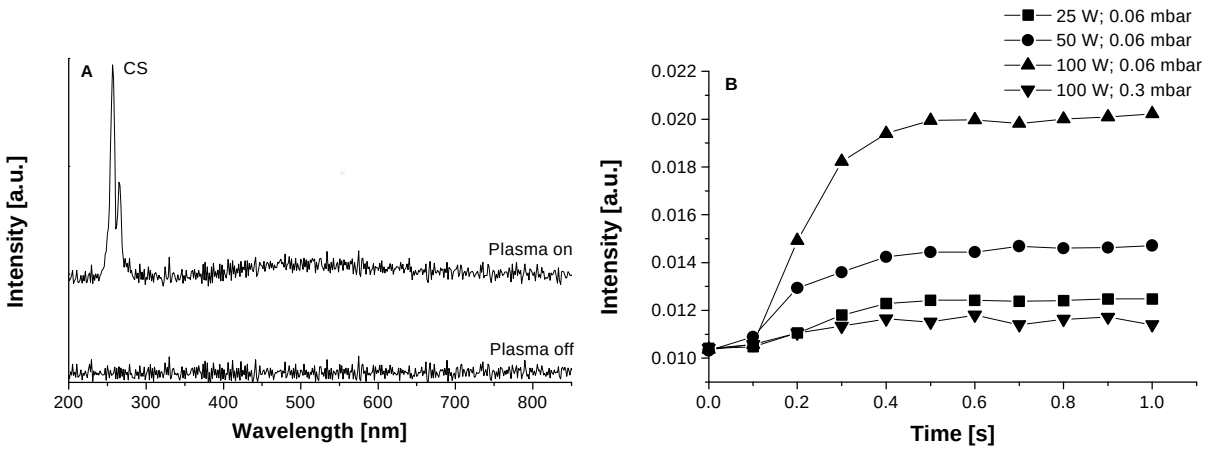

Figure 4.6. OES spectra (A) of a thiophene flow (0.06 mbar) without (bottom) and with (upper, 100 W) plasma generation. B shows the intensity of the CS peak (257 nm) at different power inputs (at 0.06 mbar) and pressures.

As was expected based on the pressure measurements, the intensity of these peaks increases with increasing power and decreasing pressure (Figure 4.6.B). The course of the CS peak in time shows that after 0.5 s the CS peak intensity reaches a plateau value, irrespective of the power input. For the high starting pressure this corresponds well with the course of the pressure during the plasma pulse (Figure 4.5). Apparently, an equilibrium between the formation and the decay of excited CS species is reached. However, at low starting pressure an increase in pressure is still observed after 0.5 s. This means that, although "netto" fragmentation still occurs (Figure 4.5), this does not result in the formation of additional excited CS species. Furthermore, Figure 4.6.B shows that short pulse times (< 0.2 s) should be used to minimise fragmentation.

Figure 4.7 shows the mass spectra of a thiophene flow through the reactor with and without plasma generation. The assignment of the peaks is summarised in Table 4.2. In the mass spectrum of a thiophene flow (without plasma generation) the most prominent peaks appear at m/e 39, 45, 58, and 84. The peak at m/e 84 can readily be assigned to the thiophene monomer. The other peaks are due to fragmentation of the thiophene molecules, which takes place in the spectrometer itself. When a plasma is generated these peaks decrease in intensity and new peaks appear in the MS spectrum, again showing that fragmentation is taking place.

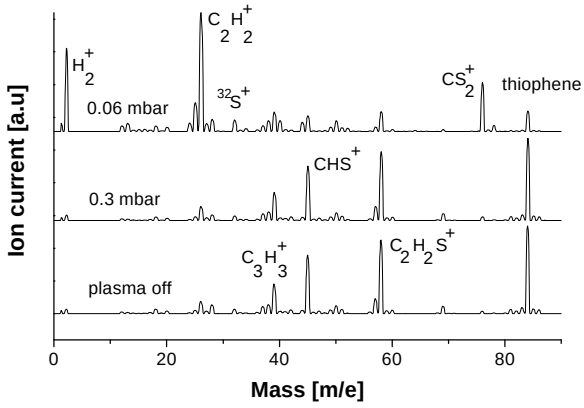

Figure 4.7. MS spectra of a thiophene flow without plasma generation (bottom) and with plasma generation (CW, 100 W) at 0.3 mbar (middle) and at 0.06 mbar (top).

Table 4.2. Peak assignment of peaks appearing (x) in the mass spectrum (range 0-225 m/e) of a thiophene flow with and without plasma generation (Figure 4.7). No peaks were observed in the range 85-225 m/e.

Peak (m/e)	Assignment	Plasma off	Plasma on
84	$C_4H_4S^+$	x	decreased
76	CS_2^+		x
58	$C_2H_2S^+$	x	decreased
45	CHS^+	x	decreased
39	$C_3H_3^+$	x	decreased
32	$^{32}S^+$		x
26	$C_2H_2^+$		x
12	C^+		x
2	H_2^+		x

In Figure 4.8, the effect of power on the decrease and increase of peaks due to plasma generation is visualised. More fragmentation occurs with increasing power input, which correlates well with the OES results.

The development of the most prominent peaks in the MS spectra in time is depicted in Figure 4.9 for two different starting pressures. At low starting pressure, the decrease of the thiophene peak and the increase of new peaks are much larger and faster than at high starting pressure. Furthermore, the peak corresponding to sulphur increases only after an “induction time”. It might be possible that sulphur is only formed at a higher degree of fragmentation.

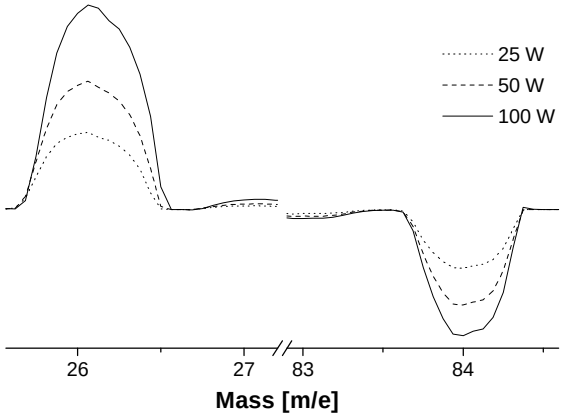

Figure 4.8. Characteristic "netto" MS peaks obtained by subtracting the mass spectrum of a thiophene flow without plasma generation from the MS spectrum of a thiophene flow with plasma generation (at different powers at 0.06 mbar).

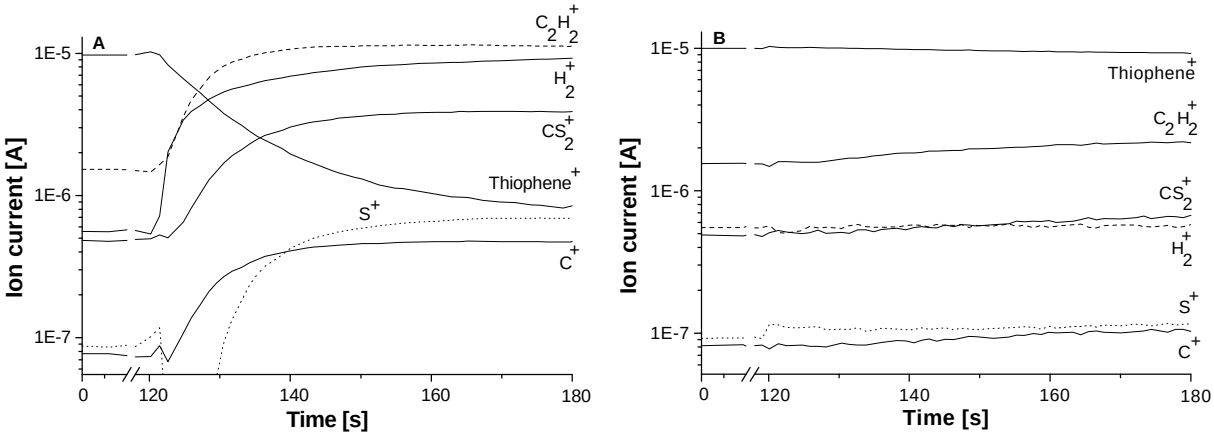

Figure 4.9. Intensity of the most prominent peaks in the MS spectrum as a function of time. A plasma (CW, 100 W) is generated at t = 120 s at a starting pressure of 0.06 mbar (A) and 0.3 mbar (B), respectively.

By definition, the ion current of a peak in a mass spectrum is related to the concentration of the species correlating with this peak via:

Equation 4.4. $$I_i = p_{ms} \,.\, c_i \,.\, S_i$$

with I_i = ion current of component i [A]

p_{ms} = pressure in the MS [mbar]

c_i = concentration of component i [-]

S_i = sensitivity factor for i [A/mbar]

As the pressure in the MS was kept constant, the course of the ion current intensity of a peak can be taken as a measure for the course of the concentration of the component correlating with this peak. For most species, absolute concentrations cannot be calculated because the sensitivity factors are not known. However, for thiophene the sensitivity factor can be calculated from the ion current of a thiophene flow without plasma generation, assuming that the thiophene concentration is 100%. In Figure 4.10 the thiophene concentration is followed during plasma generation at two different starting pressures. It shows that at high pressure, deposition takes places in an environment consisting of almost pure thiophene, whereas at low pressure the environment contains much less thiophene (and much more fragments, see also Figure 4.9).

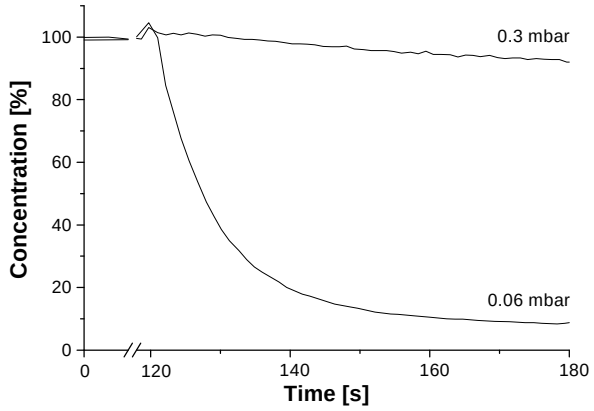

Figure 4.10. Concentration of thiophene (calculated from the ion current measured with MS) in the flow through the reactor as a function of time at two different starting pressures. A plasma (CW, 100 W) is generated at t = 120 s.

Characterisation of PPT layers. In Figure 4.2.B a detail of the samples used for the conductivity measurements is shown. The electrodes are covered by the PPT layer whereas the extensions of the electrodes are not. A good contact between the electrode extensions and the measurement leads is thus ensured. The conductivities of the iodine-doped PPT layers, summarised in Table 4.3, are much lower than the conductivity of polythiophene. This is most probably caused by the loss of conjugation due to the fragmentation of the monomer in the plasma polymerisation process.

As shown earlier, high pressures, short pulse times, high flow rates, and low power inputs result in a low amount and degree of fragmentation. Considering the fact that deposition is only taking place when a plasma is generated (see Figure 4.4), the influence of the deposition parameters on the fragmentation in the plasma phase was expected to be visible in the conductivity of the resulting PPT layers. Surprisingly, a Student's t-test revealed that only pressure has a significant effect ($P = 0.0013$) on the conductivity.

Table 4.3. Logarithm of the volume conductivities (S/cm) of PPT layers deposited under different conditions after doping in iodine vapour for 5 min. The values are averaged over positions 2-4 in the reactor using 2 samples per position ($n = 6 \pm sd$). No significant trend (Student's t-Test, $P < 0.05$) with respect to position in the reactor was observed.

Pressure (initial) (mbar)	**Power (W)**	**Pulse time (t_{on}) (s)**	**Duty cycle ($t_{on}/ (t_{on} + t_{off})$) (-)**	**Log σ_{vol} (after doping) (log S/cm)**
0.3	100	10	0.5	-5.3 ± 0.18
0.06	100	10	0.5	-7.5 ± 0.65
0.3	50	0.1	0.03	-5.6 ± 0.46
0.3	100	0.1	0.5	-5.3 ± 0.21
0.3	100	0.1	0.03	-6.2 ± 0.57

To investigate the origin of this result, the chemical structure and composition of the PPT layers were determined with FTIR and XPS, respectively.

In Figure 4.11 the FTIR spectrum of a PPT layer is compared with the spectrum of T_3. The peak assignment is summarised in Table 4.4. Several similarities between the structure of T_3 and the PPT layer can be observed. For instance, the peaks around 3100 cm^{-1} show that the monomer structure is partly preserved in the PPT layer. However, some terminal acetylene (3288 cm^{-1}) and aliphatic (2910 cm^{-1}) structures are also present, indicating that fragmentation has also occurred. Comparable spectra were obtained by Giungato *et al.* for argon-initiated PPT layers.[25]

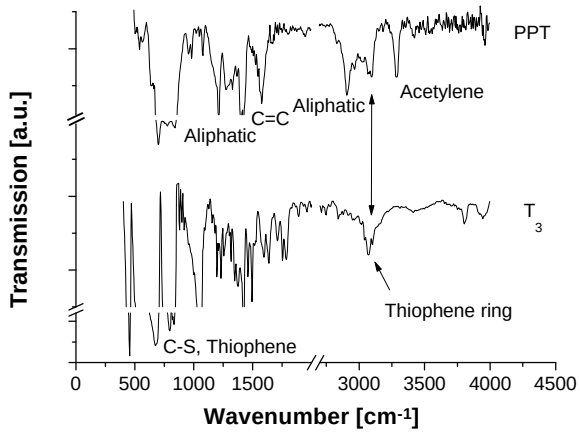

Figure 4.11. FTIR spectra of a PPT layer (top, 0.3 mbar, 50 W, 10 s on, duty cycle 0.5) and 2,2',5',2"-terthiophene (T_3) (bottom, KBr pellet).

Table 4.4. Peak assignment of peaks appearing in the FTIR spectra (see Figure 4.11) of PTT layers and 2,2',5',2"-terthiophene (T_3).[14,23,42-47]

Peak position (cm^{-1})		**Assignment**
T_3	**PPT**	
671	664	C-S
695	706	C-H, out of plane vibration, thiophene
795	784	C-H, ring vibration
834	849	C-H, out of plane deformation, thiophene
1053	-	C-H, in plane deformation, thiophene
1421	1428	C-C aliphatic or ring stretching
1594	1582	C=C
-	2832, 2910, 2972	CH_2 aliphatic
3041, 3072, 3103	3034, 3072, 3099	C=C-**H** stretch, thiophene
-	3288	C≡C-**H**

The intensities of the peaks at 3288, 3099, and 2910 cm^{-1} were used to clarify the influence of a specific deposition parameter on the structure of the resulting PPT layer. The intensities of the peaks at 3288 and 2910 cm^{-1} in the spectrum of a PPT layer deposited at a certain value (A) of a parameter (e.g., power) were normalised to the intensity of the conjugated ring peak (3099 cm^{-1}) in the same spectrum. These normalised intensities were compared with the intensities of the same peaks in the spectrum of a PPT layer deposited at different value (B) of the parameter (again normalised to the intensity of the conjugated ring peak in that spectrum). The normalised intensity ratios are shown in Figure 4.12 for all parameters. If the PPT layer only differs in thickness and the chemical structure is the same, the normalised intensity ratio

will be 1 for all three peaks.[48] Figure 4.12 shows that, in the ranges used, this is more or less the case for duty cycle, pulse time, and power. It also shows that a decrease in pressure results in a decrease of the conjugated ring structures relative to the aliphatic and terminal acetylene structures. This all correlates well with the conductivity results. It can therefore be concluded that, in accordance with the hypothesis stated earlier, the conductivity of a PPT layer increases with increasing preservation of the conjugated structure of the monomer. The most important parameter to control this is pressure (and, inherently, flow rate).

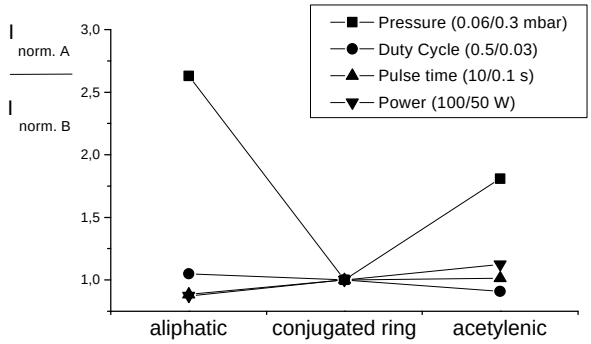

Figure 4.12. Intensity of peaks characteristic for aliphatic (2910 cm^{-1}), conjugated ring (3099 cm^{-1}) and acetylenic structures (3288 cm^{-1}) in the FTIR spectrum of a PPT layer deposited under condition A of a parameter (e.g., power) (normalised to the intensity of the peak at 3099 cm^{-1} in the spectrum) relative to the intensity of the same peaks in the FTIR spectrum of a PPT layer deposited under a different condition (B) for that parameter (again normalised to the peak at 3099 cm^{-1} in that spectrum).

The chemical composition at the surface of the PPT layers was determined with XPS. The ratio of the atom percentage of carbon over the atom percentage of a characteristic atom of the monomer (i.e., C/S ratio for a PPT layer) is often used as an indication for the preservation of the monomer in the deposited layer.[24,31,33,49-60] In our case, a C/S ratio close to that of the monomer (C/S = 4) would indicate that the monomer is incorporated in the polymer without much fragmentation. A correspondingly high conductivity would be expected. The influence of the deposition conditions and the position in the reactor on the C/S ratio of the PPT layers is depicted in Figure 4.13. Combined with Table 4.3, it shows that two samples with the same C/S ratio can show a marked difference in conductivity (cf. position 1 at low pressure and position 4 at high pressure, both at 100 W; 10 s “on”; duty cycle 0.5). Furthermore, it appears that deposition at high pressure generally results in PPT layers with a C/S ratio lower than the theoretical value for polythiophene, while the conductivity of these layers was relatively high. Apparently, a C/S ratio of 4 at the surface is not a useful indicator for the conductivity of the PPT layers.

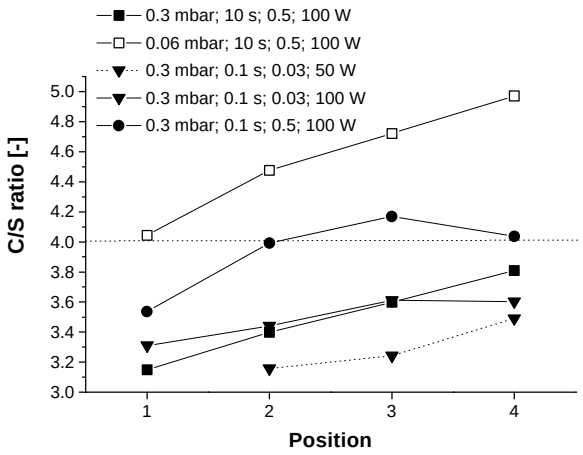

Figure 4.13. C/S ratio (determined with XPS) of PPT layers deposited under different conditions (pressure, pulse time, duty cycle, and power input) as a function of position in the reactor (n = 2, see Figure 4.1 for positions).

Most PPT layers deposited at high pressure have a C/S ratio smaller than 4. This means that at high pressure the formed species containing relatively more sulphur have a higher tendency for deposition than species containing relatively more carbon. However, at low pressure the C/S ratio is higher than 4. Apparently, the species containing relatively more sulphur formed at low pressure have a lower tendency to deposit than species containing relatively more carbon. This implies that the nature of the species formed at different pressures is different. From the FTIR, MS, and OES results it can be concluded that at low pressure the degree of fragmentation is higher than at high pressure. The OES results showed that more CS species are formed at low pressure than at high pressure. Although the MS spectra do not show a CS peak, the appearance of the CS_2^+ peak indicates that at least some of the species containing relatively more sulphur do not deposit. The induction time of the S^+ peak (Figure 4.9) shows that sulphur is formed at a later stage of the fragmentation process, i.e., when the degree of fragmentation is higher. Furthermore, at low pressure the already deposited PPT layer is more severely attacked by the plasma species. Due to the relatively labile C-S bond, more sulphur is probably liberated at low pressure than at high pressure. From these results it can be concluded that deposition under conditions which induce a higher degree of fragmentation results in PPT layers with a higher C/S ratio compared with PPT layers deposited under less fragmenting conditions.

The effect of the degree of fragmentation is also visible in the increase in C/S ratio with increasing distance from the monomer inlet. Species that deposit far away from the monomer inlet have been subjected to the plasma for a longer period of time. The degree of fragmentation is therefore higher with a correspondingly higher C/S ratio.

The effect of power on the C/S ratio is explained by the increase in electron density with increasing power input. At higher power input more electrons with sufficient energy to break the labile C-S bond attack the deposited layer. More sulphur will be liberated and a higher C/S ratio is obtained. Furthermore, the increase in electron density results in an increase in the number of collisions between electrons and other plasma species. As each collision may cause fragmentation, the degree of fragmentation will also increase, with a corresponding increase in C/S ratio.

Using longer pulse times results in a plasma resembling a continuous wave (CW) plasma. As mentioned earlier, layers deposited by a pulsed plasma show a better retention of the monomer structure than layers resulting from a CW plasma.[29,30,37] However, in our case a shorter pulse time (at the same duty cycle) results in a higher C/S ratio (i.e., higher degree of fragmentation). Apparently, the degree of fragmentation is more dependent on t_{on} then on t_{off}. This can be explained by the relation between t_{off} and the replenishing of the reactor with new monomer. The residence time (τ = volume/flow) of the monomer at 0.3 mbar in our system was around 1 s. Assuming the reactor is ideally stirred with a normal distribution of the residence time, after $t = 3\tau$, 99.9% of the total volume of the reactor will be replenished with monomer.[61,62] This means that when the off period is > 3τ, all gas phase fragments resulting from the plasma generation will have been removed from the reactor. The plasma is then always generated in a pure monomer environment. If the off period is < 3τ, the plasma is generated in an environment already containing fragments. This results in a higher degree of fragmentation with a correspondingly higher C/S ratio. The higher C/S ratios found for the higher duty cycles (i.e., shorter “off” times) confirm this explanation.

Transparency. With ellipsometry it is also possible to determine the transparency of a layer irrespective of the underlying substrate. Ellipsometric measurements were carried out on both nondoped and iodine-doped (5 min) PPT layers deposited on a silicon wafer. The data obtained could be fitted with a so-called 3-layer model: the ambient air, a thin PPT layer and the substrate, taking the native silicon oxide layer on the silicon wafer into account. For the doped samples the use of an additional thin layer (i.e., diffusion front) did not lead to a

significant improvement of the fit. The optical properties of the PPT layer were modelled with a Lorentzian absorption profile. The parameters, i.e., the PPT layer thickness and the characteristic parameters for the Lorentzian profile were optimised in a non-linear fit. The effective optical thickness was calculated and the transparency was calculated using Equation 4.3. As an example, the transparency of a 30 nm thick PPT layer is shown in Figure 4.14. A very high transparency (> 95%) is obtained over the whole visible range. When doped for 5 min in iodine vapour, the transparency decreases considerably, but is still > 80%. This is probably due to absorption by iodine taken up during the doping process. The surface conductivity of such a layer was calculated to be around 1.5×10^{-11} S, which is in the range of antistatic applications.

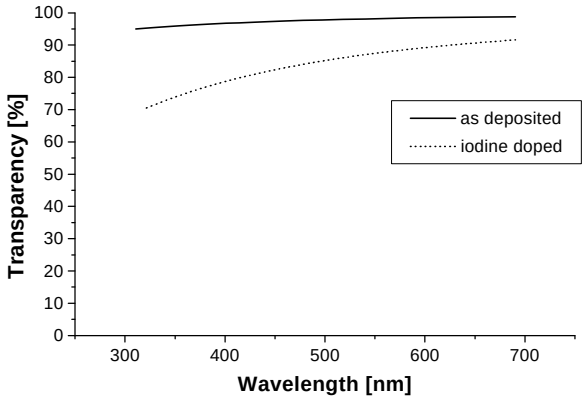

Figure 4.14. Transparency (calculated using Equation 4.3) of an undoped (solid line) and doped (5 min iodine vapour, dotted line) PPT layer (30 nm) deposited at 0.3 mbar (100 W, 10 s on, duty cycle 0.5) as a function of wavelength.

Conclusions

Highly transparent layers with conductivities in the range of antistatic applications have been obtained by plasma polymerisation of thiophene and doping with iodine. From the investigated deposition parameters, only pressure had a significant effect on the conductivity of the PPT layers. This could be related to the amount of preserved thiophene structures in the deposited PPT layer. At higher pressure more thiophene structures are built in, resulting in a higher conductivity. Opposite to what is generally accepted, a C/S ratio close to that of the starting monomer does not give conclusive information about the preservation of the monomer structure in the deposited layer. A pulsed plasma as a means to decrease the degree of fragmentation is most effective when the reactor is replenished with new monomer during the “off” time. Due to fragmentation that always takes place, plasma polymerisation does not seem to be an appropriate technique to obtain conductive layers for applications requiring high conductivities.

References

[1] Ellis, J. R. In *Handbook of conducting polymers*; Skotheim, T. A., Ed.; Marcel Dekker: New York, **1986**; Vol. 1, pp 489-500.

[2] Saunders, H. E. *Machine Design* **1992**, 161-165.

[3] Bäuerle, P. *Adv. Mater.* **1993**, *5*, 879-885.

[4] Miller, J. S. *Adv. Mater.* **1993**, *5*, 587-589.

[5] Beyer, G. *Polym. News* **1993**, *18*, 325-327.

[6] Mooney, P. J. *JOM* **1994**, *March*, 44-45.

[7] Schopf, G.; Kossmehl, G. *Adv. Polym. Sci.* **1997**, *129*.

[8] Tourillon, G. In *Handbook of conducting polymers*; Skotheim, T. A., Ed.; Marcel Dekker: New York, **1986**; Vol. 1, pp 293-350.

[9] Leclerc, M.; Faïd, K. *Adv. Mater.* **1997**, *9*, 1087-1094.

[10] Yamamoto, T.; Sanechika, K.; Yamamoto, A. *J. Polym. Sci., Polym. Lett. Ed.* **1980**, *18*, 9-12.

[11] Feast, W. J.; Tsibouklis, J.; Pouwer, K. L.; Groenendaal, L.; Meijer, E. W. *Polymer* **1996**, *37*, 5017-5047.

[12] Tenhoeve, W.; Wynberg, H.; Havinga, E. E.; Meijer, E. W. *J. Am. Chem. Soc.* **1991**, *113*, 5887-5889.

[13] Garnier, F.; Deloffre, F.; Horowitz, G.; Hajlaoui, R. *Synth. Met.* **1993**, *57*, 4747-4754.

[14] Glenis, S.; Benz, M.; LeGoff, E.; Kanatzidis, M. G.; Groot, D. C. d.; Schindler, J. L.; Kannewurf, C. R. *Synth. Met.* **1995**, *75*, 213-221.

[15] Zotti, G.; Salmaso, R.; Gallazzi, M. C.; Marin, R. A. *Chem. Mater.* **1997**, *9*, 791-795.

[16] Yin, W.; Li, J.; Gu, T.; Wu, J. *J. Appl. Polym. Sci.* **1997**, *63*, 13-16.

[17] Laakso, J.; Osterholm, J. E.; Nyholm, P. *Synth. Met.* **1989**, *28*, C467-C471.

[18] Isotalo, H.; Ahlskog, M.; Stubb, H.; Laakso, J.; Karna, T.; Jussila, M.; Osterholm, J. E. *Synth. Met.* **1993**, *57*, 3581-3586.

[19] Meador, M. A. B.; Hardy-Green, D.; Auping, J. V.; Gaier, J. R.; Ferrara, L. A.; Papadopoulos, D. S.; Smith, J. W.; Keller, D. J. *J. Appl. Polym. Sci.* **1997**, *63*, 821-834.

[20] Tanaka, K.; Yoshizawa, K.; Takeuchi, T.; Yamabe, T.; Yamauchi, J. *Synth. Met.* **1990**, *38*, 107-116.

[21] Sadhir, R. K.; K.F. Schoch, J. *Polym. Prepr.* **1992**, *33*, 412-413.

[22] Sadhir, R.; K.F. Schoch, J. *Thin Solid Films* **1993**, *223*, 154-160.

[23] Sadhir, R.; K.F. Schoch, J. *Polym. Prepr.* **1995**, *34*, 679-680.

[24] Tanaka, K.; Okazaki, S.; Inomata, T.; Kogoma, M. *8th Symp. Plasma Sci. Mater.*, **1995**, 33-37.

[25] Giungato, P.; Ferrara, M. C.; Musio, F.; d'Agostino, R. *Plasmas Polym.* **1996**, *1*, 283-297.

[26] Kiesow, A.; Heilmann, A. *Thin Solid Films* **1999**, *344*, 338-341.

[27] Boenig, H. V. In *Encycl. Polym. Sci. Eng.;* Mark, H. F. and Kroschwitz, J. I., Ed.; **1986**; Vol. 11, pp 248-261.

[28] Yasuda, H. *Plasma polymerization*; Academic Press: Orlando, 1985.

[29] Calderon, J. G.; Timmons, R. B. *Polym. Prepr.* **1997**, *38*, 1073-1074.

[30] Mackie, N. M.; Fisher, E. R. *Polym. Prepr.* **1997**, *38*, 1059-1060.

[31] Wang, J.-H.; Chen, X.; Chen, J.-J.; Calderon, J. G.; Timmons, R. B. *Plasmas Polym.* **1997**, *2*, 245-260.

[32] Calderon, J. G.; Timmons, R. B. *Macromolecules* **1998**, *31*, 3216-3224.

[33] Han, L. M.; Timmons, R. B. *Chem. Mater.* **1998**, *10*, 1422-1429.

[34] Wynberg, H.; Metselaar, J. *Synth. Commun.* **1984**, *14*, 1-9.

[35] Carpita, A.; Rossi, R.; Veracini, C. A. *Tetrahedron* **1985**, *41*, 1919-1929.

[36] Wentink, D. J. *Optical reflection studies of Si and Ge (001) surfaces*; University of Twente: Enschede, **1996**.

[37] Uchida, T.; Senda, K.; Vinogradov, G. K.; Morita, S. *Thin Solid Films* **1996**, *281-282*, 536-538.

[38] Uchida, T.; Vinogradov, G. K.; Morita, S. *J. Electrochem. Soc.* **1997**, *144*, 1434-1439.

[39] OldeRiekerink, M. B., Personal communication.

[40] d'Agostino, R. *Plasma deposition, treatment, and etching of polymers*; Academic Press: Orlando, **1990**.

[41] Pearse, R. W. B.; Gaydon, A. G. *The identification of molecular spectra*; 4th ed.; Chapman and Hall: London, **1976**.

[42] Fadini, A.; Schnepel, F.-M. In *Vibrational Spectroscopy*; Fadini, A., Schnepel, F. M., Wibbelman, C. and Masson, M., Ed.; Ellis Horwood: Chichester, **1989**.

[43] Agosti, E.; Zerbi, G. *Synth. Met.* **1996**, *79*, 107-113.

[44] Kobayashi, M.; Chen, J.; Chung, T. C.; Moraes, F.; Heeger, A. J.; Wudl, F. *Synth. Met.* **1984**, *9*, 77-86.

[45] Matsuura, Y.; Oshima, Y.; Misaki, Y.; Fujiwara, H.; Tanaka, K.; Yamabe, T.; Hotta, S. *Synth. Met.* **1996**, *82*, 155-158.

[46] Bernède, J. C.; Trégouet, Y.; Gourmelon, E.; Martinez, F.; Neculqueo, G. *Polym. Degr. Stab.* **1997**, *55*, 55-64.

[47] Ryan, M. E.; Hynes, A. M.; Wheale, S. H.; Badyal, J. P. S.; Hardacre, C.; Ormerod, R. M. *Chem. Mater.* **1996**, *8*, 916-921.

[48] Kruse, A.; Schlett, V.; Baalmann, A.; Hennecke, M. *Fresenius' J. Anal. Chem.* **1993**, *346*, 284-289.

[49] Gengenbach, T. R.; Griesser, H. J. *J. Polym. Sci. Part A: Polym. Chem.* **1998**, *36*, 985-1000.

[50] Inagaki, N.; Tasaka, S.; Ishii, K. *J. Appl. Polym. Sci.* **1993**, *48*, 1433-1440.

[51] Daw, R.; Al, S.; Beck, A. J.; Brook, I. M.; Short, R. D. *Polym. Prepr.* **1997**, *38*, 1012-1013.

[52] O'Toole, L.; Short, R. D. *J. Chem. Soc. Faraday Trans.* **1997**, *93*, 1141-1145.

[53] Lopèz, G. P.; Ratner, B. D. *J. Polym. Sci. Part A: Polym. Chem.* **1992**, *30*, 2415-2425.

[54] Tanaka, K.; Nishio, S.; Matsuura, Y.; Yamabe, T. *J. Appl. Phys.* **1993**, *73*, 5017-5022.

[55] Xie, X.; Thiele, J. U.; Steiner, R.; Oelhafen, P. *Synth. Met.* **1994**, *63*, 221-224.

[56] Grünwald, H.; Munro, H. S.; Wilhelm, T. *Mater. Sci. Eng.* **1991**, *A 139*, 356-358.

[57] Munro, H. S.; Grünwald, H. *J. Polym. Sci. Part A: Polym. Chem.* **1985**, *23*, 479-488.

[58] Bhuiyan, A. H.; Bhoraskar, S. V. *Thin Solid Films* **1993**, *235*, 43-46.

[59] Gong, X.; Dai, L.; Mau, A. W. H.; Griesser, H. J. *J. Polym. Sci. Part A: Polym. Chem.* **1998**, *36*, 633-643.

[60] Tanaka, K.; Yamabe, T.; Takeuchi, T.; Yoshizawa, K.; Nishio, S. *J. Appl. Phys.* **1991**, *70*, 5653-5660.

[61] Westerterp, K. R.; Swaaij, W. P. M. v.; Beenackers, A. A. C. M.; Kramers, H. *Residence time distribution and mixing in continuous flow reactors*; 2nd ed.; John Wiley & Sons: Chichester, **1984**.

[62] *The Handbook of Chemistry and Physics*; Lide, D. R., Ed.; 77th ed.; CRC Press: Boca Raton, **1996-1997**.

5

Plasma polymerisation of thiophene derivatives*

To obtain plasma polymerised (PP) layers with a high retention of the conjugated monomer structure, fragmentation during deposition should be minimised. Different methylated and halogenated thiophenes were used as monomers in plasma polymerisation and the influence of the substituent(s) on fragmentation during deposition was investigated. Using optical emission spectroscopy (OES) and mass spectroscopy (MS) it was found that methylated thiophenes show a low degree of fragmentation during deposition, whereas for halogenated thiophenes a high degree of fragmentation was observed. For a specific substituent, fragmentation was less for thiophene derivatives with substitution on the 2-position than on the 3-position. Disubstituted thiophenes always showed less fragmentation than their mono-substituted analogues. Due to the lower degree of fragmentation, PP layers from methylated thiophenes contained a higher amount of conjugated structures. Consequently, a higher conductivity was measured for these PP layers after iodine doping.

Introduction

Plasma polymerisation can be used to deposit thin, well adhering films onto almost any substrate.[1,2] Additional advantages are that no solvent is used and complex geometries can be handled in one step. A plasma consists of many different reactive species (e.g., radicals, ions, electrons). As a result, multiple interactions are possible and the exact chemical structure of a surface generated by a plasma is hard to predict.[3-8]

When monomers are used that upon plasma polymerisation result in conjugated structures, the plasma polymerised (PP) layer may be conductive. Because polythiophene is known for its high and stable conductivity, thiophene has frequently been used as monomer for plasma polymerisation.[9-14] The effect of conjugation length on the conductivity of polythiophene has been studied in detail.[15,16] It was shown that the conductivity of oligothiophenes increases with increasing conjugation length up to 6-11 monomer units, after which the conductivity becomes constant. Consequently, to obtain PP thiophene (PPT) layers with a high conductivity, the conjugated structure of the monomer should be retained in the PP layer and therefore, fragmentation during deposition should be minimised.

In an earlier study, we found that the conductivity of PPT layers was higher when the deposition pressure was higher.[14] It was concluded that this was due to the fact that less fragmentation occurred during deposition at higher pressure, resulting in a higher retention of the conjugated structure of the monomer in the PPT layer.

* The work described in this chapter has been submitted for publication in *Langmuir*.

It can be hypothesised that, besides the process parameters such as pressure, the chemical structure of the monomer can also be used to minimise fragmentation during deposition. In principle, substituent(s) can affect fragmentation in two ways: it can stabilise the monomer thus preventing fragmentation, or it can act as a preferred leaving group, thereby providing better control over the fragmentation process. For instance, benzo-[b]-thiophene was used as a monomer for plasma polymerisation to increase the retention of the thiophene ring.[17] It was observed that the aromatic skeleton of the monomer was retained in the deposited layers to a higher extent than in PPT layers. However, it was not clear whether this was due to retention of the thiophene or the benzene ring. Considering the higher stability of benzene compared to thiophene, probably the benzene ring is retained more. The conductivity of the PP-benzo-[b]-thiophene layers was not different from PPT layers. Earlier we showed that the conductivity of a PPT layer depends on the conjugation length and on the number and mobility of the charge carriers generated by charge transfer (CT) complexes.[18] The characteristics of the PP-benzo-[b]-thiophene layers and the PPT layers with respect to these factors were apparently not sufficiently different to have an effect on the conductivity.

In other studies, 2-iodothiophene was used as a monomer to deposit PP layers from RF (13.56 MHz)[19] and MW (2.45 GHz)[20] plasmas. It was found that iodine was preferentially lost from the monomer in both cases. Fourier transform infrared spectroscopy (FTIR) measurements showed that at high plasma frequency, the use of 2-iodothiophene gave more fragmentation than thiophene, whereas at low frequency more conjugated structures were retained in the PP- 2-iodothiophene layer than in the PPT layer.

Both the character and position of the substituent may have an effect on fragmentation during deposition. Substituents which act as a leaving group will probably create a reactive site at their former position on the parent molecule, whereas stabilising effects may also be induced on positions further away from the substituent. Consequently, the number of substituents will also have an influence on fragmentation.

In the present study, the effect of the nature, position, and number of substituents on the fragmentation of the thiophene derivative during deposition was investigated. PP layers were deposited from plasmas of different methylated and halogenated thiophene derivatives. OES and MS were used to study the plasma phase. The deposited layers were analysed using FTIR and X-ray induced photoelectron spectroscopy (XPS). To study the relationship between fragmentation during deposition and the chemical structure and conductivity of the resulting PP layer, the conductivity of the PP layers was measured after iodine doping.

Experimental

Materials. Besides thiophene, three series of thiophene derivatives (2-substituted, 3-substituted, and 2,5-disubstituted) were used as monomer. Within these series, the substituent (Me, Cl, Br) was varied.

Thiophene (purity > 99.5%, T), 2,5-dimethylthiophene (> 99%, 2,5-DiMeT), 2-chlorothiophene (> 97%, 2-ClT), 2-methylthiophene (> 98 %, 2-MeT), 3-methylthiophene (> 98%, 3-MeT), iodine (doubly sublimated), H_2SO_4 (96 %, analytical grade), and H_2O_2 (33%, medicinal purity) were purchased from Merck (Darmstadt, Germany). 2,5-Dichlorothiophene (98%, 2,5-DiClT), 2,5-dibromothiophene (95%, 2,5-DiBrT), 2-bromothiophene (> 98%, 2-BrT), and 3-bromothiophene (97%, 3-BrT) were obtained from Sigma-Aldrich (Zwijndrecht, the Netherlands). Solvents were of analytical grade purity and purchased from Biosolve (Valkenswaard, the Netherlands). All chemicals were used as received. Water used was doubly deionised. Glass slides (∅ 2.5 cm, used for FTIR analysis) with a sputtered gold layer were obtained from the FFW division (University of Twente, Enschede, the Netherlands). Glass slides (∅ 1.5 cm, used for XPS analysis) were purchased from Knittel (Braunschweig, Germany). The samples used for the conductivity measurements (glass slides with four electrodes with extensions to contact areas for the measurement leads)[14] were supplied by the MESA Institute (University of Twente, Enschede, the Netherlands), as were the 4" Si wafers from which Si-samples (∅ 1.5 cm, used for ellipsometry) were cut.

Cleaning. All glassware, glass substrates and tools were cleaned ultrasonically, consecutively three times in toluene, n-hexane, acetone, water, and acetone and subsequently dried at 125 ºC. The Si samples were cleaned ultrasonically three times in chloroform and then submersed in Piranha solution consisting of 70% H_2SO_4 and 30% H_2O_2 for 30 min. After thorough rinsing with water, acetone and n-hexane, the samples were dried at room temperature.

Plasma polymerisation. The plasma apparatus consisted of a tubular glass reactor with three externally placed, capacitively coupled electrodes.[14] The powered (hot) electrode was placed at the centre of the reactor. Two glass plates were placed between the hot and the grounded (cold) electrodes, which were positioned at 30 cm on either side of the hot electrode. The flow of monomer vapour through the reactor was regulated using needle valves and calculated from the time needed to obtain a certain pressure increase, once pumping of the reactor was stopped, assuming ideal gas behaviour. The flow of non-condensing gases was controlled by mass flow controllers (MKS Instruments, Andover, USA). The system (without the substrates) was first cleaned by applying an air plasma (5 sccm/min, 125 W, 0.13 mbar) for 60 min. The substrates were placed at the centre between the hot and cold electrode at the side of the monomer inlet and the reactor was evacuated to $< 5.10^{-3}$ mbar. The substrates were cleaned with an air plasma (5 sccm/min, 85 W, 0.13 mbar) for 5 min, after which the reactor was again evacuated to $< 5.10^{-3}$ mbar. Subsequently, a monomer flow was established through the reactor and after 1 min, pulsed plasma depositions were carried out. For each monomer the conditions were chosen such that a homogeneous plasma was obtained at the lowest possible power input (see Table 5.1). The on time was always 1 s. The off time was chosen such that the reactor was replenished with new monomer during this period (see also Table 5.1). After deposition, the monomer flow was sustained for another 2 min and the reactor was brought to atmospheric pressure with air. The samples were stored at –18 ºC.

Table 5.1. Conditions used for the plasma deposition of thiophene and thiophene derivatives. Plasma "on" time was always 1 s.

	2,5-DiClT	**2,5-DiBrT**	**2,5-DiMeT**	**2-ClT**	**2-BrT**	**2-MeT**	**3-BrT**	**3-MeT**	**T**
Pressure [mbar]	0.038	0.024	0.04	0.05	0.045	0.06	0.043	0.05	0.06
Power [W]	30-31	20-22	24-25	19-20	17-21	18-21	19-22	30-31	21
Off time [s]	7.5	15	5	6	7.5	5	7.5	6	5

Characterisation of plasma phase. MS was carried out to analyse the gas composition at the outlet of the reactor. The spectrometer was a differentially pumped QMS 421 mass spectrometer (Balzers, Utrecht, the Netherlands). The gas was introduced into the MS using a leak valve. The MS spectra were corrected for pressure differences by dividing the ion current by the pressure in the spectrometer. In this way, ion currents of a certain mass (m/e) can be compared as they were concentrations.

OES analysis was carried out using an MCPD-1000 spectrophotometer (Otsuka, Osaka, Japan) with a slit width of 0.2 mm. The measuring probe was placed at the reactor entrance, in line of sight with the plasma. Spectra were recorded from 180 to 875 nm with a step width of 2 nm. For practical reasons, a continuous plasma was used for both the MS and the OES measurements.

Characterisation of the PP layers. For FTIR analysis, PP layers were deposited on gold-coated glass discs (∅ 2.5 cm) and spectra were recorded using a BioRad FTS-60 (Biorad, Cambridge, UK) in the reflectance mode. A background spectrum was recorded using a clean substrate.

XPS analysis was carried out on layers deposited on glass discs (∅ 1.5 cm) using an S probe (Surface Science Instruments, Mountain View, CA, USA) with a monochromatic Al K_α source (1486.6 eV). The input power was 220 W and the analysed spot size was 250×1000 μm. Survey scans (1100 - 0 eV binding energy (BE) window) were recorded with a pass energy (PE) of 150 eV. The concentrations of the various elements were calculated from the relative peak areas, using sensitivity factors (SF) from literature.[21] High-resolution (HR) detail scans (20 eV BE window) were taken at 50 eV PE. From the iodine doped samples, HR XPS spectra (400 μm spot, 100 W) were obtained using a VG Σ-Probe (VG Scientific, East-Grinstead, UK). Besides detail scans (20 eV BE and 20 eV PE), survey scans (1100 eV BE window, 150 eV PE) were taken to calculate the atomic concentration using SF supplied by the manufacturer.

The thickness of the PP layers deposited on Si samples was determined with a variable angle ellipsometer with a QTH 200 lightsource, a M44 detector, and an EC 120 control module (J.A. Woollam Co., Lincoln, NE, USA). A two-layer model (Cauchy-layer on top of a Si-substrate) was used in the fitting procedure. The thickness and the Cauchy parameters (A and b) were adjusted iteratively to obtain an optimal fit. A Levenberg-Marquardt algorithm was used for the minimisation of the mean-squared error between the fit and the experimental data.[22]

The conductivity of the layers was determined using specially designed substrates for the plasma deposition[14] (configuration in accordance with ASTM D257). During plasma deposition, the extensions of the electrodes were covered with glass slides to prevent deposition, thus ensuring a good contact with the measurement leads. After deposition, the samples were doped for 5 min by placing them in a sealed container containing iodine crystals. Two electrometers (Keithley Instruments, Cleveland, USA) were used to apply a current over the outer electrodes and to measure the voltage over the inner electrodes. After applying the current for 1 min, the voltage was read. The volume conductivity of the deposited layer was calculated with the appropriate formulas (ASTM D257).

Results & Discussion

Characterisation of the plasma phase. During plasma polymerisation of the different monomers, a difference in colour of the plasmas was observed, indicating a variation in the species present in the plasma. OES and MS were used to determine these species. In Figure 5.1, the OES spectra of plasmas of all monomers are depicted. All spectra show the presence of CS species, which is considered as a measure for fragmentation of the thiophene structure.[14] In an earlier study with thiophene, we observed an effect of pressure (0.06 vs. 0.3 mbar) on fragmentation during deposition.[14] Therefore, to properly evaluate the influence of substituents on fragmentation, the deposition conditions should be similar for all

monomers. The differences in deposition conditions in the present study (see Table 5.1) are small enough to allow a comparison of the fragmentation.

It can be concluded from the OES results that fragmentation increases in the order MeT's < T < halogenated thiophenes. This shows that fragmentation is suppressed by electron-donating substituents, whereas it is enhanced by electron-withdrawing substituents. This suggests that the electron-deficient species present in a plasma (e.g., radicals and positive ions) play a role in the fragmentation process.

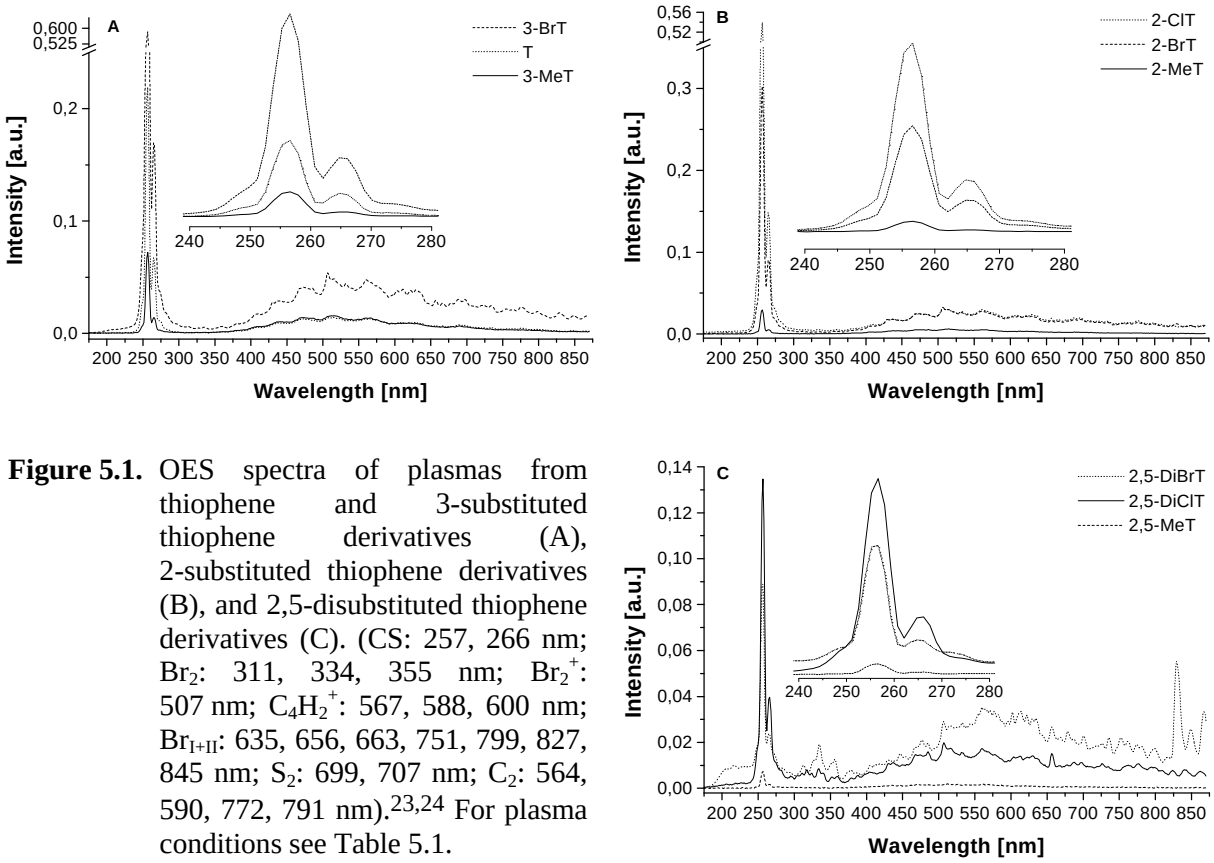

Figure 5.1. OES spectra of plasmas from thiophene and 3-substituted thiophene derivatives (A), 2-substituted thiophene derivatives (B), and 2,5-disubstituted thiophene derivatives (C). (CS: 257, 266 nm; Br_2: 311, 334, 355 nm; Br_2^+: 507 nm; $C_4H_2^+$: 567, 588, 600 nm; Br_{I+II}: 635, 656, 663, 751, 799, 827, 845 nm; S_2: 699, 707 nm; C_2: 564, 590, 772, 791 nm).[23,24] For plasma conditions see Table 5.1.

More fragmentation occurs in the plasmas of ClT's than of BrT's. A recent study by Yasuda *et al.* showed that the stability of an element towards plasma decreases with increasing electron affinity.[25] Although the difference in electron affinity between chlorine and bromine is small,[23] it may explain the observed differences between the OES spectra of the ClT's and BrT's. Further research is needed to obtain conclusive information.

The effect of the position of the substituent on fragmentation becomes clear when the series of 2- and 3-substituted thiophenes are compared. For a specific substituent, more fragmentation occurs for substitution on the 3-position than on the 2-position.

In many studies an effect of substituent nature and position on the reactivity of thiophene derivatives towards a number of species (i.e., nucleophiles,[26] electrophiles,[27,28] radicals,[29]

and UV light[30,31]) has been observed,[32,33] but due to the uncertainty of the mechanism of deposition at this point the conclusions from these studies cannot be directly applied to the plasma polymerisation process.[2]

The plasmas of the 2,5-series all show less fragmentation than T and their corresponding mono-substituted analogues, while the same relation between electron affinity and fragmentation (i.e., MeT < BrT < ClT) is found. This indicates that similar processes resulting in CS formation occur in plasmas of mono- and disubstituted thiophenes, but that the extent of CS formation decreases with increasing number of substituents. Besides less CS formation, other differences exist as is indicated by the presence and absence of atomic bromine and Br_2 in the plasmas of 2,5-DiBrT and the BrT's, respectively. This could be related to weakening of the C-Br bond due to the presence of a second electronegative bromine group on the monomer.

In Figure 5.2, the difference between the MS spectra of a monomer flow with and without plasma generation is shown for the various monomers. No CS species are present in the MS spectra, implying that the CS species observed with OES have reacted or are deposited before they reach the MS or that they cannot be detected by the MS, which shows the complementality of the two analysis techniques. Upon generation of a plasma, the MS spectra of T and the MeT's hardly change. Compared with T, a lower amount of carbon containing fragments is observed in the MS spectra of the MeT's. Together with the OES results, this shows that substitution of T with electron-donating substituents is an effective way to decrease the fragmentation during deposition. For the halogenated thiophenes, next to some peaks corresponding to carbon-containing fragments, an intense H_2 peak is observed. This can be related to the electron affinity of the substituent in these cases, which weakens the C-H bond.

For a specific substituent, more H_2 is formed in the plasmas of the 3-series than of the 2-series. Together with the OES results, this suggests that the liberation of hydrogen and the formation of CS are related. This implies that when hydrogen is liberated from the 3-position, more CS formation (i.e., fragmentation) occurs compared with the 2-position.

In the MS spectra of the ClT's a HCl peak is observed, whereas no HBr is detected for the BrT's. Consequently, the H_2 peak is relatively low for the ClT's compared with the BrT's. As mentioned before, this might be related to the difference in electron affinity but further research is needed to obtain conclusive information.

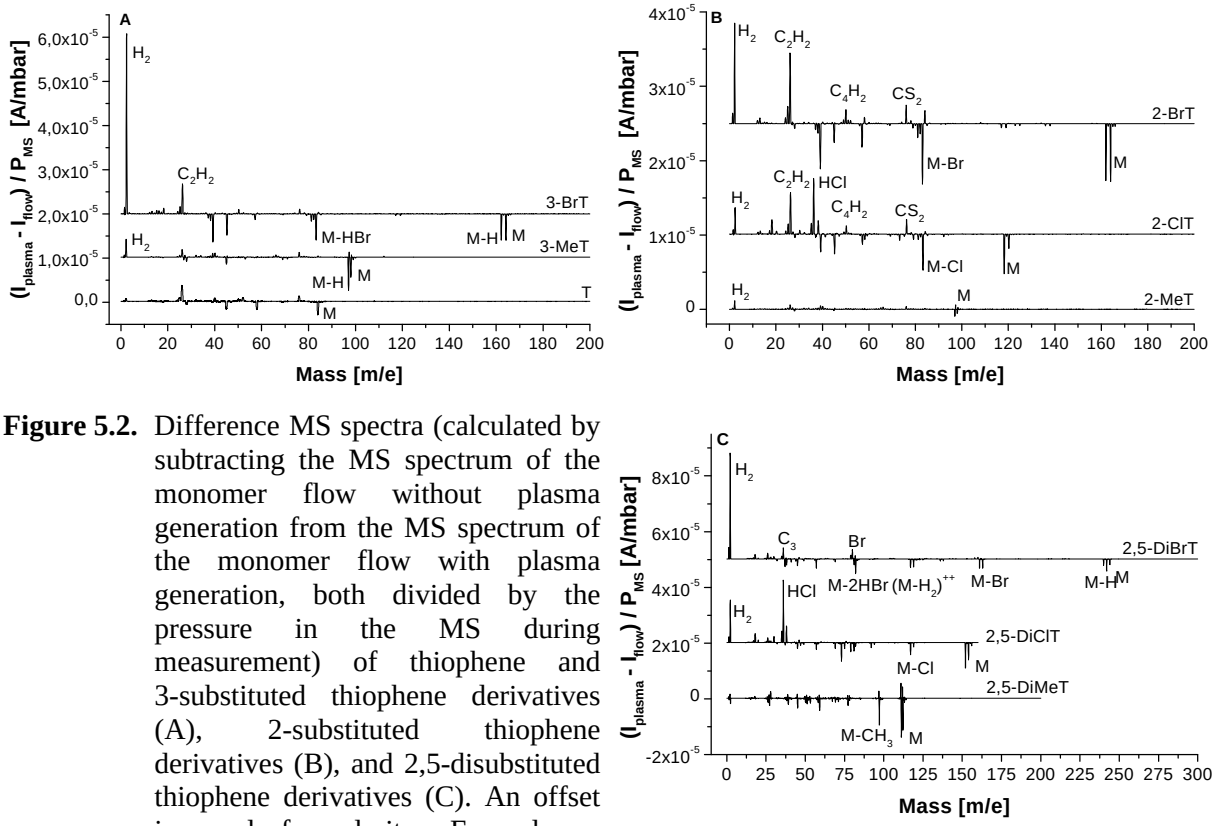

Figure 5.2. Difference MS spectra (calculated by subtracting the MS spectrum of the monomer flow without plasma generation from the MS spectrum of the monomer flow with plasma generation, both divided by the pressure in the MS during measurement) of thiophene and 3-substituted thiophene derivatives (A), 2-substituted thiophene derivatives (B), and 2,5-disubstituted thiophene derivatives (C). An offset is used for clarity. For plasma conditions see Table 5.1.

Summarising, it was observed that fragmentation during deposition is suppressed by electron-donating substituents, whereas it is enhanced by electron-withdrawing substituents. For a specific substituent, substitution on the 3-position results in more fragmentation during deposition compared with substitution on the 2-position. Furthermore, fragmentation is less when the number of substituents is higher.

Characterisation of the PP layers. XPS analysis was performed to determine the chemical composition of the PP layers. The results are summarised in Table 5.2. For T and the MeT's, the carbon concentration relative to the sulphur concentration is lower than expected from theory, while for the other monomers the C/S ratio is equal to or higher than the theoretical value. Considering the OES results, it seems that PP layers deposited from monomers showing little fragmentation during deposition contain relatively more sulphur. This is consistent with the results obtained in an earlier study on the effect of deposition conditions on fragmentation of thiophene.[14]

The halogen removal from halogenated thiophenes is apparent from the lower than theoretical halogen content. The loss of chlorine from 2-ClT is relatively high, compared with the loss of bromine from the mono-BrT's. Together with the high C/S ratio of the ClT's, this corresponds well with the high amount of fragmentation observed in these cases as measured with OES and MS.

Table 5.2. Chemical composition (determined with XPS) at the surface of plasma polymerised thiophene derivatives (n = 3 ± sd). For plasma conditions see Table 5.1

Monomer	**PP layer**	**C (atom%)**	**S (atom%)**	**Halogen (atom%)**	**O (atom%)**
T	theory	80	20	-	-
	PPT	72.0 ± 0.1	23.6 ± 0.7	-	4.4 ± 0.7
2,5-DiMeT	theory	85.7	14.3	-	-
	PP-2,5-DiMeT	80.8 ± 0.3	17.5 ± 0.1	-	1.7 ± 0.3
2,5-DiHaloT	theory	57.1	14.3	28.6	-
	PP-2,5-DiClT	64.3 ± 0.4	13.2 ± 0.1	20.0 ± 0.6	2.5 ± 0.1
	PP-2,5-DiBrT	63.0 ± 1.3	16.2 ± 0.8	18.8 ± 0.4	2.0 ± 1.5
MeT	theory	83.3	16.7	-	-
	PP-2-MeT	79.8 ± 0.7	19.1 ± 0.1	-	1.1 ± 0.8
	PP-3-MeT	78.7 ± 1.3	18.5 ± 0.6	-	2.7 ± 1.9
HaloT	theory	66.7	16.7	16.7	-
	PP-2-ClT	72.1 ± 0.1	16.9 ± 0.1	6.8 ± 0.2	4.1 ± 0.2
	PP-2-BrT	68.3 ± 0.8	19.1 ± 0.2	11.2 ± 0.4	1.4 ± 1.0
	PP-3-BrT	67.2 ± 1.6	17.6 ± 0.8	12.4 ± 1.2	2.8± 2.0

HR C1s spectra were acquired to investigate whether conjugated structures are present in the deposited layers (Figure 5.3). If so, π-π^* shake-up satellites should be visible at about 6 - 7 eV higher BE than the primary peak.[34] Figure 5.3 shows that only PP-MeT layers contain conjugated structures that can be detected by XPS, which is consistent with the low amount of fragmentation observed earlier. This shows that CS formation is indeed a good indicator for the amount of fragmentation of the thiophene ring.

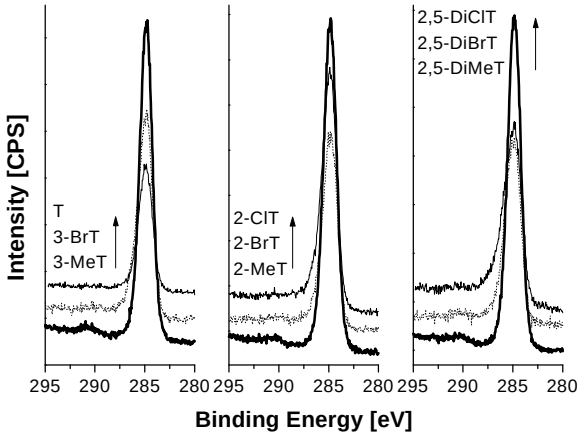

Figure 5.3. HR XPS spectra of the C1s region at the surface of PP layers from thiophene and 3-substituted thiophene derivatives (left), 2-substituted thiophene derivatives (middle), and 2,5-disubstituted thiophene derivatives (right). Spectra are arranged in the direction of the arrow, using an offset for reasons of clarity. For plasma conditions see Table 5.1.

FTIR was used to investigate the chemical structure of the PP layers. In Figure 5.4, the FTIR spectra of the PP layers are given. In all FTIR spectra absorption bands of H-atoms as expected based on the monomer structure (α-H and/or β-H atoms)[35] are also present in the respective PP layers, showing that, to some extent, the monomers are built in without fragmentation.

Both the PPT and the PP-ClT layers contain terminal acetylene groups, which are formed by a reaction either in the plasma phase or at the surface of a deposited PP-layer. The spectra of the PP-ClT layers show that -C≡C- groups are also present in these layers. Together with the formation of HCl as determined with MS (Figure 5.2), this shows that liberation of chlorine and hydrogen from adjacent positions has occurred. The presence of aliphatic CH_2 groups in the PPT layer is consistent with the almost negligible small H_2 peak in the difference MS spectra.

Tanaka *et al.* also used T and 3-MeT as monomers, but they did not observe the characteristic absorption around 3100 cm^{-1} in the FTIR spectra.[12] This is probably related to their use of argon as a carrier gas in combination with a different reactor (bell jar) and electrode configuration (internal). This may have an effect on the fragmentation during deposition and possibly also on the deposition mechanism.

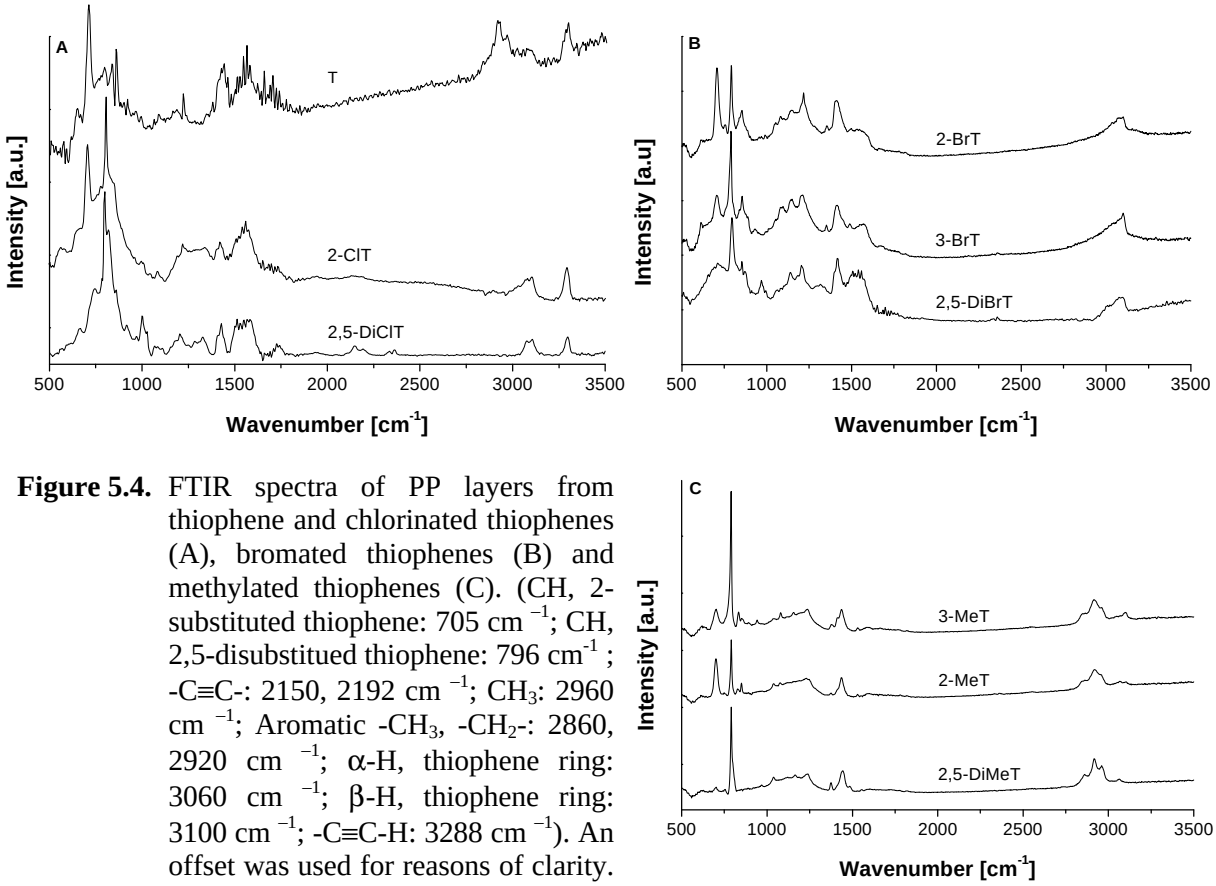

Figure 5.4. FTIR spectra of PP layers from thiophene and chlorinated thiophenes (A), bromated thiophenes (B) and methylated thiophenes (C). (CH, 2-substituted thiophene: 705 cm^{-1}; CH, 2,5-disubstitued thiophene: 796 cm^{-1} ; -C≡C-: 2150, 2192 cm^{-1}; CH_3: 2960 cm^{-1}; Aromatic -CH_3, -CH_2-: 2860, 2920 cm^{-1}; α-H, thiophene ring: 3060 cm^{-1}; β-H, thiophene ring: 3100 cm^{-1}; -C≡C-H: 3288 cm^{-1}). An offset was used for reasons of clarity. For plasma conditions see Table 5.1.

The conductivity of the PP layers was measured after 5 min iodine doping and the results are given in Figure 5.5. In another study, it was observed that the conductivity showed a complex dependence on doping time.[18] A separate experiment (data not shown) showed that although the conductivity increased with doping time, Figure 5.5 can be considered as representative for the conductivity of the PP layers. Clearly, the PP-MeT layers are the most conductive in all series, showing a positive relation between the amount of conjugated structures and the conductivity of a PP layer. This was also found in a number of other studies.[13,36-40]

Within a series, the conductivity decreases with increasing electron affinity of the substituents. Together with the OES and MS results, this shows that with increasing fragmentation during deposition the conductivity of the resulting PP layer decreases. This is in good agreement with earlier results.[14] However, it seems that this relation cannot be used to predict the conductivity of PP layers in different series. For instance, the OES spectra of the 2,5-series show less fragmentation than the 2- and 3-series, whereas the conductivity is lower in the 2,5-series. This shows that other effects impaired by the substituents (e.g., coplanarity of thiophene rings)[16,41] also have an effect on the conductivity.

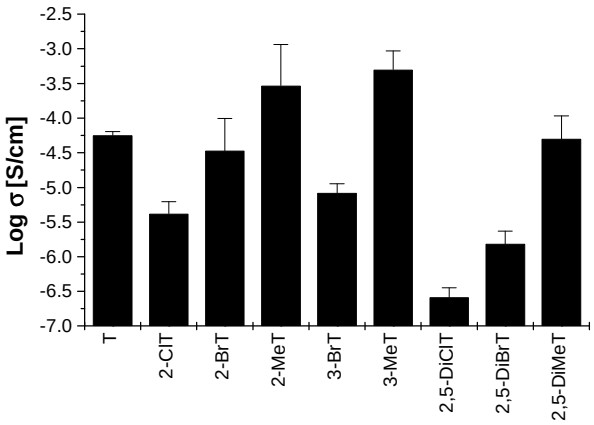

Figure 5.5. Logarithm of the volume conductivity (S/cm) of PP layers from derivatised thiophenes after 5 min iodine doping (n = 3 ± sd). For plasma conditions see Table 5.1.

In the HR XPS spectra of the I_{3d5} region of the doped PP layers (Figure 5.6) two peaks can be observed. In literature, the low BE peak is assigned to charge transfer (CT) complexes with conjugated structures in the form of I_3^- and/or I_5^-, whereas the peak at higher BE is due to covalently bound iodine and/or adsorbed I_2.[42-44] The PP layers are rendered conductive by charge carriers generated by the CT complexes, which are in equilibrium with absorbed I_2.[18] The amount of CT complexes as measured with XPS cannot be directly related to the conductivity results due to the vacuum applied for the measurement. Assuming that the relative decrease due to the applied vacuum is equal for both peaks in all layers, the XPS results can be used as a measure of the ability of the PP layer to form charge carriers upon iodine doping.

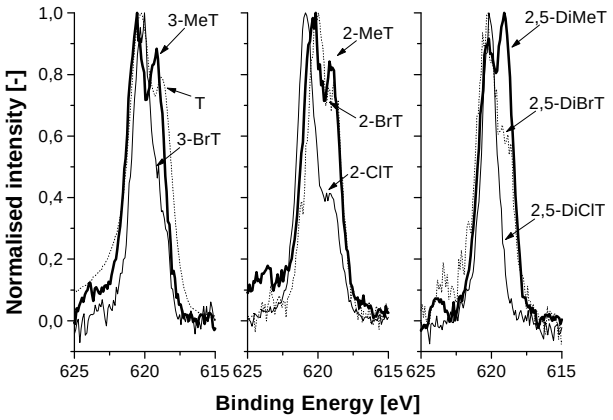

Figure 5.6. Normalised HR XPS spectra of the I_{3d5} region of PP layers from thiophene and 3-substituted thiophene derivatives (left), 2-substituted thiophene derivatives (middle), and 2,5-disubstituted thiophene derivatives (right) after doping for 5 min with iodine. For plasma conditions see Table 5.1. Iodine concentrations: T: 4.1%; 3-BrT: 1.5%; 3-MeT: 2.5%; 2-ClT: 3.5%; 2-BrT: 1.5%; 2-MeT: 2.0%; 2,5-DiClT: 1.3%; 2,5-DiBrT: 1.1%; 2,5-DiMeT: 2.4%.

In all series, the PP-MeT layers contain the largest amount of CT complexes relative to the absorbed and covalently bound iodine. This shows that a relatively high concentration of unfragmentated thiophene structures is present in these PP layers. Furthermore, after iodine doping, the PP-ClT layers contain a high amount of covalently bound/absorbed iodine. As iodine reacts with the PP layers for instance with acetylene groups,[18,45] it seems most probable that the high BE peak stems mainly from covalently bound iodine in these cases. These results are consistent with the HR XPS data (Figure 5.3). The absolute amount of CT complexes in the PP-MeT layers is not always the highest while the conductivity is. This shows that the environment in which the charge carriers are generated also plays a role in determining the conductivity.

Conclusions

The monomer structure can be used to minimise fragmentation during plasma polymerisation, resulting in PP layers with a high conductivity upon iodine doping. Electron-donating substituents on thiophene such as methyl groups suppress fragmentation, whereas it is enhanced by substitution with electron-withdrawing groups. For electron-withdrawing substituents, a higher electron affinity results in a higher degree of fragmentation. Fragmentation is always less when the number of substituents is increased. For a specific substituent, substitution on the 2-position results in less fragmentation compared with substitution on the 3-position. Due to the low amount of fragmentation during deposition, only PP layers of thiophene substituted with electron-donating substituents contain conjugated structures detectable with XPS. Consequently, after iodine doping a higher conductivity is found for the methyl substituted thiophenes compared with non-substituted thiophene and halogenated thiophenes. However, because substituents can also affect the conductivity in other ways (e.g., coplanarity of thiophene rings), prudence is called for when applying the relationship between fragmentation and conductivity to compare series varying in number and position of the substituents.

Acknowledgements

The authors thank Joop de Vries from Groningen University (Groningen, the Netherlands) and VG Scientific (East-Grinstead, UK) for performing the high resolution XPS measurements.

References

[1] Boenig, H. V. In *Encycl. Polym. Sci. Eng.;* Mark, H. F. and Kroschwitz, J. I., Ed.; **1986**; Vol. 11, pp 248-261.

[2] Yasuda, H. *Plasma polymerization*; Academic Press: Orlando, **1985**.

[3] Terlingen, J. G. A. *Introduction of functional groups at polymer surfaces by glow discharge techniques*; University of Twente: Enschede, **1993**.

[4] Suhr, H. In *Techniques and applications of plasma chemistry*; Hollahan, J. and Bell, A. T., Ed.; Wiley: New York, **1974**, pp 57-111.

[5] Coburn, J. W.; Chen, M. *J. Appl. Phys.* **1980**, *51*, 3134-3136.

[6] Gazicki, M.; Yasuda, H. *J. Appl. Pol. Sci., Appl. Pol. Symp.* **1984**, *38*, 35-44.

[7] d'Agostino, R. *Plasma deposition, treatment, and etching of polymers*; Academic Press: Boston, **1990**.

[8] *Techniques and applications of plasma chemistry*; Hollahan, J. and Bell, A. T., Ed.; John Wiley & Sons: New York, **1974**.

[9] Giungato, P.; Ferrara, M. C.; Musio, F.; d'Agostino, R. *Plasmas Polym.* **1996**, *1*, 283-297.

[10] Sadhir, R.; K.F. Schoch, J. *Thin Solid Films* **1993**, *223*, 154-160.

[11] Sadhir, R.; K.F. Schoch, J. *Polym. Prepr.* **1995**, *34*, 679-680.

[12] Tanaka, K.; Yoshizawa, K.; Takeuchi, T.; Yamabe, T.; Yamauchi, J. *Synth. Met.* **1990**, *38*, 107-116.

[13] Tanaka, K.; Okazaki, S.; Inomata, T.; Kogoma, M. *8th Symp. Plasma Sci. Mater.*, 1995, pp 33-37.

[14] Groenewoud, L. M. H.; Engbers, G. H. M.; Terlingen, J. G. A.; Wormeester, H.; Feijen, J. *Langmuir* **2000**, *16*, 6278-6286.

[15] Tenhoeve, W.; Wynberg, H.; Havinga, E. E.; Meijer, E. W. *J. Am. Chem. Soc.* **1991**, *113*, 5887-5889.

[16] Garnier, F.; Deloffre, F.; Horowitz, G.; Hajlaoui, R. *Synth. Met.* **1993**, *57*, 4747-4754.

[17] Tanaka, K.; Yamabe, T.; Takeuchi, T.; Yoshizawa, K.; Nishio, S. *J. Appl. Phys.* **1991**, *70*, 5653-5660.

[18] Groenewoud, L. M. H.; Engbers, G. H. M.; White, R.; Feijen, J. *Synth. Met., submitted*.

[19] Ryan, M. E.; Hynes, A. M.; Wheale, S. H.; Badyal, J. P. S.; Hardacre, C.; Ormerod, R. M. *Chem. Mater.* **1996**, *8*, 916-921.

[20] Kruse, A.; Schlett, V.; Baalmann, A.; Hennecke, M. *Fresenius' J. Anal. Chem.* **1993**, *346*, 284-289.

[21] Wagner *Surf. Interface Anal.* **1981**, *3*, 211-225.

[22] Jellison jr., G. E. J. *Thin Solid Films* **1998**, *33*, 313-314.

[23] Yasuda, H.; Yasuda, T. *J. Polym. Sci. Part A; Polym. Chem.* **2000**, *38*, 943-953.

[24] *The Handbook of Chemistry and Physics*; Lide, D. R. Ed., 77th ed.; CRC Press: Boca Raton, **1996-1997**.

[25] Spinelli, D.; Consiglio, G.; Dell'erba, C.; Novi, M. In *Thiophene and its derivatives*; Gronowitz, S., Ed.; John Wiley & Sons: New York, **1985**.

[26] Belen'kii, L. I. *Hetrocycles* **1994**, *37*, 2029-2049.

[27] Taylor, R. In *Thiophene and its derivatives*; Gronowitz, S., Ed.; J. Wiley &Sons: New York, **1985**.

[28] Porter, A. E. A. In *Thiophene and its derivatives*; Gronowitz, S., Ed.; J. Wiley & Sons: New York, **1985**.

[29] Wynberg, H.; Kellog, R. M.; Driel, H. v.; Beekhuis, G. E.; Buter, J. *J. Am. Chem. Soc.* **1966**, *88, 89*, 5047-5048, 3487-3505.

[30] Lablache-Combier, A. In *Thiophene and its derivatives*; Gronowitz, S., Ed.; John Wiley & Sons: New York, **1985**.

[31] Reinecke, M. G.; Pedaja, P. In *Thiophene and its derivatives*; Gronowitz, S., Ed.; John Wiley & Sons: New York, **1985**.

[32] *Thiophene and its derivatives*; Gronowitz, S., Ed.; John Wiley & Sons: New York, **1985**.

[33] Briggs, D.; Seah, M. P. *Practical surface analysis*; 2nd ed.; John Wiley & Sons: New York, **1986**; Vol. 1.

[34] http://www.aist.go.jp/RIODB/SDBS/menu-e.html .

[35] Bhuiyan, A. H.; Bhoraskar, S. V. *J. Mat. Sci.* **1989**, *24*, 3091-3095.

[36] Gong, X.; Dai, L.; Mau, A. W. H.; Griesser, H. J. *J. Polym. Sci. Part A: Polym. Chem.* **1998**, *36*, 633-643.

[37] Xie, X.; Thiele, J. U.; Steiner, R.; Oelhafen, P. *Synth. Met.* **1994**, *63*, 221-224.

[38] Osada, Y.; Yasunaga, H.; Wang, F. S.; Chen, J. *J. Appl. Phys.* **1988**, *4*, 1476-1483.

[39] Lee, K. P.; Park, S. Y.; Kim, N.; Song, S. K. *Mol. Cryst. Liq. Cryst.* **1993**, *224*, 53-59.

[40] Tourillon, G.; GArnier, F. *J. Phys. Chem.* **1983**, *87*, 2289-2292.

[41] Hsu, S. L.; Signorelli, A. J.; Pez, G. P.; Baughman, R. H. *J. Chem. Phys.* **1978**, *69*, 106-111.

[42] Salaneck, E. W.; Thomas, H. R.; Bigelow, R. W.; Duke, C. B.; Plummer, E. W.; Heeger, A. J.; MacDiarmid, A. G. *J. Chem. Phys.* **1980**, *72*, 3674-3678.

[43] Petit, M. A.; Soum, A. H. *J. Polym. Sci. B* **1987**, *25*, 423-433.

[44] Boyd, G. V. In *The chemsitry of triple bonded functional groups*; Patai, S., Ed.; J. Wiley & Sons: New York, **1994**; Vol. 2.

[45] Pearse, R. W. B.; Gaydon, A. G. *The identification of molecular spectra*; 4th ed.; Chapman and Hall: London, **1976**.

6

Mechanism of plasma polymerisation of thiophene and thiophene derivatives*

The effect of the nature, position, and number of substituents on the chemistry of the deposition process in plasma polymerisation has been investigated. It was found that for mono-halogenated thiophenes deposition preferably proceeds via the dissociation of C-H bonds from positions adjacent to the substituent. The ease of radical formation increases with increasing electron affinity of the substituent. Radicals formed on carbon atoms also attached to sulphur induce fragmentation of the thiophene ring. Consequently, for a specific substituent, substitution on the 3-position results in more fragmentation than substitution on the 2-position. The dissociation of the C-halogen bond in dihalogenated thiophenes is energetically more favourable than in mono-halogenated thiophenes due to the presence of a second halogen. The deposition of methylated thiophenes was found to proceed via C-H bond dissociation from the CH_3 substituent. As a result, the thiophene ring is preserved to a high extent, which after iodine doping, gives rise to a high conductivity for the plasma polymerised layers of methylated thiophene derivatives.

Introduction

Plasma polymerisation is frequently used to deposit thin films. A plasma consists of a variety of reactive species (e.g., electrons, ions, and radicals). Many different reactions can therefore occur,[1-6] and as a consequence the exact chemical structure of layers resulting from plasma polymerisation is not precisely predictable. As doped polythiophene is known for its high and stable conductivity,[7] thiophene is often used as a monomer in plasma polymerisation.[8-16] In an earlier study, we have shown that the monomer structure has an influence on the fragmentation of thiophene during deposition.[17] It was observed that fragmentation during deposition was enhanced by substitution of thiophene with electron-withdrawing substituents, whereas it was suppressed by electron-donating substituents. The conductivity of the plasma polymerised (PP) layers after iodine doping was higher when there was less fragmentation during deposition.

Selection of substituted thiophenes that will show little fragmentation during deposition should be based on the chemistry of the polymerisation process. From conventional chemistry it is known that the reactivity of thiophene derivatives towards different species (e.g., nucleo- and electro-philes) as well as the preferable reaction site is influenced by the type and position of the substituent(s).[18] Although plasma polymerisations have been studied for a long time, the chemistry taking place during deposition is still not clear.[19-21]

* The work described in this chapter has been submitted for publication in *Langmuir*.

Mechanisms involving ions,[22,23] radicals, and atomic processes have been described to explain the experimental data.[21] At the present time, many investigators support the polymerisation mechanism as proposed by Yasuda *et al.*[4,19,24,25] In this stepwise initiation-recombination sequence, radicals are formed upon the generation of a discharge. These primary radicals recombine to a species that again can be radical initiated etc.

The site and ease of radical formation in this process may well be affected by the monomer structure. Therefore, the present study is directed to the mechanism of plasma deposition of different thiophene derivatives, varying in nature, position, and number of substituents. The plasma phase was characterised using optical emission spectroscopy (OES) and mass spectrometry (MS). Deposition of PP layers was followed *in situ* using a quartz crystal thickness monitor (QCM). The deposited PP layers were characterised by X-ray induced photoelectron spectroscopy (XPS), Fourier transform infrared spectroscopy (FTIR), and nuclear magnetic resonance spectroscopy (NMR). The conductivity of the PP layer after iodine doping was also determined.

Experimental

Materials. Beside thiophene (T), three series of thiophene derivatives (2-substituted, 3-substituted, and disubstituted (2,5 and 3,4)) were used as monomers. Within these series, the substituent (Me, Cl, Br) was varied.

Thiophene (purity > 99.5%, T), 2,5-dimethylthiophene (> 99%, 2,5-DiMeT), 2-chlorothiophene (> 97%, 2-ClT), 2-methylthiophene (> 98%, 2-MeT), 3-methylthiophene (> 98%, 3-MeT), iodine (doubly sublimated), H_2SO_4 (96%, analytical grade), H_2O_2 (33%, medicinal purity), and CD_2Cl_2 (> 99.9%, 99.5% deuterated) were purchased from Merck (Darmstadt, Germany). 2,5-Dichlorothiophene (98%, 2,5-DiClT), 2,5-dibromothiophene (95%, 2,5-DiBrT), 3,4-dibromothiophene (98%, 3,4-DiBrT), 2-bromothiophene (> 98%, 2-BrT), and 3-bromothiophene (97%, 3-BrT) were obtained from Sigma-Aldrich (Zwijndrecht, the Netherlands). Other solvents were of analytical grade purity and were purchased from Biosolve (Valkenswaard, the Netherlands). Water used was doubly deionised. All chemicals were used as received. Glass slides (∅ 2.5 cm, used for FTIR analysis) with a sputtered gold layer were obtained from the FFW division (University of Twente, Enschede, the Netherlands). Glass slides (∅ 1.5 cm, used for XPS analysis) were purchased from Knittel (Braunschweig, Germany). The samples used for the conductivity measurements (glass slides with four electrodes with extensions to contact areas for the measurement leads)[16] were supplied by the MESA Institute (University of Twente, Enschede, the Netherlands), as were the 4” Si wafers from which Si-samples (∅ 1.5 cm, used for ellipsometry) were cut.

Cleaning. All glassware, glass substrates and tools were cleaned ultrasonically, consecutively three times in toluene, n-hexane, acetone, water, and acetone and subsequently dried at 125 ºC. The Si samples were cleaned ultrasonically three times in chloroform and were put in Piranha solution consisting of 70 % H_2SO_4 and 30 % H_2O_2 for 30 min. After thorough rinsing with water, acetone and n-hexane, the samples were dried at room temperature.

Plasma polymerisation. The plasma apparatus consisted of a tubular glass reactor with three externally placed, capacitively coupled electrodes.[16] The powered (hot) electrode was placed at the centre of the reactor. Two glass plates were placed between the hot and the grounded (cold) electrodes, which were positioned at 30 cm on either side of the hot electrode. The flow of monomer

vapour through the reactor was regulated using needle valves and calculated from the time needed to obtain a certain pressure increase, once pumping of the reactor was stopped, assuming ideal gas behaviour. The flow of non-condensing gases was controlled by mass flow controllers (MKS Instruments, Andover, USA). The system (without the substrates) was first cleaned by applying an air plasma (5 sccm/min, 125 W, 0.13 mbar) for 60 min. The substrates were placed in the centre between the hot and cold electrode at the side of the monomer inlet and the reactor was evacuated to $< 5.10^{-3}$ mbar. The substrates were cleaned with an air plasma (5 sccm/min, 85 W, 0.13 mbar) for 5 min, after which the reactor was again evacuated to $< 5.10^{-3}$ mbar. Subsequently, a monomer flow was established through the reactor and after 1 min, pulsed plasma depositions were carried out. For each monomer the conditions were chosen such that a homogeneous plasma was obtained at the lowest possible power input (Table 6.1). The on time was always 1 s. The off time was chosen such that the reactor was replenished with new monomer during this period (see also Table 6.1). The mass increase of deposited PP layers was followed in situ with a QSG 301 (Balzers, Utrecht, the Netherlands) quartz crystal thickness monitor (QCM). The density was set at 2.0 g/cm^3 for convenience of data processing. After deposition, the monomer flow was sustained for another 2 min and the reactor was brought to atmospheric pressure with air. The samples were stored at –18 ºC.

Table 6.1. Conditions used for the plasma deposition of thiophene and thiophene derivatives. Plasma "on" time was always 1 s.

	2,5-DiClT	**2,5-DiBrT**	**3,4-DiBrT**	**2,5-DiMeT**	**2-ClT**	**2-BrT**	**2-MeT**	**3-BrT**	**3-MeT**	**T**
Pressure [mbar]	0.038	0.024	0.017	0.04	0.05	0.045	0.06	0.043	0.05	0.06
Power [W]	30-31	20-22	20	24-25	19-20	17-21	18-21	19-22	30-31	21
Off time [s]	7.5	15	20	5	6	7.5	5	7.5	6	5

Characterisation of plasma phase. MS was carried out to analyse the gas composition at the outlet of the reactor. The spectrometer was a differentially pumped QMS 421 mass spectrometer (Balzers, Utrecht, the Netherlands). The gas was introduced into the MS using a leak valve. The MS spectra were corrected for pressure differences by dividing the ion current by the pressure in the spectrometer. In this way, ion currents of a certain mass can be compared, as they were concentrations.

OES analysis was carried out using an MCPD-1000 spectrophotometer (Otsuka, Osaka, Japan) with a slit width of 0.2 mm. The measuring probe was placed at the reactor entrance, in line of sight of the plasma. Spectra were recorded from 180 to 875 nm with a step width of 2 nm.

For practical reasons a continuous plasma was used for both the MS and the OES measurements.

Characterisation of the PP layers. The thickness of PP layers deposited on Si samples was determined with a variable angle ellipsometer with a QTH 200 lightsource, a M44 detector, and an EC 120 control module (J.A. Woollam Co., Lincoln, NE, USA). In the fitting procedure, a two-layer model (Cauchy-layer on top of a Si-substrate) was used. The thickness and the Cauchy parameters (A and b) were adjusted iteratively to obtain an optimal fit. A Levenberg-Marquardt algorithm was used for the minimisation of the mean-squared error between the fit and the experimental data.[26]

XPS analysis was carried out on PP layers deposited on glass discs (∅ 1.5 cm) using an S probe (Surface Science Instruments, Mountain View, CA, USA) with a monochromatic Al K_α source (1486.6 eV). The input power was 220 W and the analysed spot size was 250 × 1000 μm. Survey scans (1100-0 eV binding energy (BE) window) were recorded with a pass energy (PE) of 150 eV. The concentrations of the various elements were calculated from the relative peak areas, using sensitivity factors (SF) from literature.[27] High-resolution (HR) detail scans (20 eV BE window) were taken at 50 eV PE.

For FTIR analysis, PP layers were deposited on gold-coated glass discs (∅ 2.5 cm) and spectra were recorded using a BioRad FTS-60 (Cambridge, UK) in the reflectance mode. A background spectrum was recorded using a clean substrate.

The conductivity of the PP layers was determined using specially designed substrates for the plasma deposition[16] (configuration in accordance with ASTM D257). During plasma deposition, the extensions of the electrodes were covered with glass slides to locally prevent deposition, thus ensuring a good contact with the measurement leads. After deposition, the samples were doped for 5 min by placing them in a sealed container containing iodine crystals. Two electrometers (Keithley Instruments, Cleveland, USA) were used to apply a current over the outer electrodes and to measure the voltage over the inner electrodes. After applying the current for 1 min, the voltage was read. The volume conductivity of the deposited layer was calculated with the appropriate formulas.[16]

For PP layers that were soluble in CH_2Cl_2 (determined with ellipsometry), nuclear magnetic resonance (NMR) measurements were carried out in CD_2Cl_2 on a Varian 400 (Varian, Palo Alto, CA, USA). Both ^1H and ^1H-^{13}C correlation spectra were collected at 400 and 100.6 MHz, respectively.

Results and Discussion

Plasma polymerisation. QCM measurements (e.g., in Figure 6.1) showed that in all cases deposition only takes place during the plasma "on" time. This was also found by Uchida *et al.* for the plasma polymerisation of acetylene.[28,29] These results exclude a chain-growth mechanism during the "off" time of radicals produced during the plasma "on" time, as suggested by Ryan *et al.*[30]

Because formation of the PP layer only takes place during the plasma "on" time, the deposition rate can be calculated from the thickness (determined with ellipsometry) and the total plasma "on" time (Figure 6.2).

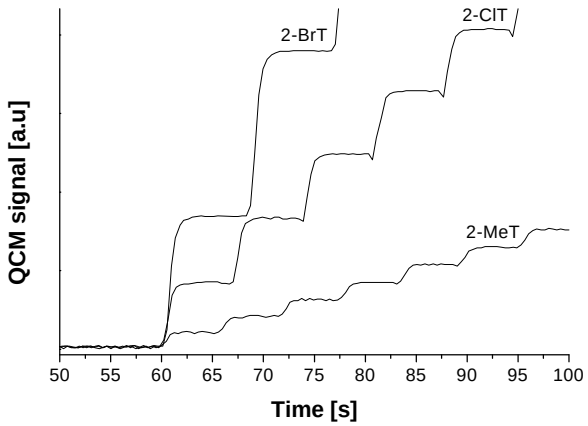

Figure 6.1. QCM signal as a function of time during pulsed (1 s on) plasma polymerisation of 2-substituted thiophene derivatives. First pulse was generated at t = 60 s. For plasma conditions see Table 6.1.

Within a series, the halogenated thiophenes show a higher deposition rate than the MeT's, with a faster deposition for the ClT's than for the BrT's. Comparing these data with the amount of fragmentation observed in a previous study,[17] it appears that more fragmentation results in a higher deposition rate. This is consistent with the deposition mechanism proposed by Yasuda *et al.*,[19,24,25] in which PP layers are formed by recombination of radicals in the gas phase and at the surface. Fragmentation increases the number of radicals, which consequently results in an increase in deposition rate.

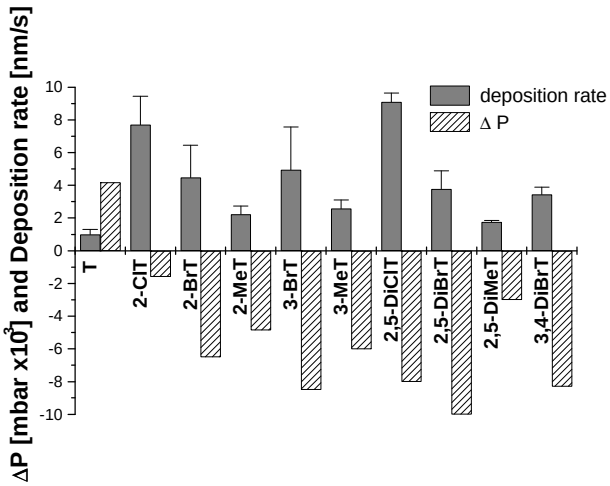

Figure 6.2. Deposition rate (calculated form the total plasma "on" time and the thickness determined with ellipsometry, n = 3 ± sd) and pressure difference between plasma "on" and "off" for plasmas of thiophene and thiophene derivatives. For plasma conditions see Table 6.1.

The pressure difference upon plasma generation is directly related to the difference in the number of particles in the reactor via the gas law, assuming that the temperature remains constant. Other measurements showed that this assumption is valid for a number of plasmas (e.g., CO_2, CF_4) for plasma "on" times < 10 s.[31] During plasma polymerisation, plasma species are brought in by flow (monomer) and are generated by fragmentation, whereas they are removed by flow, deposition, and recombination. If it is assumed that, when the pressure differences are small, the flow of condensable species in and out of the reactor is the same,[19] the loss of particles from the reactor due to deposition is related to the deposition rate, assuming that the relation between molecular weight and density is equal for all PP layers. The maximal pressure difference in the reactor between plasma "on" and "off" (also shown in Figure 6.2) can thus be related to the fragmentation and recombination in the plasma phase.

Of all monomers, only thiophene shows an increase in pressure upon plasma generation. In combination with the low deposition rate (i.e., low fragmentation), this indicates that noncondensable species are formed. For the other monomers a negative pressure difference is observed, which shows that the generation of particles by fragmentation is less than the removal of particles by recombination and deposition in these cases. The combination of a high deposition rate together with a small pressure difference upon plasma generation for 2-ClT shows that a relatively high amount of fragmentation occurs. The DiBrT's show just the opposite behaviour of 2-ClT, indicating that recombination in the plasma phase is relatively high for these monomers. The other pressure differences are more or less consistent with the deposition rates.

Characterisation of the plasma phase. In a previous study, OES measurements were carried out to determine the emitting species present in the plasma.[17] It was found that the intensity of the peak corresponding to CS species in a series increased in the order MeT<T<BrT<ClT. Furthermore, for a specific substituent, substitution on the 3-position resulted in a higher amount of CS formation than substitution on the 2-position. Disubstituted thiophenes always showed less CS formation than their mono-substituted analogues.

The OES spectra of the plasmas of the DiBrT's are depicted in Figure 6.3. Atomic bromine and Br_2 are observed in the OES spectra of both DiBrT's, which were almost not detected for the mono-BrT's. Apparently, the presence of a second bromine group facilitates liberation of bromine. Furthermore, the lower CS formation in the 3,4-DiBrT plasma compared with 2,5-DiBrT shows an influence of the position of substitution on the fragmentation that is opposite of what was observed earlier (i.e., 3-substitution more CS formation than 2-substitution). This indicates that different processes take place in the plasmas of DiBrT's and mono-BrT's.

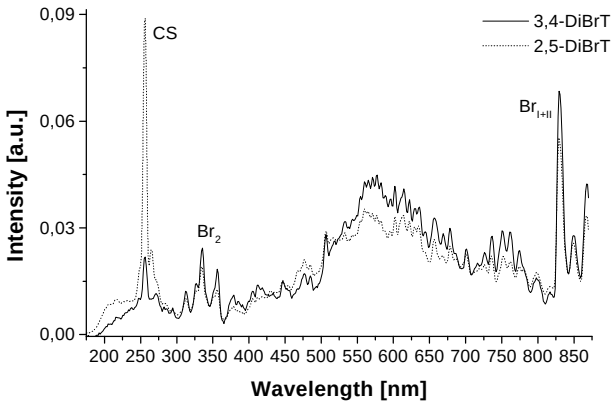

Figure 6.3. OES spectra of plasmas from 2,5-DiBrT (dotted line) and 3,4-diBrT (solid line). For plasma conditions see Table 6.1.

When longer plasma times were applied, a colour change was observed for the DiBrT's during the first few seconds of plasma generation. Although depositions were carried out with an "on" time of 1 s, this phenomenon is interesting in view of the mechanism and because deposited PP layers are exposed to the plasma for longer times than 1 s. Therefore, OES spectra were taken continuously during plasma generation of 10 s (Figure 6.4).

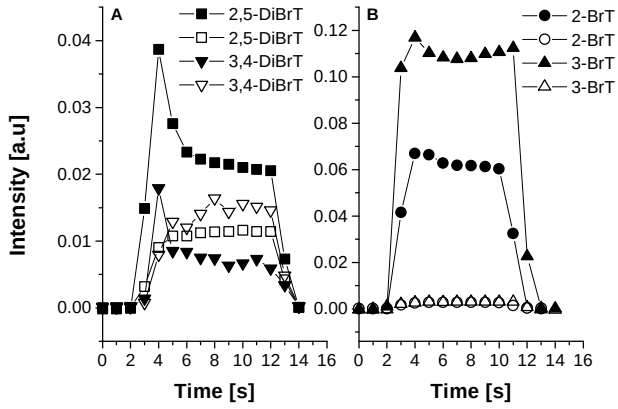

Figure 6.4. Intensity of the peaks at 257 nm (CS, solid symbols) and 829 nm (Br_{I+II}, open symbols) in the OES spectra of (A) DiBrT's (2,5-DiBrT, squares and 3,4-diBrT, down-triangle) and of (B) mono-substituted BrT's (2-BrT, circles and 3-BrT, up-triangle) as a function of time. Plasma is turned on at t ≈ 2 s for a duration of 10 s. For plasma conditions see Table 6.1.

For the DiBrT's, the peak corresponding to CS species (257 nm) shows a maximum just after the plasma was turned on, whereas later on, the peak corresponding to atomic bromine (829 nm) levels off to its maximal value. The initial "burst" in the CS peak is probably due to the impact of electrons that in a plasma have a high mobility and sufficient energy to break chemical bonds (3-5 eV).[1] The decrease in the CS peak suggests that the absorption of

UV light induces the liberation of bromine. In a plasma, many pathways for energy dissipation can be followed.[20] The path requiring the least energy is favoured over others, although these may still occur. Consequently, the amount of liberated bromine is related to the ease with which the C-Br bond is broken. For the mono-BrT's, the decrease in intensity of the CS peak relative to the increase in atomic bromine is less than for the DiBrT's, showing that the presence of a second bromine weakens the C-Br bond. Dissociation of the C-Br bond is further facilitated because the radical generated by this process is stabilised by the remaining bromine substituent. The higher deposition rate for the DiBrT's compared with the mono-BrT's (see Figure 6.2) confirms this explanation. The liberated bromine radical can pick up an electron or recombine to Br_2. For the mono-BrT's, the resulting radical on the thiophene ring is less stabilised, which makes this process unfavourable relative to other processes (e.g., hydrogen liberation).[19] There might also be a difference in absorption at 257 nm between the mono- and di-BrT's, but considering the energy of the UV light generated by the CS species (4.6 eV) in relation to the C-Br bond energy (3.8 eV), it is not expected to have such a pronounced effect. It can therefore be concluded that the number of substituents has an effect on energetically favourable pathway of energy dissipation.

The intensity of the bromine peak relative to the decrease in intensity of the CS peak after the initial burst is higher for 3,4-DiBrT than for 2,5-Di-BrT. This implies that the liberation of bromine from 2,5-DiBrT requires more energy compared with 3,4-DiBrT, showing an effect of substituent position. In 3,4-DiBrT, the remaining bromine group is adjacent to the leaving bromine, whereas for 2,5-DiBrT the electronegative effects (both the weakening of the C-Br bond and the stabilisation of the resulting radical) have to be transferred over a number of bonds. This may result in a lowering of the energy required for the bromine liberation process for 3,4-DiBrT compared with 2,5-DiBrT.

The much higher CS peak for 2,5-DiBrT compared with 3,4-DiBrT can be explained by the fact that bromine liberation from 2,5-DiBrT generates a radical on the carbon atom that is also involved in a relatively unstable C-S bond. For the mono-BrT's the opposite effect of substituent position on the CS peak was found, i.e., higher for 3-BrT than for 2-BrT. This suggests that in these cases liberation of hydrogen is favoured over bromine. The OES results of the mono-BrT's would then imply that substitution on the 3-position weakens the C-H bond on the 2-position more than the other way around. A similar substitution effect is observed for the reactivity of thiophene derivatives towards nucleophiles and radicals,[32,33] which increases with increasing electron affinity of the substituent. The C-H bond is becoming increasingly electron poor (i.e., weakened) with increasing electron affinity of the

substituent. This makes dissociation of the C-H bond easier, irrespective of the process (e.g., UV absorption, electron impact). The CS formation (Me < T < Br < Cl, and 3- > 2-substitution)[17] and the deposition rates (Figure 6.2) are therefore consistent with the proposed mechanism of CS formation by radical formation on the carbon adjacent to sulphur, and explains the effect of substituent nature and position on fragmentation.

This explanation is confirmed by the MS results from a previous study.[17] For all halogenated thiophenes an intense H_2 peak was observed, whereas for T and the MeT's the H_2 concentration was much lower. Furthermore, the H_2 concentration in the 3-BrT plasma was higher than in the 2-BrT plasma. H_2 is formed upon abstraction of hydrogen atoms by or recombination of hydrogen radicals, the former process being less favourable.[34]

HCl was detected in the ClT plasmas, while no HBr was observed in the plasmas of the BrT's.[17] A H-Halogen species can be formed by a number of processes (e.g., recombination of halogen radicals with hydrogen radicals, abstraction of halogen atoms by hydrogen radicals or visa versa). Considering the small difference in bond energy between the C-Br and the C-Cl bond, chlorine radicals will probably also be formed. Recombination of radicals is an exothermic process, as is the abstraction of halogens by hydrogen radicals and of hydrogen atoms by chlorine radicals.[34] In contrast, the abstraction of hydrogen atoms by bromine radicals is endothermic. Furthermore, the formation of H_2 and a halogen radical by the impact of a hydrogen radical on a H-halogen species is energetically much less favourable for HCl (-5 kJ/mol) than for HBr (-69 kJ/mol). This implies that when HBr is formed it will not be stable in a plasma, which explains why HBr is not detected whereas HCl is. The lower H_2 concentration observed for the ClT's compared with the BrT's confirms this explanation.

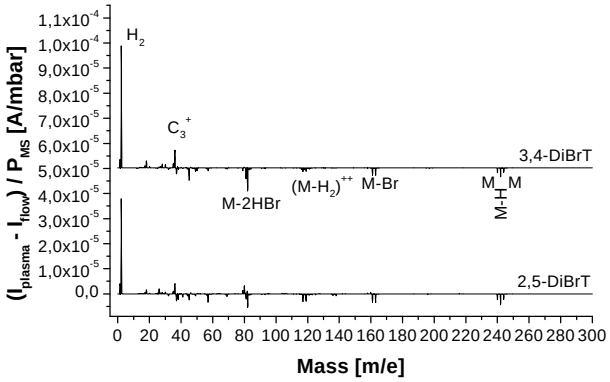

Figure 6.5. Difference MS spectra (calculated by subtracting the MS spectrum of the monomer flow without plasma generation from the MS spectrum of the monomer flow with plasma generation, both divided by the pressure in the mass spectrometer during measurement) of DiBrT's. An offset is used for clarity. For plasma conditions see Table 6.1.

Between the MS spectra of the DiBrT's (Figure 6.5) hardly any difference is observed. This implies that the CS and bromine species observed in the OES spectra are either deposited before they reach the MS and/or are transformed (either by the plasma or the MS) into species that cannot be detected by the MS. The H_2 concentration in a DiBrT plasma is higher than in a plasma of their mono-substituted analogues,[17] which can be explained by the facilitating effect of the second bromine substituent on the liberation/abstraction of both bromine and hydrogen. Analogously, the production of H_2 and HCl is higher in a plasma of 2,5-DiClT than of 2-ClT.[17] The H_2 concentration was higher for the MeT's than for T, while the CS formation was lower.[17] Together with the slightly higher deposition rates for the MeT's, this indicates that for the MeT's an other pathway resulting in hydrogen liberation takes place.

Summarising, it can be concluded that the position, number, and nature of the substituent(s) influence the deposition process via the site and ease of radical formation.

Characterisation of the PP layers. The chemical composition of the PP layers was determined with XPS (Table 6.2). The halogen removal from halogenated thiophenes is apparent from the lower than theoretical halogen content. The loss of chlorine from 2-ClT is relatively high, compared with the loss of bromine from the mono-BrT's. Together with the high C/S ratio[16] of the PP-ClT layers, this corresponds well with the high amount of fragmentation observed in these cases as measured with OES and MS.[17] For T and the MeT's, the carbon concentration relative to the sulphur concentration is lower than expected from theory, while for the other monomers the C/S ratio is equal to or higher than the theoretical value. Considering the OES results, it seems that PP layers deposited from monomers showing little fragmentation during deposition contain relatively more sulphur. This is consistent with the results obtained in an earlier study on the effect of deposition conditions on fragmentation of thiophene.[16] No difference between the DiBrT's is observed, which agrees well with the MS results. Earlier it was found that only the PP-MeT layers contained conjugated structures detectable by XPS.[17] Together with the observed OES (lower CS formation than T) and MS (more H_2 formation than T) results this shows that a pathway resulting in hydrogen liberation other than hydrogen liberation from the thiophene ring takes place for the MeT's.

Table 6.2. Chemical composition (determined with XPS) at the surface of PP layers of thiophene and thiophene derivatives ($n \geq 3 \pm sd$).

Monomer	PP layer	C (atom%)	S (atom%)	Halogen (atom%)	O (atom%)
T	theory	80	20	-	-
	PPT	72.0 ± 0.1	23.6 ± 0.7	-	4.4 ± 0.7
2,5-DiMeT	theory	85.7	14.3	-	-
	PP-2,5-DiMeT	80.8 ± 0.3	17.5 ± 0.1	-	1.7 ± 0.3
DiHaloT	theory	57.1	14.3	28.6	-
	PP-2,5-DiClT	64.3 ± 0.4	13.2 ± 0.1	20.0 ± 0.6	2.5 ± 0.1
	PP-2,5-DiBrT	63.0 ± 1.3	16.2 ± 0.8	18.8 ± 0.4	2.0 ± 1.5
	PP-3,4-DiBrT	63.9 ± 0.5	15.6 ± 0.6	19.0 ± 1.1	1.4 ± 1.4
MeT	theory	83.3	16.7	-	-
	PP-2-MeT	79.8 ± 0.7	19.1 ± 0.1	-	1.1 ± 0.8
	PP-3-MeT	78.7 ± 1.3	18.5 ± 0.6	-	2.7 ± 1.9
HaloT	theory	66.7	16.7	16.7	-
	PP-2-ClT	72.1 ± 0.1	16.9 ± 0.1	6.8 ± 0.2	4.1 ± 0.2
	PP-2-BrT	68.3 ± 0.8	19.1 ± 0.2	11.2 ± 0.4	1.4 ± 1.0
	PP-3-BrT	67.2 ± 1.6	17.6 ± 0.8	12.4 ± 1.2	2.8± 2.0

FTIR measurements of the PP layers showed that only the PPT layer contained aliphatic CH_2 units, which explains the low H_2 peak in the MS spectrum.[17] Furthermore, terminal acetylene structures were present in the PPT and PP-ClT layers, whereas disubstituted acetylene units were only detected in the PP-2,5-DiClT layer. As this was not found in the FTIR spectra of the BrT's, this shows the importance of the abstraction of hydrogen by chlorine radicals in the deposition process. The FTIR spectra of the PP-MeT layers (Figure 6.6) show that the C-H bonds present in the monomer (α-H and β-H) are also present in the respective PP-MeT layers.[35] Together with the OES, MS, and XPS results this confirms that deposition does not proceed via hydrogen liberation from the thiophene ring. To study this further, NMR spectra were taken from the PP-MeT layers (Figure 6.7), which were the only ones that were soluble in CH_2Cl_2, as was determined with ellipsometry. The peaks at 1.4 and 5.25 ppm in Figure 6.7 are due to water and nondeuterated CD_2Cl_2, respectively. A spectrum of the residue after evaporation of a solvent sample revealed that the other peaks below 2 ppm are due to impurities in CH_2Cl_2.

Based on the reference spectra of the monomers[35] and the ^{1}H-^{13}C correlation spectra (data not shown), the peaks in the region δ = 6.5-7.5 ppm can be assigned to hydrogens on different positions on the thiophene ring. The peak around 2-2.5 ppm originates from hydrogen atoms in CH_3 groups.

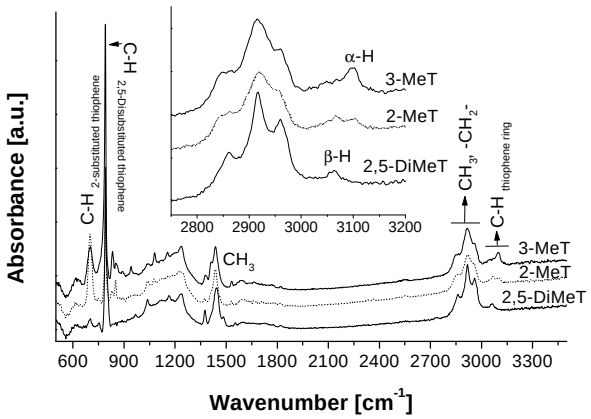

Figure 6.6. FTIR spectra of PP layers from pulsed (1 s on) plasmas of MeT's (2,5-DiMeT, bottom; 2-MeT, middle; 3-MeT, top). (CH, 2-substituted thiophene: 705 cm^{-1}; CH, 2,5-disubstitued thiophene: 796 cm^{-1}; CH_3: 2960 cm^{-1}; Aromatic -CH_3, -CH_2-: 2860, 2920 cm^{-1}; α-H, thiophene ring: 3060 cm^{-1}; β-H, thiophene ring: 3100 cm^{-1}; -C≡**C-H**: 3288 cm^{-1}). An offset is used for clarity. For plasma conditions see Table 6.1.

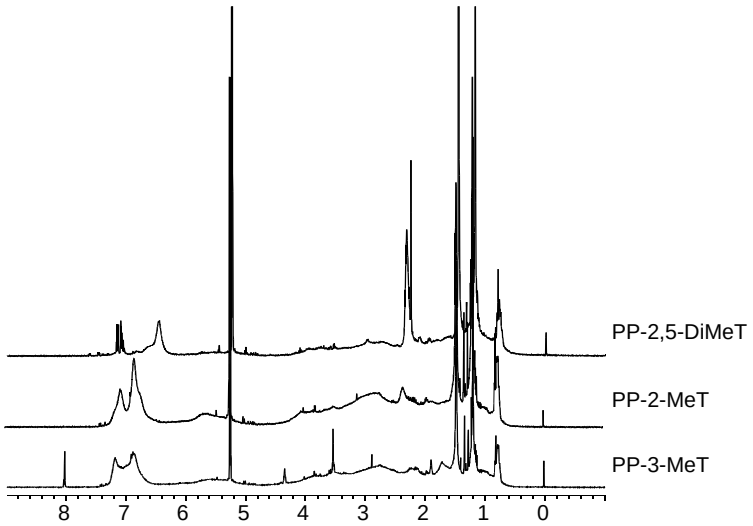

Figure 6.7. ^{1}H NMR spectra of PP layers from pulsed (1s on) plasmas of MeT's (2,5-DiMeT, top; 2-MeT, middle; 3-MeT, bottom) in CD_2Cl_2. (1.4 (H_2O), 2-2.5 (H, CH_3), 5.25 (nondeuterated CD_2Cl_2), 6.5-7.5 (H, thiophene ring) ppm). An offset was used for reasons of clarity. For plasma conditions see Table 6.1.

In all NMR spectra, the thiophene hydrogens as expected from the monomer structure are present. Some other peaks are also observed but they represent only very small amounts of H atoms. Furthermore, it cannot be excluded that small amounts of aliphatic C-H bonds are formed that would show peaks in the same region as the impurities of the solvent. This shows that almost no fragmentation of the thiophene ring occurs, while some rearrangement of hydrogen atoms has also taken place.[35] This is in good agreement with the OES, MS and FTIR results (Figure 6.6 and previous study[17]). Quantitative analysis showed that the H atoms on the thiophene ring are preserved to a greater extent relative to the H atoms in the CH_3 groups, which shows that polymerisation proceeds via dissociation of either the C-H bond in the CH_3 group or the thiophene-CH_3 bond. In the plasma polymerisation of toluene it was observed that at 1 mbar the dissociation of the C-CH_3 bond and the C-H bond of the CH_3 groups are equally favoured, while almost no hydrogen was lost from the benzene ring.[2] In our case, the low CS formation observed for the MeT's is not in accordance with a mechanism involving dissociation of the thiophene-CH_3 bond, whereas the radical formed upon dissociation of the C-H bond of the CH_3 group would be stabilised by resonance. The OES (lower CS formation than T) and MS (higher H_2 formation than T) results also suggest that deposition occurs via the liberation of the H atom from the CH_3 substituent. Based on the NMR and FTIR results, the formation of aliphatic CH_2 groups cannot be excluded. It is therefore concluded that deposition takes place via liberation of a H atom from the CH_3 substituent.

The conductivity of the PP layers after 5 min iodine doping is shown in Figure 6.8. The same trends were also observed after longer doping times (data not shown), although the absolute values differed to some extent. Figure 6.8 can thus be considered as representative for the conductivity of the PP layers. Combining Figure 6.8 with Figure 6.2, it becomes clear that a high deposition rate results in a low conductivity of the deposited PP layer. As shown above, a high deposition rate corresponds to a high amount of fragmentation during deposition. In an earlier study the same relation between fragmentation and conductivity was found for thiophene.[16]

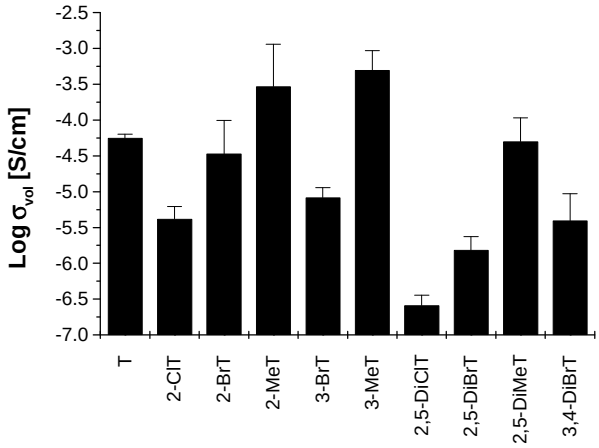

Figure 6.8. Logarithm of the volume conductivity (S/cm) of PP layers from thiophene and thiophene derivatives after 5 min iodine doping (n = 3 ± sd). For plasma conditions see Table 6.1.

The relation between the monomer structure, mechanism of deposition, and PP layer characteristics becomes clear when the results of all analysis techniques are taken into account. For instance, for the DiBrT's deposition probably proceeds via bromine liberation (Figure 6.3). Due to the position of radical formation, more fragmentation occurs for 2,5-DiBrT than for 3,4-DiBrT (Figure 6.3 and Figure 6.4), with a corresponding lower conductivity for 2,5-DiBrT (Figure 6.8). For the mono-BrT's liberation of bromine is unfavourable (Figure 6.4), resulting in a different deposition mechanism (hydrogen liberation[17]). This gives rise to radical formation on a different position on the thiophene ring compared with the DiBrT's, resulting in more fragmentation for 3-BrT than for 2-BrT. Therefore, the conductivity of the PP-2-BrT layer is higher than the PP-3-BrT layer. For the MeT's, deposition proceeds mainly via the methyl substituent (Figure 6.6 and XPS results previous study[17]) and therefore the thiophene ring is hardly fragmented (Figure 6.7), which results in a high conductivity after iodine doping (Figure 6.8). This shows that the monomer structure can effectively be used to influence the deposition mechanism via the ease and position of radical formation, thereby affecting the retention of the thiophene ring in the PP layer and thus the conductivity of the resulting PP layer.

Conclusions

The deposition of thiophene and thiophene derivatives by plasma polymerisation most probably proceeds by a mechanism involving radicals, which are generated via the most favourable energy dissipation path. The nature, number, and position of substituents on thiophene influence the deposition process via the ease and site of radical formation. With increasing electronaffinity of the substituent(s) the dissociation of the adjacent C-H and the C-substituent bond are increasingly facilitated. An increase in the number of substituents facilitates dissociation of the adjacent C-substituent bond. The position of substituent(s) affects the fragmentation during deposition of the thiophene ring via the position on which the radical is formed, with a higher fragmentation for radicals formed on carbon atoms also attached to sulphur, compared with other carbon atoms. An increase in fragmentation during deposition gives rise to an increase in deposition rate and a decrease in conductivity. Consequently, the number, position, and nature of substituents can be effectively used to alter the ease and position of radical formation, thereby affecting fragmentation during deposition and thus the characteristics of the resulting PP layer.

Acknowledgements

The authors thank Joop de Vries from Groningen University (Groningen, the Netherlands) and VG Scientific (East-Grinstead, UK) for performing the high resolution XPS measurements.

References

[1] Terlingen, J. G. A. *Introduction of functional groups at polymer surfaces by glow discharge techniques*; University of Twente: Enschede, **1993**.

[2] Suhr, H. In *Techniques and applications of plama chemistry*; Hollahan, J. and Bell, A. T., Ed.; Wiley: New York, **1974**, pp 57-111.

[3] Coburn, J. W.; Chen, M. *J. Appl. Phys.* **1980**, *51*, 3134-3136.

[4] Gazicki, M.; Yasuda, H. *J. Appl. Pol. Sci., Appl. Pol. Symp.* **1984**, *38*, 35-44.

[5] d'Agostino, R. *Plasma deposition, treatment, and etching of polymers*; Academic Press: Boston, **1990**.

[6] *Techniques and applications of plasma chemistry*; Hollahan, J. and Bell, A. T., Ed.; John Wiley & Sons: New York, **1974**.

[7] Tourillon, G. In *Handbook of conducting polymers*; Skotheim, T. A., Ed.; Marcel Dekker: New York, **1986**; Vol. 1, pp 293-350.

[8] Tanaka, K.; Yoshizawa, K.; Takeuchi, T.; Yamabe, T.; Yamauchi, J. *Synth. Met.* **1990**, *38*, 107-116.

[9] Tanaka, K.; Yamabe, T.; Takeuchi, T.; Yoshizawa, K.; Nishio, S. *J. Appl. Phys.* **1991**, *70*, 5653-5660.

[10] Sadhir, R. K.; K.F. Schoch, J. *Polym. Prepr.* **1992**, *33*, 412-413.

[11] Sadhir, R.; K.F. Schoch, J. *Thin Solid Films* **1993**, *223*, 154-160.

[12] Sadhir, R.; K.F. Schoch, J. *Polym. Prepr.* **1995**, *34*, 679-680.

[13] Tanaka, K.; Okazaki, S.; Inomata, T.; Kogoma, M. *8th Symp. Plasma Sci. Mater*., **1995**, pp 33-37.

[14] Giungato, P.; Ferrara, M. C.; Musio, F.; d'Agostino, R. *Plasmas Polym.* **1996**, *1*, 283-297.

[15] Kiesow, A.; Heilmann, A. *Thin Solid Films* **1999**, *344*, 338-341.

[16] Groenewoud, L. M. H.; Engbers, G. H. M.; Terlingen, J. G. A.; Wormeester, H.; Feijen, J. *Langmuir* **2000**, *16*, 6278-6286.

[17] Groenewoud, L. M. H.; Engbers, G. H. M.; Feijen, J. *Langmuir* **2000**, *submitted*.

[18] *Thiophene and its derivatives*; Gronowitz, S., Ed.; J. Wiley & Sons: New York, **1985**.

[19] Yasuda, H. *Plasma polymerization*; Academic Press: Orlando, **1985**.

[20] Polak, L. S.; Lebedev, Y. A. *Plasma Chemistry*; 1st ed.; Cambridge International Sci. Publ.: Cambridge, **1998**.

[21] Inagaki, N. *Plasma Surface Modification and Plasma Polymerization*; Technomic Publishing Co. Inc.: Lancaster, **1996**.

[22] O'Toole, L.; Beck, A. J.; Ameen, A. P.; Jones, F. R.; Short, R. D. *J. Chem. Soc. Faraday Trans.* **1995**, *91*, 3907-3912.

[23] O'Toole, L.; Short, R. D. *J. Chem. Soc. Faraday Trans.* **1997**, *93*, 1141-1145.

[24] Yasuda, H. *J. Macromol. Sci.* **1976**, *A10*, 383-420.

[25] Yasuda, H.; Yasuda, T. *J. Polym. Sci. Part A: Polym. Chem.* **2000**, *38*, 943-953.

[26] Jellison, G. E. j. *Thin Solid Films* **1998**, *33*, 313-314.

[27] Wagner *Surf. Interface Anal.* **1981**, *3*, 211-225.

[28] Uchida, T.; Senda, K.; Vinogradov, G. K.; Morita, S. *Thin Solid Films* **1996**, *281-282*, 536-538.

[29] Uchida, T.; Vinogradov, G. K.; Morita, S. *J. Electrochem. Soc.* **1997**, *144*, 1434-1439.

[30] Ryan, M. E.; Hynes, A. M.; Wheale, S. H.; Badyal, J. P. S.; Hardacre, C.; Ormerod, R. M. *Chem. Mater.* **1996**, *8*, 916-921.

[31] OldeRiekerink, M. B., personal communication.

[32] Porter, A. E. A. In *Thiophene and its derivatives*; Gronowitz, S., Ed.; J. Wiley & Sons: New York, **1985**; Vol. 1.

[33] Spinelli, D.; Consiglio, G.; Dell'erba, C.; Novi, M. In *Thiophene and its derivatives*; Gronowitz, S., Ed.; John Wiley & Sons: New York, **1985**; Vol. 44.

[34] Solomons, T. W. G. *Organic Chemistry*; 3rd ed.; John Wiley & Sons: New York, **1988**.

[35] http://www.aist.go.jp/RIODB/SDBS/menu-e.html .

7

On the iodine doping process of plasma polymerised thiophene layers*

To make a fair comparison of the conductive properties of plasma polymerised thiophene (PPT) layers deposited under different conditions, optimal doping procedures should be applied. The iodine doping process of PPT layers deposited at high (HP) and low (LP) pressure has been studied in detail. Doping time, thickness, and exposure time to air before and after doping were varied. Iodine doping generates charge carriers by the formation of charge transfer (CT) complexes, which are in equilibrium with absorbed iodine. The conductivity of the LP-PPT layers decreases with increasing thickness due to (vacuum-) UV modification. Upon exposure to air before doping, LP-PPT layers loose their capability to form CT complexes, whereas the HP-PPT layers do not. Consequently, the conductivity for LP-PPT layers exposed to air before doping decreases with exposure time. After iodine doping, a lower rate of oxidation upon exposure to air is observed compared with as deposited PPT layers. Furthermore, the conductivity decreases slowly due to diffusion of absorbed iodine out of the PPT layers. The conductivity of the HP-PPT layers increases faster with doping time and shows a higher stability towards exposure to air after doping than LP-PPT layers. Consequently, the optimal doping procedure may vary for PPT layers deposited under different conditions.

Introduction

Plasma polymerisation can be used to obtain very thin, pinhole-free, and tightly adhering layers on almost any substrate.[1,2] When monomers are used that yield conjugated structures upon plasma polymerisation, the deposited layers may become conductive after the introduction of charge carriers by dopants.[3-5] Iodine is frequently used as a dopant because of the ease of the doping procedure. It was shown by several techniques (e.g., UV and X-ray induced photoelectron spectroscopy (UPS and XPS), Raman, and UV-Vis spectroscopy) that, next to absorbed I_2, charge transfer (CT) complexes in the form of I_3^- and/or I_5^- are formed upon iodine doping of polyacetylene.[6-8] The same CT complexes of iodine were found after iodine doping of other conjugated polymers,[9-13] trimers,[14] and monomers.[15] It is now generally accepted that the conductivity in conjugated polymers after doping is governed by the charge carriers generated by these CT complexes.

As doped polythiophene is known for its high and stable conductivity,[16] thiophene is often used as a monomer in plasma polymerisation.[17-25] In an earlier study we have shown that the amount of incorporated thiophene structures in plasma polymerised thiophene (PPT) layers increases with decreasing degree of fragmentation during deposition.[25] In our experimental setting, pressure was the only process parameter which influenced the degree of

* The work described in this chapter has been submitted for publication in *Synthetic Metals*.

fragmentation during deposition. At high pressure fragmentation is suppressed and, with the doping procedure used, a higher conductivity was found for PPT layers deposited at high pressure (0.3 mbar) as compared to PPT layers deposited at low pressure (0.06 mbar).

It is known that iodine reacts with non-conjugated unsaturated structures in rubbers,[26,27] whereas it forms CT complexes with conjugated structures in polyacetylene.[6-8] Due to fragmentation, the PPT layers contain different chemical structures, of which the type and amount are influenced by the deposition conditions. The effect of iodine doping may be different for these different chemical structures. Furthermore, PPT layers contain a considerable amount of radicals and other unstable entities that can react with atmospheric oxygen after deposition. Consequently, the time and the exposure conditions between deposition and doping might be important factors for the conductivity of the PPT layers. To form CT complexes, iodine has to diffuse into the PPT layers,[28] requiring adequate doping times with respect to the thickness of the layer.

In the cited studies on PPT layers, optimisation of the doping procedure in order to obtain a maximal conductivity of the PPT layers was not performed. The doping time varied from 5 min[25] to overnight,[19-21] irrespective of the thickness of the layer, whereas sometimes vacuum was applied after doping to remove excess iodine.[22] To make a fair comparison of the conductive properties of PPT layers deposited under different conditions, optimal doping procedures should be applied. Furthermore, the conductive properties of doped PPT layers should be related to the chemical structure of the PPT layer before and after doping.

In the present study, PPT layers deposited at high (HP) and low (LP) pressure having different chemical structures were doped with iodine. To study the effect of the diffusion of iodine on the conductivity, PPT layers of varying thickness were doped with iodine for different times. The effect of exposure of the PPT layers to atmospheric conditions for various times before and after doping on the conductivity was also investigated. Characterisation of the PPT layers was carried out using XPS, Fourier transform infrared spectroscopy (FTIR), and conductivity measurements.

Experimental

Materials. Thiophene (99,5% purity) and iodine (doubly sublimated) were purchased from Merck (Darmstadt, Germany) and used as received. All solvents were of analytical grade purity and purchased from Biosolve (Valkenswaard, the Netherlands). Water used was doubly deionised. Glass slides (∅ 2.5 cm, used for FTIR analysis) with a sputtered chromium and gold layer were obtained from the FFW division (University of Twente, Enschede, the Netherlands). Glass slides (∅ 1.5 cm, used for XPS analysis) were purchased from Knittel (Braunschweig, Germany). The samples used for the conductivity measurements (glass slides with four parallel electrodes with extensions to contact

areas for the measurement leads,[25] configuration in accordance with ASTM D257) were supplied by the MESA Institute (University of Twente, Enschede, the Netherlands).

Cleaning. All glassware, substrates and tools were cleaned ultrasonically, consecutively three times in toluene, n-hexane, acetone, water, and acetone and subsequently dried at 125 ºC.

Plasma polymerisation. The plasma apparatus consisted of a tubular glass reactor with three externally placed, capacitively coupled electrodes.[25] The powered (hot) electrode was placed at the centre of the reactor. Two glass plates were placed between the hot and the grounded (cold) electrodes, which were positioned at 30 cm on either side of the hot electrode. The flow of monomer vapour through the reactor was regulated using needle valves and calculated from the time needed to obtain a certain pressure increase, once pumping of the reactor was stopped, assuming ideal gas behaviour. Mass flow controllers (MKS Instruments, Andover, USA) controlled the flow of noncondensing gases. The system (without the substrates) was first cleaned by applying an air plasma (5 sccm/min, 125 W, 0.13 mbar) for 60 min. The substrates were placed at the centre between the hot and cold electrode at the side of the monomer inlet and the reactor was evacuated to $< 5.10^{-3}$ mbar. The substrates were cleaned with an air plasma (5 sccm/min, 85 W, 0.13 mbar) for 5 min, after which the reactor was again evacuated to $< 5.10^{-3}$ mbar. Subsequently, a monomer flow was established through the reactor and after 2 min, pulsed plasma depositions (10 s on, 10 s off) were carried out. The starting pressure (0.06 and 0.3 mbar) and the number of pulses were varied to obtain PPT layers of varying chemical structure and thickness. After deposition, the monomer flow was sustained for another 2 min and the reactor was brought to atmospheric pressure with air. The samples were stored at -18 ºC.

Characterisation of PPT layers. The thickness of PPT layers deposited on the samples used for the conductivity measurements was determined with a Dektak IIA (Sloan Technology Corporation, Santa Barbara, USA). During plasma deposition, the extensions of the electrodes were covered with glass slides to locally prevent deposition, thus enabling a good contact with the measurement leads for the conductivity measurements. The needle was moved over the boundary between areas of the substrate, which were covered and not covered during plasma deposition. The height difference was taken as the thickness of the deposited layer.

The conductivity of the PPT layers was determined using specially designed substrates for the plasma deposition.[25] Two Keithley 617 Electrometers (Keithley Instruments, Cleveland, USA) were used to apply a current over the outer electrodes and to measure the voltage over the inner electrodes. After applying the current for 1 min, the voltage was read. The volume conductivity of the deposited layer was calculated using the appropriate formulas (ASTM D257).

The samples were doped by placing them in a sealed container containing iodine crystals for a certain period of time. If applicable, samples were subjected to atmospheric conditions at room temperature before and after iodine doping.

For FTIR analysis, PPT layers were deposited on gold-coated glass discs (∅ 2.5 cm) and spectra were recorded using a BioRad FTS-60 (Biorad, Cambridge, UK) in the reflectance mode. A background spectrum was recorded using a clean substrate.

XPS analysis of PPT layers was carried out on layers deposited on glass discs (∅ 1.5 cm) using a Kratos XSAM 800 (Manchester, UK) equipped with a Mg/Al K_α source (1253.6 and 1486.6 eV, respectively). The analyser was placed perpendicular to the sample surface. The input power was 150 W (10 mA, 15 kV). The analysed spot size was ∅ 6 mm. Survey scans (1100 - 0 eV binding energy (BE) window) were recorded with a pass energy (PE) of 100 eV and a dwell of 0.1 s. Relative peak areas for the different elements were calculated by numerical integration of the detail scans (20 eV BE window, 20 eV PE) using empirically determined sensitivity factors. After normalisation, the concentrations of the various elements were obtained.

High resolution (HR) XPS spectra (20 eV PE) were obtained using a VG Σ Probe (VG Scientific, East-Grinstead, UK) with a monochromatic Al K_α source (1486.6 eV, 400 μm spot size, 100 W). For each sample data were collected until the spectra were of sufficient quality.

Results & Discussion

Plasma polymerisation of thiophene. FTIR spectra of PPT layers deposited at high (HP) and low (LP) pressure are given in Figure 7.1.A. The absorption bands at 705 cm^{-1} and around 3100 cm^{-1} show that the thiophene structure is partly preserved in the PPT layers.[29,30] However, some terminal acetylene (3288 cm^{-1}) and aliphatic (2910 cm^{-1}) structures are also present, indicating that fragmentation has occurred. From Figure 7.1.B it is clear that the relative amount of preserved thiophene structures is higher for the HP-PPT layer than for the LP-PPT layer. An earlier study showed that, with the doping procedure used, this results in a higher conductivity after iodine doping for the HP-PPT layers, which might be related to a longer conjugation length in these layers.[25] To get insight into the doping process, HP- and LP-PPT layers were doped in iodine vapour for different times. The samples were exposed to atmospheric conditions before and after doping. The effect of the three parameters (doping time, pre- and post-doping exposure to air) on the conductivity and the chemical structure of the two types of PPT layers will be discussed in detail below.

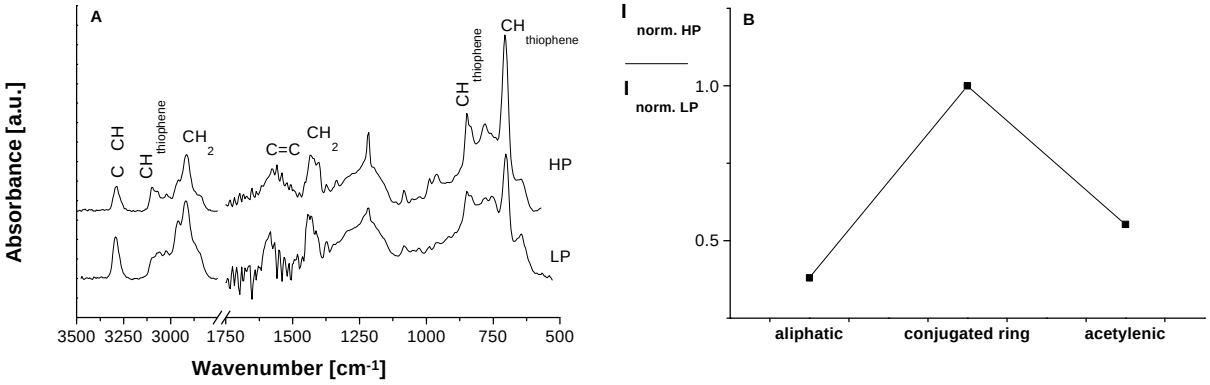

Figure 7.1. A. FTIR spectra of PPT layers (100 W, 10 s on, 10 s off) deposited at 0.06 mbar (LP, bottom, 10 pulses) and 0.3 mbar (HP, top, 20 pulses). B. Intensity of absorption bands characteristic for acetylenic (3288 cm^{-1}), conjugated ring (3099 cm^{-1}), and aliphatic structures (2910 cm^{-1}) (normalised to the intensity of the absorption band at 3099 cm^{-1} in that spectrum) in the FTIR spectrum of a layer deposited at 0.3 mbar (HP) relative to the normalised intensity of the same absorption bands in the FTIR spectrum of a layer deposited at 0.06 mbar (LP).

Doping. The effect of iodine doping time on the conductivity of LP- and HP-PPT layers is depicted in Figure 7.2. For the LP-PPT layers, the conductivity increases with doping time during the first 40 min, whereas for the HP-PPT layers already after 5 min iodine doping a constant conductivity is found. Since it is not expected that small differences in density, which may exist between HP- and LP-PPT layers, will result in substantial different iodine

diffusion rates in the PPT layers, the observed different time dependencies of the conductivity on iodine doping time must result from a difference in the rate of charge carrier formation. This is confirmed by Zhang *et al.*, who found instantaneous doping of polythiophene and polythiophene derivative films.[31] It can be hypothesised that the difference in the rate of formation of charge carriers is due to a difference in conjugation length, which is presumably longer in the HP-PPT layers. Charge carriers are delocalised over a number of monomer units.[32] At longer conjugation lengths there will be an increased rate of formation of charge carriers due to a lower activation energy. Consequently, the conductivity will show a faster increase in time.

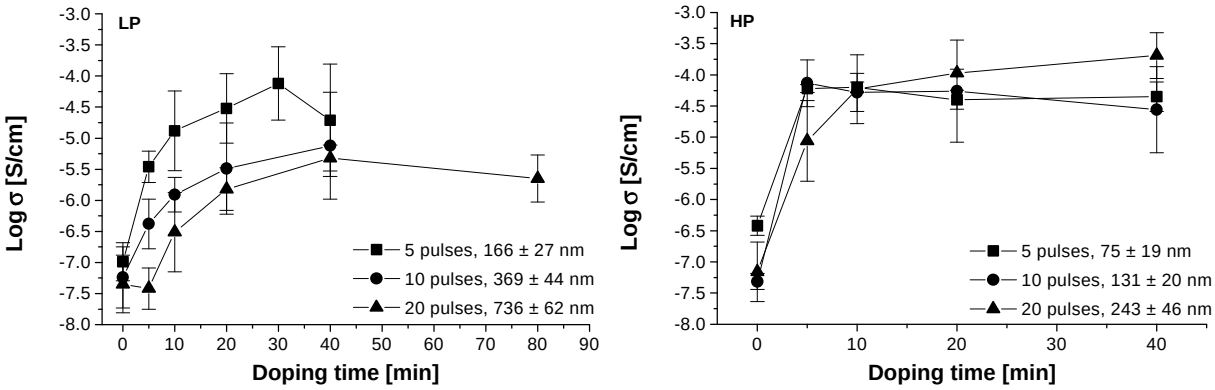

Figure 7.2. Logarithm of the volume conductivity (S/cm) of PPT layers (100 W, 10 s on, 10 s off) deposited at 0.06 mbar (LP) and at 0.3 mbar (HP) as a function of iodine doping time ($n \geq 3 \pm sd$).

Conductivity is determined by the number of charge carriers and their mobility throughout the PPT layer. For conductivity, the charge carriers have to move along as well as between (hopping) the PPT chains. The hopping transport was found to be the rate-determining step in several conductive polymers, including iodine doped polyalkylthiophenes.[33] The energy barrier for hopping is lower when the delocalisation of the charge carriers is higher. Therefore, the hopping efficiency depends on the conjugation length. When the conjugation length is longer the delocalisation of charge is easier, resulting in a lower activation energy for the hopping process. This is shown by an increase in the carrier mobility in oligothiophenes with increasing conjugation length up to the hexamer.[34]

To make inter-chain hopping possible, the chains have to be in close proximity of each other. Therefore, the diffusion of chains is also of importance, but this is not expected to be different for the PPT layers.

On the basis of the amount of preserved thiophene structures (Figure 7.1) and the similar diffusion properties of the PPT chains in the PPT layers, the hopping efficiency of charge carriers (and consequently the conductivity) is expected to be higher in the HP-PPT layers than in the LP-PPT layers. However, the maximum conductivity of the LP-PPT layer deposited in 5 pulses is not significantly different from the conductivity of the HP-PPT layers. Apparently, the number of charge carriers is higher in the LP-PPT layers compared to the HP-PPT layers.

For the HP-PPT layers the conductivity is independent of the thickness of the layer, whereas for the LP-PPT layers the conductivity decreases with increasing thickness. This implies that, due to the interaction with plasma species, deposited LP-PPT layers become less conductive during the deposition of subsequent layers. As deposition only takes place during the plasma ”on” time,[25] the time PPT layers are exposed to the plasma is a linear function of the thickness. During 1 pulse of 10 s a PPT layer of ± 13 (HP) or ± 35 (LP) nm is formed. The only species in plasma that penetrates far enough to modify the “bulk” of a deposited layer is the (vacuum-) UV light. In literature, several authors have pointed to the possibility of (vacuum-) UV modification of deposited layers during deposition.[35,36] Optical emission spectroscopy (200-875 nm) showed a peak at 257 nm in the thiophene plasmas, with a higher intensity for the LP plasma than for the HP plasma.[25] The energy of this light (4.56 eV) is sufficient to break chemical bonds (3-5 eV) in the PPT layers, which may result in the destruction of thiophene structures and/or the formation of cross-links. Consequently, the number of charge carriers and the diffusion of PPT chains is lowered, which explains the decrease in conductivity of the LP-PPT layers with increasing thickness. For the HP-PPT layers the modification induced by the UV light is apparently not sufficient to have an effect on the conductivity.

The FTIR spectra depicted in Figure 7.3 show the effect of iodine doping on the structure of the HP-PPT layers. Qualitatively, the LP-PPT layers gave comparable spectra. Upon doping with iodine the absorption bands at 3288 cm^{-1} and 705 cm^{-1} decrease in intensity, showing that hydrogen atoms in acetylenic and thiophene (α-H) structures disappear by a reaction with iodine. Furthermore, the intensity of the absorption bands at around 1425 cm^{-1} is strongly increased, and a new absorption band appears at 1540 cm^{-1}. These absorption bands can be ascribed to C=C groups in mono-substituted thiophenes (1425 and 1540 cm^{-1}) and -$\mathbf{CH_2}$I or -CI=$\mathbf{CH_2}$ groups (1425 cm^{-1}), respectively.[29,30]

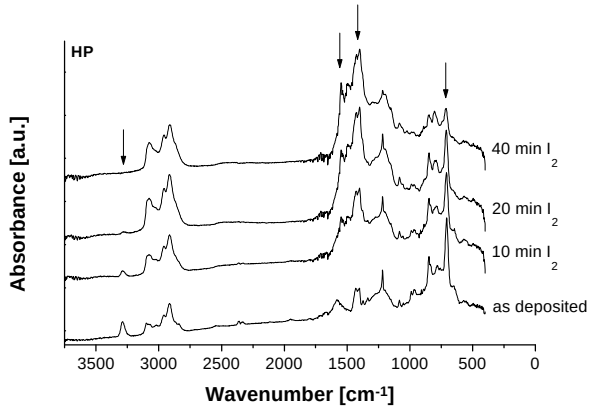

Figure 7.3. FTIR spectra of HP-PPT layers (20 pulses of 10 s on, 10 s off, 100 W, 0.3 mbar) after deposition (bottom) and doping with iodine for different times. For each spectrum a new PPT layer was used.

Considering the complex chemical structure of the PPT layers, many reactions with iodine may occur. Iodine probably reacts with residual radicals in the PPT layers via PPT• + $I_2 \rightarrow$ PPTI + I•. Iodine radicals can also be formed by the homolytic dissociation of iodine due to the influence of light.[37] Iodine radicals may be able to abstract hydrogen atoms from thiophene structures because the aromatic structure can delocalise the resulting radical. Subsequently, thus formed HI can react with terminal acetylene structures via RC≡CH + HI $\rightarrow$ RCI=CH_2.[38] The radical on the thiophene structure can in its turn react with other iodine radicals to form mono-substituted thiophenes etc. The main conclusion that can be drawn from the FTIR results is that side-reactions occur during iodine doping of PPT layers.

In the HR XPS spectra of the I_{3d5} region two different peaks can be observed (Figure 7.4). The high BE peak can be assigned to either iodine atoms covalently bound to carbon and/or absorbed I_2. The low BE peak originates from CT complexes in the form of I_3^- and/or I_5^-, probably with the thiophene structures in the PPT layers.[6-8] Comparing the I_{3d5} region of the HP- and the LP-PPT layers (Figure 7.4), it becomes clear that the HP-PPT layers have formed relatively more CT complexes. Together with the iodine atom % (LP: 4.6% and HP: 4.2%) this could be related to the conductivity results, if the vacuum applied during the XPS measurements (10 min, $<10^{-6}$ mbar) would have no effect on the conductivity. However, when the PPT layers were doped and subjected to vacuum (0.1 mbar) for 10 min the conductivity dropped considerably (Figure 7.5). Tanaka *et al.* also found a low conductivity of iodine doped PPT layers after applying vacuum (10^{-8} S/cm), but they did not compare it with the conductivity before the application of vacuum.[22]

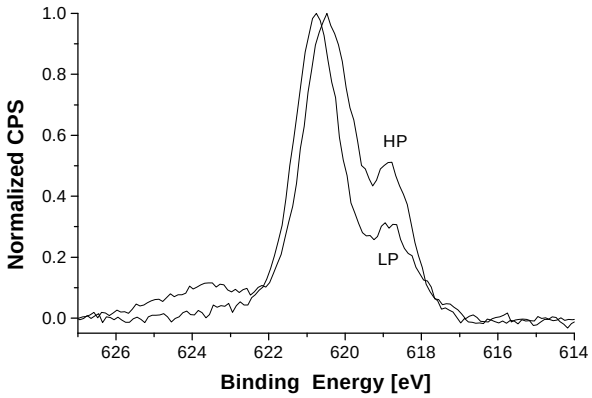

Figure 7.4. High resolution XPS spectra of the I_{3d5} region of PPT layers (100 W, 10 s on, 10 s off) deposited at 0.06 mbar (LP) and 0.3 mbar (HP) after doping with iodine for 5 min.

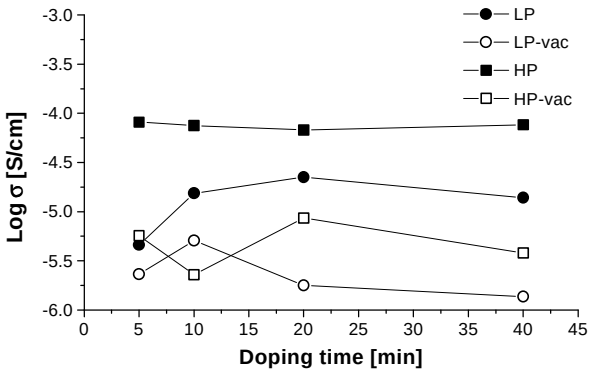

Figure 7.5. Logarithm of the volume conductivity (S/cm) of PPT layers (100 W, 10 s on, 10 s off) deposited at 0.06 mbar (LP, circles, 5 pulses) and at 0.3 mbar (HP, squares, 10 pulses) as a function of iodine doping time, just after doping (solid symbols) and after 10 min exposure to vacuum (10^{-1} mbar, open symbols).

This implies that the XPS results cannot be directly related to the conductivity determined immediately after doping. Moreover, the variation of the conductivity as a function of doping time is no longer observed after post-doping exposure to vacuum. This indicates that the removal of absorbed I_2 from the layers strongly influences the conductivity. The low conductivity of iodine (10^{-9} S/cm)[39] excludes absorbed iodine as being responsible for the observed conductivity. To study this further, the iodine concentration and the ratio of the low and high BE peak areas in the I_{3d5} region were studied as a function of post-doping vacuum exposure time (Figure 7.6). To minimise the effect of X-ray damage on the results, a new analysis spot was taken for every data point. For both layers, the iodine concentration decreases almost linearly, whereas there is only a slight decrease in the peak area ratio. This shows that an equilibrium exists between the CT complexes and absorbed iodine.

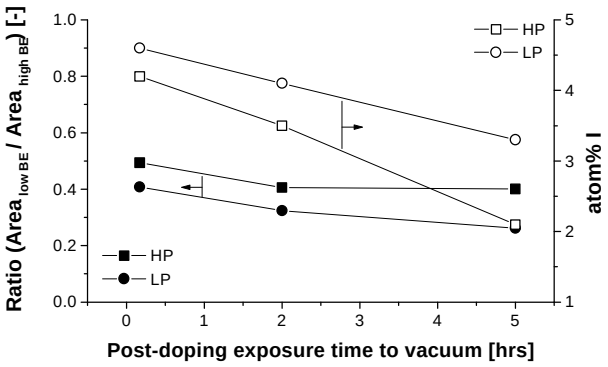

Figure 7.6. Ratio of peak areas of the low and high BE peak in the I_{3d5} region (left axis, solid symbols) and iodine concentration (right axis, open symbols) as measured with XPS at the surface of iodine doped (40 min) PPT layers (100 W, 10 s on, 10 s off) deposited at 0.06 mbar (LP, circles) and 0.3 mbar (HP, squares) as a function of time under vacuum ($<10^{-6}$ mbar).

Figure 7.6 also shows a slight decrease in the peak area ratio, which is due to the fact that the high BE peak also stems from covalently bound iodine. The peak area ratio decreases relatively more for the LP-PPT layers, whereas the decrease in iodine concentration is less than for the HP-PPT layers. This means that there is more covalently bound iodine in the LP-PPT layers, which is consistent with the FTIR results (Figure 7.1 and Figure 7.3).

The decrease in conductivity upon the application of vacuum was found to be irreversible. This must be due to a reaction of iodine with the PPT layers, resulting in a loss of the capability of the PPT layer to form CT complexes upon redoping with iodine.

Osterholm *et al.* describe the effect of vacuum on the equilibrium between iodine and CT complexes in polyacetylene as follows:[40]

Equation 7.1. $2(CH)_x^+ + I_5^- + I_3^- + I_2 \hat{U} 2(CH)_x^+ + 2I_3^- + 2I_2$

The equilibrium is continuously shifted to the right by the application of vacuum. Based on Equation 7.1 this should be a reversible process, which is consistent with results found earlier for polyacetylene.[8,41] It was also noted that at later stages, the transformation of I_3^- to I_2 and I^- occurred.

Because in literature the assignment of the peaks in the I_{3d5} region of iodine doped polymers to I_5^- and I_3^- is inconsistent,[6-8] we do not distinguish between I_5^- and I_3^-. The following equilibrium is proposed for our PPT layers:

Equation 7.2. $2(PPT)^{+\cdot} + I_5^- + I_3^- + I_2 \hat{U} 2(PPT)^{+\cdot} + 2I_3^- + 2I_2 \hat{U} 2(PPT)^{+\cdot} + 2I^- + 4I_2$

or

$(PPT)^{++} + I_5^- + I_3^- + I_2 \hat{U} (PPT)^{++} + 2I_3^- + 2I_2 \hat{U} (PPT)^{++} + 2I^- + 4I_2$

The equilibrium is continuously shifted to the right by the vacuum, resulting in an increasing concentration of I_3^- and I^-, on which the charge is less delocalised than on I_5^-. Furthermore, the delocalisation of charge on the PPT chains is probably less than on the PA chains studied by Osterholm *et al.* The low delocalisation on both the iodine ions and the PPT chains facilitates an ionic addition reaction of I^- and possibly I_3^- with charge carriers.[42] As a result, the capability of forming CT complexes is lost irreversibly. If radicals remain on the non-degenerated conjugated polymers they are not stable and will therefore terminate quickly, either internally (recombination of radicals) or externally (e.g., reaction with I_2).

Based on these results it can be concluded that conductivity is governed by charge carriers generated by CT complexes, which are in equilibrium with absorbed iodine. Their mobility is determined by the diffusion of PPT chains. The application of vacuum induces a reaction of iodine with the PPT layer, resulting in an irreversible loss of conductivity.

Exposure to air. Both LP- and HP-PPT layers were subjected to atmospheric conditions for several days before doping with iodine. The FTIR spectra of PPT layers that were exposed to air (Figure 7.7) show a strong increase of the intensity of the absorption bands at 1702 (C=O) and 3500 cm^{-1} (C=O and/or OH). The increase is larger for the LP-PPT layers than for the HP-PPT layers. Furthermore, absorption bands appear at 1050 and 1180 cm^{-1}, which are due to the oxidation of sulphur into >S=O and -SO_2- groups, respectively. The HP-PPT layers only show the formation of >S=O groups.

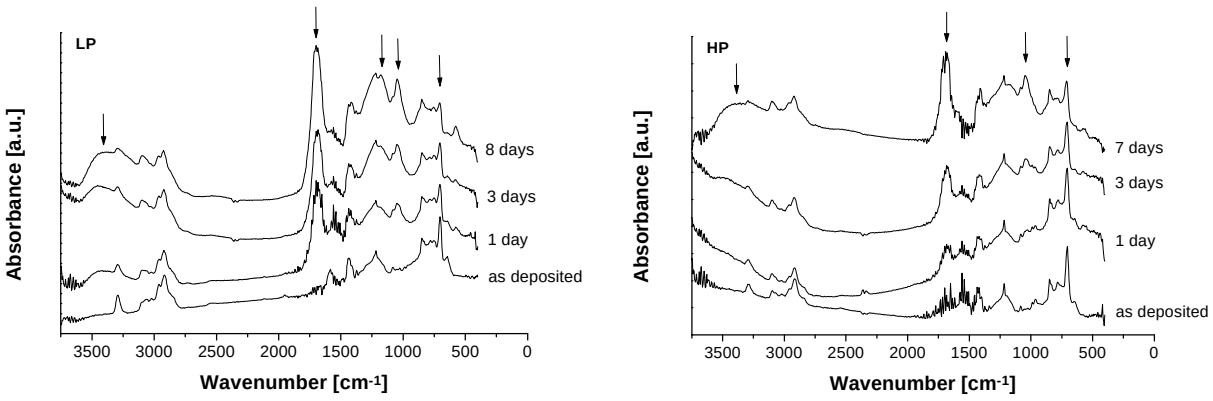

Figure 7.7. FTIR spectra of PPT layers (100 W, 10 s on, 10 s off) deposited at 0.06 mbar (LP, 10 pulses) and 0.3 mbar (HP, 10 pulses) as deposited (bottom) and after different exposure times to air.

These differences can be explained by the higher degree of fragmentation in the LP-PPT layers, which could be the result of the higher degree of fragmentation of the monomer during deposition at LP[25] and/or the higher intensity of the UV light in the LP plasma. Due to these processes, more and maybe different structures that are susceptible to oxidation, are present in the LP-PPT layers. For both layers, a decrease in the intensity of the absorption band at 705 cm^{-1} (CH in thiophene ring) with exposure time is observed. Apparently, the thiophene rings oxidise in time.

The XPS results (data not shown) were consistent with the FTIR results. Both types of PPT layers show an increase of the oxygen concentration with oxidation time, but the increase is less for the HP-PPT layers (from 2 to 10 atom% O in 7 days, compared with 2 to 14% for LP-PPT layers). The HR XPS spectra of the S_{2p} region of the oxidised PPT layers showed the presence of sulphur in -SO_2-groups in the LP-PPT layers but not in the HP-PPT layers, which is in agreement with the FTIR results.

After the exposure to air, the PPT layers were doped with iodine. The influence of pre-doping exposure time on the conductivity after doping is shown in Figure 7.8. No effect is observed for the HP-PPT layers, whereas the LP-PPT layers are less conductive after 7 days of pre-doping exposure time.

As stated earlier, the number of charge carriers and their inter- and intra-chain mobility determine the conductivity. Furthermore, diffusion of chains has to take place to make inter-chain hopping possible. It is not expected that the diffusion of PPT chains is influenced by the oxidation. Therefore, the decrease in conductivity after exposure to air for the

LP-PPT layers must be due to a decrease in the number of charge carriers formed upon iodine doping and/or a decrease in the mobility of the charge carriers. It can be hypothesised that the number of charge carriers decreases due to a decrease in conjugation length after oxidation. It is possible that the conjugation length in the LP-PPT layers is shortened to such an extent that they cannot or only slowly form a CT complex with iodine. With decreasing conjugation length, the energy barrier for hopping will increase, resulting in a loss of mobility. The mobility of charge carriers is also reduced due to the presence of carbonyl groups (localisation effect) formed upon exposure to air.[43] For the HP-PPT layers, the decrease in conjugation length and the localisation effect of carbonyl groups are apparently not sufficient to affect the rate of formation, the number, and the mobility of generated charge carriers, the combination of which is responsible for the observed conductivity.

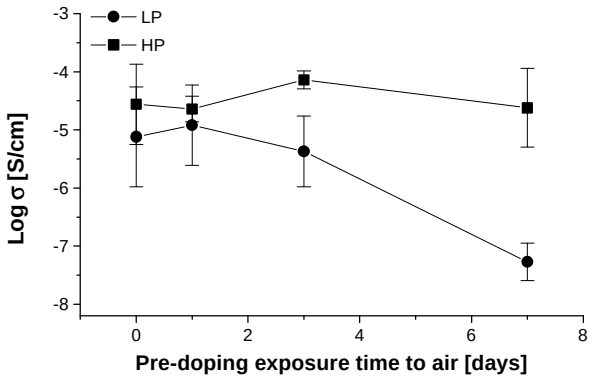

Figure 7.8. Logarithm of the volume conductivity (S/cm) after 40 min iodine doping of PPT layers (100 W, 10 s on, 10 s off) deposited at 0.06 mbar (LP, 10 pulses) and 0.3 mbar (HP, 10 pulses) as a function of pre-doping exposure time to air (n = 3 ± sd).

The FTIR spectra of the PPT layers exposed to air for 7 days and doped afterwards are given in Figure 7.9. No changes in the spectrum of the LP-PPT layers are observed after iodine doping, although there are still acetylenic structures present that normally react with iodine (cf. Figure 7.3). It might be that the diffusion of iodine in the oxidised layer is slower and/or that no HI is formed upon doping because the residual radicals have reacted with oxygen during the exposure to air. The HP-PPT layers show an effect comparable to that just after deposition (cf. absorption bands at 3288 and 705 cm^{-1}), which is in good agreement with the conductivity results.

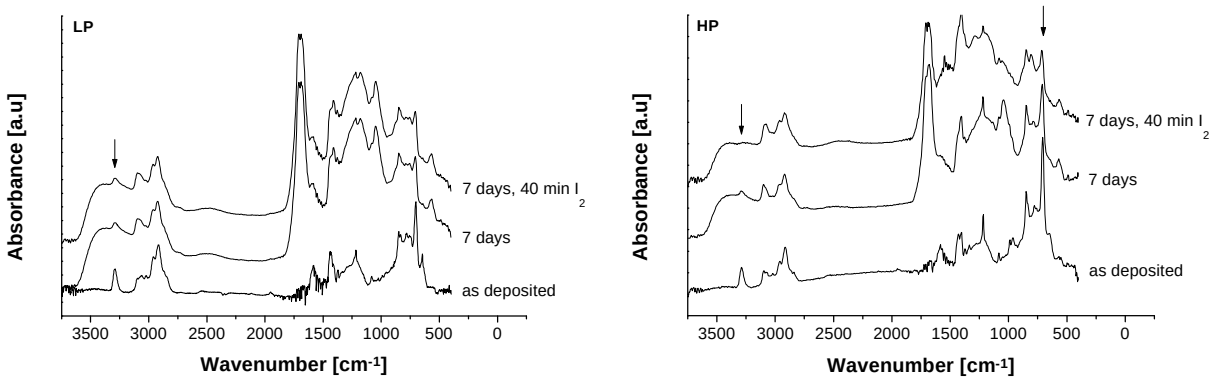

Figure 7.9. FTIR spectra of PPT layers (100 W, 10 s on, 10 s off) deposited at 0.06 mbar (LP, 10 pulses) and 0.3 mbar (HP, 10 pulses) just after deposition (bottom), after 7 days of exposure to air (middle), and 7 days of exposure to air and 40 min of iodine doping (top).

XPS measurements showed a decrease in the iodine concentration with increasing pre-doping exposure time (data not shown). In literature, the reaction with iodine and the oxidation process are found to be competitive.[28] After exposure to air, structures that form C-I bonds upon iodine doping have already reacted to a certain extent with atmospheric oxygen. Figure 7.10 shows that the relative intensity of the low BE peak in the I_{3d5} region is independent of exposure time for the HP-PPT layer, whereas it decreases for the LP-PPT layer. Assuming that the effect of vacuum on the decrease of CT complexes is equal for the layers, this shows that when iodine diffuses into LP-PPT layers that are exposed to air, less CT complexes are formed compared with LP PPT layers immediately after deposition. In the HP-PPT layers CT complex formation is unaffected by exposure to air. This confirms the hypothesis that the ability of the LP-PPT layers to form CT complexes decreases upon exposure to air due to a decrease in conjugation length.

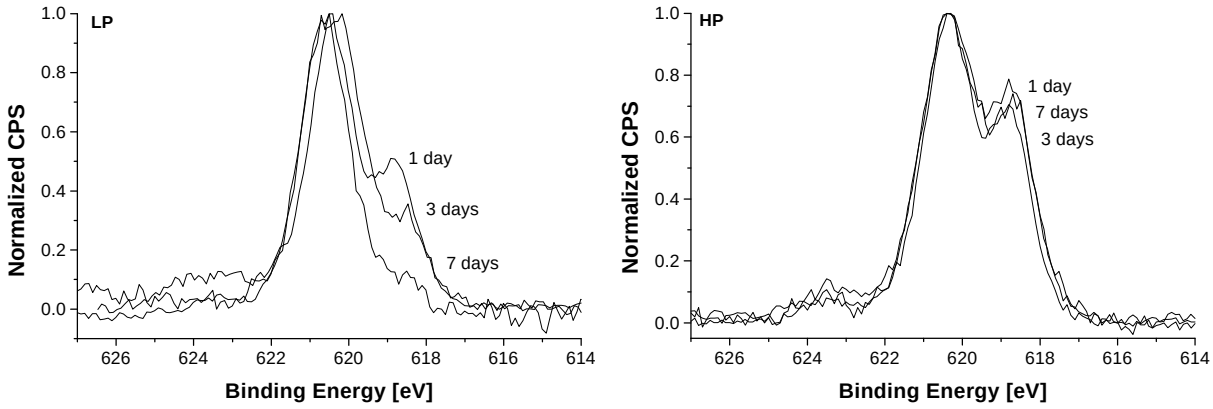

Figure 7.10. High resolution XPS spectra of the I_{3d5} region of PPT layers (100 W, 10 s on, 10 s off) deposited at 0.06 mbar (LP) and 0.3 mbar (HP) after 40 min iodine doping at different pre-doping exposure times to air.

Post-doping exposure to air. The effect of post-doping exposure to air on the conductivity of the PPT layers is depicted in Figure 7.11. For both PPT layers the conductivity decreases gradually, which is probably due to the diffusion of absorbed iodine out of the PPT layers. This process is analogous to the application of vacuum (cf. Figure 7.5). The decrease in conductivity is much slower than when vacuum is applied because the pressure difference is lower by a factor 10^4. Chilkoti *et al.* also found a much faster decrease of the conductivity of iodine doped polyisoprene in vacuum compared with exposure to air.[44]

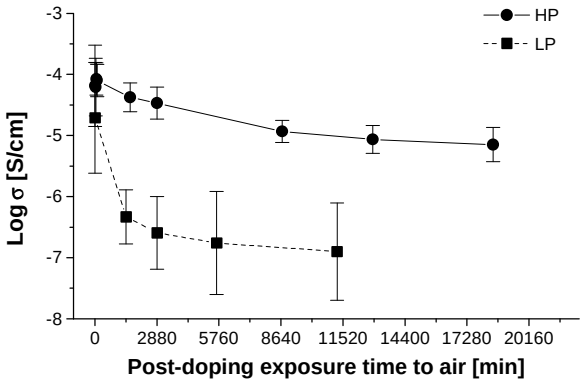

Figure 7.11. Logarithm of the volume conductivity (S/cm) of PPT layers (100 W, 10 s on, 10 s off) deposited at 0.06 mbar (LP, 5 pulses) and 0.3 mbar (HP, 10 pulses) as a function of exposure time to air after 40 min iodine doping (n = 3 ± sd).

XPS (Figure 7.12) and FTIR (data not shown) measurements showed that both layers are only slightly oxidised upon post-doping exposure to air. The iodine uptake reduces the rate of increase in oxygen concentration upon exposure to air compared with nondoped PPT layers. This is because part of the structures susceptible to oxidation (e.g., residual radicals) has reacted with iodine.

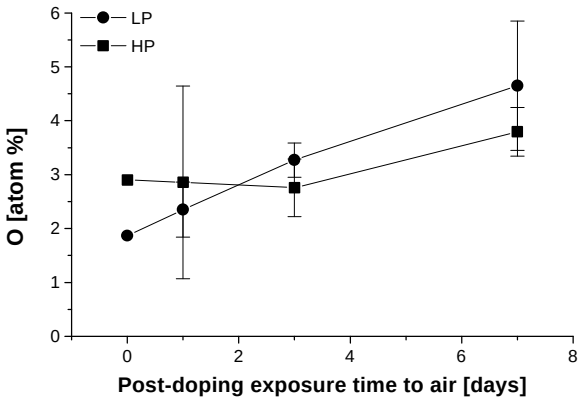

Figure 7.12. Oxygen concentration (determined with XPS) at the surface of PPT layers (100 W, 10 s on, 10 s off) deposited at 0.06 mbar (LP) and 0.3 mbar (HP) after 40 min iodine doping as a function of exposure time to air after doping (n = 2 or n = 3 ± sd).

Conclusions

Conductivity in PPT layers is governed by charge carriers, generated by CT complexes in equilibrium with absorbed iodine. The rate of formation of charge carriers is higher for PPT layers containing thiophene structures with a longer conjugation length. Modification of a deposited PPT layer by (vacuum-) UV light during deposition of subsequent PPT layers can lower the conductivity after iodine doping via the formation of cross-links and the destruction of thiophene structures. The application of vacuum after doping induces a reaction of iodine with the PPT layers resulting in an irreversible loss of conductivity. Upon exposure to air, oxidation of carbon and sulphur atoms occurs. When this results in a loss of the capability to form CT complexes, a lower conductivity after oxidation is observed. Iodine doping reduces the rate of oxidation upon exposure to air. Exposure to air after iodine doping results in a gradual decrease of the conductivity due to a slow diffusion of absorbed iodine out of the PPT layers. The conductivity of PPT layers deposited under less fragmenting conditions (i.e., high pressure) is less affected by pre- and post-doping exposure to air.

As a consequence, the optimal doping procedure may vary for PPT layers deposited under different conditions. Therefore, a detailed study of the doping parameters (doping time, pre- and post-doping exposure time and conditions, etc.) is needed to identify the optimal iodine doping procedure for a specific PPT layer.

Acknowledgement

The authors thank VG Scientific (East-Grinstead, UK) for the unrestricted use of the Σ probe.

References

[1] Boenig, H. V. In *Encycl. Polym. Sci. Eng.*; Mark, H. F. and Kroschwitz, J. I., Ed., **1986**; Vol. 11, pp 248-261.

[2] Yasuda, H. *Plasma polymerization*; Academic Press: Orlando, **1985**.

[3] Pekker, S.; Janossy, A. In *Handbook of conducting polymers*; Skotheim, T. A., Ed.; Marcel Dekker: New York, **1986**; Vol. 1, pp 45-79.

[4] Chance, R. R.; Boudreaux, D. S.; Bredas, J. L.; Silbey, R. In *Handbook of conducting polymers*; Skotheim, T. A., Ed.; Marcel Dekker: New York, **1986**; Vol. 2, pp 825-857.

[5] Brédas, J. In *Handbook of conducting polymers*; Skotheim, T. A., Ed.; Marcel Dekker: New York, **1986**; Vol. 2, pp 859-914.

[6] Hsu, S. L.; Signorelli, A. J.; Pez, G. P.; Baughman, R. H. *J. Chem. Phys.* **1978**, *69*, 106-111.

[7] Salaneck, E. W.; Thomas, H. R.; Bigelow, R. W.; Duke, C. B.; Plummer, E. W.; Heeger, A. J.; MacDiarmid, A. G. *J. Chem. Phys.* **1980**, *72*, 3674-3678.

[8] Petit, M. A.; Soum, A. H. *J. Polym. Sci. B* **1987**, *25*, 423-433.

[9] Bhuiyan, A. H.; Bhoraskar, S. V. *Thin Solid Films* **1993**, *235*, 43-46.

[10] Tu, D. M.; Zhuang, G. P.; Kao, K. C. *J. Appl. Polym. Sci.* **1991**, *43*, 1625-1632.

[11] Kakimoto, M.; Ueno, H.; Kojima, H.; Yamaguchi, Y.; Nishimura, A. *J. Polym. Sci. Part A: Polym. Chem.* **1996**, *34*, 2753-2758.

[12] Tanaka, K.; Ohzeki, K.; Yamabe, T. *Synth. Met.* **1984**, *9*, 41-52.

[13] Napo, K.; Safoula, G.; Bernede, J. C.; D'Almeida, K.; Touirhi, S.; Alimi, K.; Barreau, A. *Polym. Degr. Stab.* **1999**, *66*, 257-262.

[14] Bocchi, V.; Colombo, A.; Porzio, W. *Synth. Met.* **1996**, *80*, 309-313.

[15] Tassaing, T.; Besnard, M.; Yarwood, J. *Chem. Phys.* **1998**, *226*, 71-82.

[16] Tourillon, G. In *Handbook of conducting polymers*; Skotheim, T. A., Ed.; Marcel Dekker: New York, **1986**; Vol. 1, pp 293-350.

[17] Tanaka, K.; Yoshizawa, K.; Takeuchi, T.; Yamabe, T.; Yamauchi, J. *Synth. Met.* **1990**, *38*, 107-116.

[18] Tanaka, K.; Yamabe, T.; Takeuchi, T.; Yoshizawa, K.; Nishio, S. *J. Appl. Phys.* **1991**, *70*, 5653-5660.

[19] Sadhir, R. K.; K.F. Schoch, J. *Polym. Prepr.* **1992**, *33*, 412-413.

[20] Sadhir, R.; K.F. Schoch, J. *Thin Solid Films* **1993**, *223*, 154-160.

[21] Sadhir, R.; K.F. Schoch, J. *Polym. Prepr.* **1995**, *34*, 679-680.

[22] Tanaka, K.; Okazaki, S.; Inomata, T.; Kogoma, M. *8th Symp. Plasma Sci. Mater.* **1995**, 33-37.

[23] Giungato, P.; Ferrara, M. C.; Musio, F.; d'Agostino, R. *Plasmas Polym.* **1996**, *1*, 283-297.

[24] Kiesow, A.; Heilmann, A. *Thin Solid Films* **1999**, *344*, 338-341.

[25] Groenewoud, L. M. H.; Engbers, G. H. M.; Terlingen, J. G. A.; Wormeester, H.; Feijen, J. *Langmuir* **2000**, *16*, 6278-6286.

[26] Dai, L. M.; Mau, A. W. H.; Griesser, H. J.; Winkler, D. A. *Macromolecules* **1994**, *27*, 6728-6735.

[27] Owen, E. D.; Al-Moh'd, H. S. M. *Polymer* **1997**, *38*, 3533-3538.

[28] Pochan, J. M. In *Handbook of conducting polymers*; Skotheim, T. A., Ed.; Marcel Dekker: New York, **1986**; Vol. 2, pp 1383-1405.

[29] *The handbook of infrared and raman characteristic frequencies of organic molecules*; Lin-Vien, D.; Colthup, N. B.; Fateley, W. G.; Grasselli, J. G., Ed.; Academic Press: Boston, **1991**.

[30] *Infrared characteristic group frequencies*; Socrates, G., Ed.; 2nd ed.; J. Wiley & Sons: Chichester, **1994**.

[31] Zhang, D. Y.; Porter, T. L. *Synth. Met.* **1995**, *74*, 55-58.

[32] *Handbook of conducting polymers*; Skotheim, T. A., Ed.; Marcel Dekker: New York, **1986**; Vol. 1 and 2.

[33] Yoon, C. O.; Reghu, M.; Moses, D.; Heeger, A. J.; Cao, Y.; Chen, T. A.; Wu, X.; Rieke, R. D. *Synth. Met.* **1995**, *75*, 229-239.

[34] Garnier, F.; Deloffre, F.; Horowitz, G.; Hajlaoui, R. *Synth. Met.* **1993**, *57*, 4747-4754.

[35] Yasuda, H. *J. Macromol. Sci.* **1976**, *A10*, 383-420.

[36] Polak, L. S.; Lebedev, Y. A. *Plasma Chemistry*; Cambridge International Sci. Publ.: Cambridge, **1998**.

[37] Solomons, T. W. G. *Organic Chemistry*; 3rd ed.; John Wiley & Sons: New York, **1988**.

[38] Boyd, G. V. In *The chemistry of triple bonded functional groups*; Patai, S., Ed.; J. Wiley & Sons: New York, **1994**; Vol. 2.

[39] *The elements*; Emsley, J., Ed.; 3rd ed.; Claredon Press: Oxford, **1998**.

[40] Osterholm, J.-E.; Yasuda, H. K.; Levenson, L. L. *J. Appl. Polym. Sci.* **1983**, *28*, 1265-1275.

[41] Chiang, C. K.; Park, Y. W.; Heeger, A. J.; Shirakawa, H.; Louis, E. J.; MacDiarmid, A. G. *J. Chem. Phys.* **1978**, *69*, 5098-5104.

[42] Pross, A. *Acc. Chem. Res.* **1985**, *18*, 212-219.

[43] Tanaka, K.; Nishio, S.; Matsuura, Y.; Yamabe, T. *Synth. Met.* **1994**, *64*, 209-215.

[44] Chilkoti, A.; Ratner, B. D. *Chem. Mater.* **1993**, *5*, 786-792.

8

Effect of dopants on the transparency and stability of the conductivity of plasma polymerised thiophene layers*

Iodine is frequently used as dopant for plasma polymerised thiophene (PPT) layers, but suffers from several drawbacks such as the rapidly decaying conductivity upon exposure to air, and the absorption of light by iodine species that are present in the doped PPT layer (i.e., I_2, I_3^-, and I_5^-). This limits the utilisation of these layers in applications that require a high transparency and a stable conductivity. Two alternative dopant systems (thiantrenium perchlorate ($ThClO_4$) and nitrosonium hexafluorphosphate ($NOPF_6$)) have been evaluated and with both alternatives highly transparent (> 90% over the whole visible range) PPT layers were obtained of which the conductivity (10^{-4} S/cm) was stable during the period of evaluation (2 weeks).

Introduction

For many applications, conductive polymers should have a conductivity that is stable in time, while for some applications (e.g., antistatic coatings for photographic films) transparency is also of major importance. Conjugated polymers such as polythiophene become conductive when charge carriers, generated by dopants, are present.[1-3] However, due to their conjugated structure, conductive polymers are non-transparent. Transparent and conductive polymeric systems can be obtained when thin conductive polymer layers are applied on transparent substrates. Plasma polymerisation has been frequently used to deposit thin plasma polymerised thiophene (PPT) layers,[4-10] thereby keeping the transparency high.[11]

Iodine is often used as a dopant for PPT layers because of the ease of the doping procedure. In an earlier study it was shown that complicated chemistry is involved in the iodine doping of PPT layers, with the conductivity of the PPT layers being dependent on the conjugation length of thiophene structures in the PPT layers, the doping time, and the time (and conditions) before and after doping.[12] In practice, the application of these iodine doped PPT layers is hindered by the low stability of the conductivity (decrease by 2 orders of magnitude in 2 days). Furthermore, for applications that require a high transparency, the strong absorption of light by iodine species is a major problem.

Using other dopants, PPT layers with a high transparency and conductivity that is stable in time might be obtained. During doping, charge is transferred from the dopant to the polymer,

* The work described in this chapter has been submitted for publication in *Synthetic Metals*.

while charge neutrality is retained by the simultaneous incorporation of counter-ions.[13] Oxidation of the polymer (i.e., electrons from polymer to dopant) results in a hole-conducting polymer (p-type), whereas an electron-conducting polymer (n-type) is formed upon reduction. A high degree of charge delocalisation on both the conjugated polymer and the counter-ion is needed to obtain a stable conductivity.[14] Generally, the conductivity from n-type dopants is less stable than from p-type dopants due to the formation of unstable carbanions in the former case.[15] Therefore, to obtain layers with a high and stable conductivity, strong oxidators should be used in combination with counter-ions that delocalise the charge to a high extent.[14,16] Furthermore, to obtain transparent layers the combination of the reduced oxidator, the oxidised conductive polymer, and the counter-ion should not absorb light in the visible range. From the wealth of p-type dopant systems used in literature,[17-22] thiantrenium perchlorate ($ThClO_4$)[23,24] and nitrosonium hexafluorphosphate ($NOPF_6$)[17,25,26] seem very promising alternatives for iodine (Figure 8.1). Both thiantrenium radical cations and NO cations are strong oxidators that after reduction are transparent in the visible region or evaporate as a gas, respectively. Furthermore, the counter-ions (ClO_4^-, PF_6^-) are also transparent.

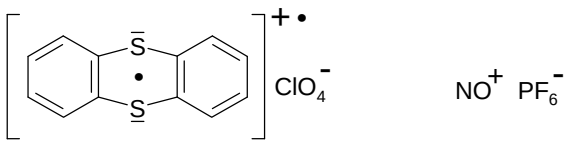

Figure 8.1. Chemical structure of thiantrenium perchlorate (left, $ThClO_4$)[27,28] and hexafluorophosphate (right, $NOPF_6$).

In this study, the effect of $ThClO_4$, and $NOPF_6$ doping on the conductivity (and the stability thereof) and the transparency of PPT layers is compared with iodine doping. Earlier it was found that PPT layers deposited at high pressure (HP) contain more thiophene structures than PPT layers deposited at low pressure (LP), which results in a faster initial increase in conductivity with iodine doping time.[11,12] Therefore, in the present study, HP- and LP-PPT layers were used in the doping experiments. The distribution of the counter-ions in the PPT layers was measured by recording Auger electron spectroscopy (AES) and X-ray induced photoelectron spectroscopy (XPS) sputter profiles of PPT layers doped for different times. The type of charge carriers with respect to the number of spins was determined using electron spin resonance (ESR) measurements. To study the stability of the doped PPT layers, the conductivity of these layers was measured as a function of exposure time to air. Transparency of the PPT layers in the visible region was also determined.

Experimental

Materials. Thiophene (99,5% purity), iodine (doubly sublimated), H_2SO_4 (96%, analytical grade), and H_2O_2 (33%, medicinal purity) were purchased from Merck (Darmstadt, Germany). $ThClO_4$ (Figure 8.1) was synthesised according to literature[27] and supplied by the Technical University of Eindhoven (Eindhoven, the Netherlands). $NOPF_6$ (96%) was purchased from Alfa Aesar (Klasruhe, Germany). All chemicals were used as received. Solvents were of analytical grade purity and purchased from Biosolve (Valkenswaard, the Netherlands). CH_2Cl_2 used for the doping experiments was purified according to literature to remove the stabiliser (ethanol).[29] Other solvents were used as received. Water used was doubly deionised. Glass slides (∅ 1.5 cm, used for XPS and UV-Vis measurements) were purchased from Knittel (Braunschweig, Germany). The substrates used for the conductivity measurements (glass slides with four parallel electrodes with extensions to contact areas for the measurement leads,[11] configuration in accordance with ASTM D257) were supplied by the MESA Institute (University of Twente, Enschede, the Netherlands), as were the 4" Si wafers from which Si-substrates (∅ 1.5 cm, used for ellipsometry) were cut.

Cleaning. All glassware, substrates and tools were cleaned ultrasonically, consecutively three times in toluene, n-hexane, acetone, water, and acetone and subsequently dried at 125ºC. The Si substrates were cleaned ultrasonically three times in chloroform and were put in Piranha solution consisting of 70 % H_2SO_4 and 30 % H_2O_2 for 30 min. After thorough rinsing with water, acetone and n-hexane, the substrates were dried at room temperature.

Plasma polymerisation. The plasma apparatus consisted of a tubular glass reactor with three externally placed, capacitively coupled electrodes.[11] The powered (hot) electrode was placed at the centre of the reactor. Two glass plates were placed between the hot and the grounded (cold) electrodes, which were positioned at 30 cm on either side of the hot electrode. The flow of monomer vapour through the reactor was regulated using needle valves and calculated from the time needed to obtain a certain pressure increase, once pumping of the reactor was stopped, assuming ideal gas behaviour. The flow of noncondensing gases was controlled by mass flow controllers (MKS Instruments, Andover, USA). The system (without the substrates) was first cleaned by applying an air plasma (5 sccm/min, 125 W, 0.13 mbar) for 60 min. The substrates were placed in the centre between the hot and cold electrode at the side of the monomer inlet and the reactor was evacuated to $< 5.10^{-3}$ mbar. The substrates were cleaned with an air plasma (5 sccm/min, 85 W, 0.13 mbar) for 5 min, after which the reactor was again evacuated to $< 5.10^{-3}$ mbar. Subsequently, a monomer flow was established through the reactor and after 2 min, pulsed plasma depositions (10 s on; 10 s off) were carried out. The starting pressure (0.06 and 0.3 mbar) and the number of pulses (0.06 mbar: 5 pulses and 0.3 mbar: 10 pulses) were varied to obtain PPT layers of varying chemical structure and comparable thickness. After deposition, the monomer flow was sustained for another 2 min, whereafter the reactor was brought to atmospheric pressure with air. After deposition, the samples were stored at –18 ºC.

Doping procedure for the PPT layers. Iodine doping was carried out in the gas-phase by placing the samples for a certain period of time in a sealed container containing iodine crystals.

For solution doping, the samples were completely submersed in the doping solution for a certain period of time. The preparation of the doping solutions and the doping experiments therewith were carried out in an inert atmosphere (< 2 ppm H_2O, 0 ppm O_2). The doping solution consisted of 70 mg $ThClO_4$ or 40 mg of $NOPF_6$, respectively, in 100 ml of CH_2Cl_2, degassed by several pump-freeze-thaw cycles.

After doping the samples were subjected to atmospheric conditions at RT for different times until further analysis was carried out.

Characterisation of PPT layers. The thickness of PPT layers deposited on Si substrates (∅ 1.5 cm) was determined with a variable angle ellipsometer with a QTH 200 lightsource, a M44 detector, and an EC 120 control module (J.A. Woollam Co., Lincoln, NE, USA). In the fitting procedure, a two-layer model (Cauchy-layer on top of a Si-substrate) was used. The thickness and the Cauchy parameters (A and b) were adjusted iteratively to obtain an optimal fit. A Levenberg-Marquardt algorithm was used for the minimisation of the mean-squared error between the fit and the

experimental data.[30] The thickness determined in this way was used for the calculation of the conductivity and for the stability measurements.

For the determination of the stability of the PPT layers in CH_2Cl_2, the thickness of the PPT layers was measured with ellipsometry and, after submersion in CH_2Cl_2 and subsequent application of vacuum (≈ 10 mbar, 24 hrs), the thickness was measured again.

For the conductivity measurements the PPT layers were deposited on specially designed substrates.[11] During plasma deposition the extensions of the electrodes were covered with glass slides to locally prevent deposition, thus enabling a good contact with the measurement leads used for the conductivity measurements. Two electrometers (Keithley Instruments, Cleveland, USA) were used to apply a current over the outer electrodes and to measure the voltage over the inner electrodes. After applying the current for 1 min, the voltage was read. The volume conductivity of the deposited layer was calculated using the appropriate formulas (ASTM D257).

AES measurements (10 keV, 0.10 μA) were carried out on PPT layers deposited on Si substrates using a PHI 600 SAM (Physical Electronics, Minneapolis, MA, USA).

XPS spectra were obtained using an Escalab 250 (VG Scientific, East-Grinstead, UK) with a 500 μm spot size, a power input of 100 W, at 20 eV pass energy (PE), and equipped with a monochromatic Al K_α source (1486.6 eV).

Sputter profiles of $ThClO_4$ doped PPT layers were obtained by repetitive AES and XPS sputter-measure cycles. Sputtering was carried out by argon ions in both the AES (sputter time 1 min, ion energy 1.5 keV, spot size 1 mm^2) and the XPS (VG: 30 - 120 s, 500 eV, 9 mm^2 spot size) measurements.

ESR spectra were recorded on a Bruker ESP 300E X-band spectrometer (Bruker Instruments, Billerica, MA, USA) operating with a standard cavity, an ER 035M NMR Gauss meter, and a Hewlett Packard 5350B frequency counter (Hewlett Packard, Palo Alto, CA, USA).

The transparency in the visible range (350 – 800 nm) of PPT layers deposited on glass slides, was determined with UV-Vis spectroscopy using a Cary 300 (Varian, Palo Alto, CA, USA) with a 1 nm stepsize at a scan rate of 10 nm/s. The UV-Vis spectra were corrected for the glass substrate by using the spectrum of a clean glass substrate as baseline.

Results & Discussion

Doping time. In the following section, the effect of doping time on the conductivity, the chemical composition, and the transparency of doped HP- and LP-PPT layers will be discussed in detail for each dopant.

Using ellipsometry it was observed that the thickness of the HP- and the LP-PPT layers after submersion in CH_2Cl_2 and subsequent application of vacuum remained within 5% of the original value. The solution doping method can thus be applied to these layers.

Conductivity. The conductivity of the HP- and LP-PPT layers as a function of doping time is given in Figure 8.2. The maximum conductivity (± 10^{-4} S/cm) is about the same for both the HP- and the LP-PPT layers, irrespective of the type of dopant, showing that the chemical structure of the as deposited PPT layer is the determining factor for the conductivity in all cases.

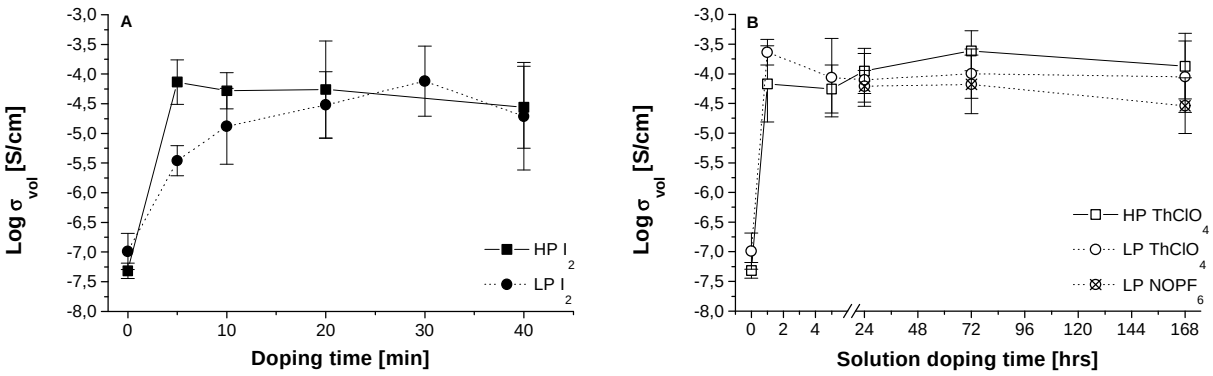

Figure 8.2. Logarithm of the volume conductivity (S/cm, n = 3 ± sd) of iodine (A), and solution (B, $NOPF_6$: crosses, $ThClO_4$: open symbols) doped PPT layers (100 W, 10 s on, 10 s off) deposited at 0.06 mbar (LP, 5 pulses, circles, dotted lines) and 0.3 mbar (HP, 10 pulses, squares, solid lines) as a function of doping time.

Upon iodine doping, the initial increase in conductivity is faster for the HP-PPT layers compared with the LP-PPT layers. This can be explained by the longer conjugation length in the HP-PPT layers. At longer conjugation lengths, both the rate of formation and the mobility of charge carriers are higher.[12] The same maximal conductivity is reached, which shows that the number of charge carriers in the LP-PPT layers is higher than in the HP-PPT layers.

Upon solution doping with $ThClO_4$, the conductivity does not increase for doping times > 2 hrs. Furthermore, no difference between the HP- and the LP-PPT layers is observed. Considering the higher oxidation strength of the NO cation compared with thiantrenium cation radicals,[31] no difference between the PPT layers was expected for this dopant. For practical reasons, only LP-PPT layers were used for the $NOPF_6$ doping experiments.

Chemical composition. For the $ThClO_4$ doped PPT layers, AES sputter profiles were acquired to determine the distribution of the dopant into the PPT layer (e.g., in Figure 8.3). Thiantrenium (only C and S) is indiscernible from the PPT layer itself and therefore the ClO_4^- counter-ion was used to follow the diffusion of the dopant. Figure 8.3 shows that chlorine is measured throughout this layer, which indicates that the dopant has diffused through the layer. Surprisingly, oxygen is only detected at the interfaces (surface and Si substrate). Examination of the individual spectra of the O_{1s} region showed that there is a difference in the binding state of the oxygen at the surface and at the substrate interface (data not shown). The surface oxygen is probably bonded to carbon and/or chlorine, whereas the oxygen signal at the substrate interface originates from the native oxide layer on the substrate (SiO_2).

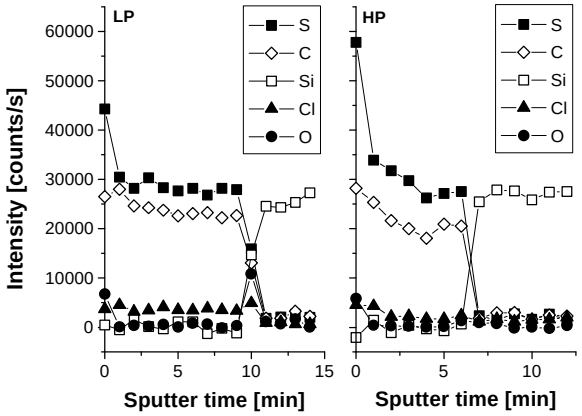

Figure 8.3. AES sputter profiles (Ar^+ ions of 1.5 keV) of PPT layers (100 W, 10 s on, 10 s off) deposited at 0.06 mbar (LP, 5 pulses) and 0.3 mbar (HP, 10 pulses) doped with $ThClO_4$ for 3 days.

With AES no differences in the binding state of the chlorine were observed. Therefore, XPS was used to get more information about the chemical state of the chlorine. In the Cl_{2p} region (data not shown) two peaks around 208 eV and 200 eV were observed, which are indicative of perchlorate species (208 eV) and Cl^- and/or C-Cl species (200 eV), respectively.[32] In Figure 8.4 the XPS sputter profile of the oxygen and the chlorine species in a $ThClO_4$ doped PPT layer is given as an example. In contrast to the AES sputter profiles, oxygen is present throughout the PPT layer. Taking the sensitivity factors of the elements into account an O/Cl ratio of 4 to 1 is calculated, showing that the dopant has indeed diffused throughout the whole PPT layer. Apparently, ClO_4^- is modified during the acquisition of AES sputter profiles. This could be due to the higher energy of the sputtering Ar^+ ions used for AES compared with XPS (1.5 keV and 500 eV, respectively) and/or to the different sources of energy used in the analysis techniques (electrons and X-rays, respectively). The high oxygen concentration at the surface is probably due to a reaction of residual radicals in the PPT surface layer with oxygen when the reactor is brought to atmospheric pressure with air. Based on all AES and XPS sputter profiles, it was concluded that, at least after 2 hrs, $ThClO_4$ has diffused throughout the layer. This is consistent with the conductivity results (see Figure 8.2).

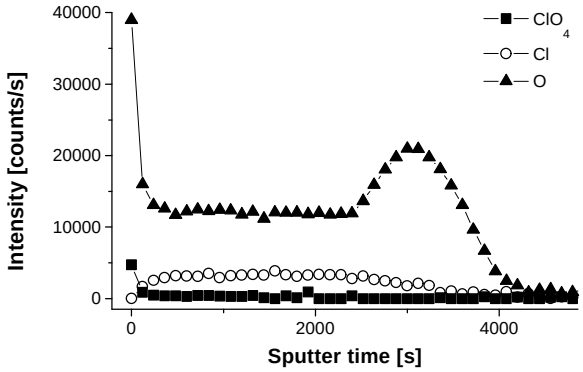

Figure 8.4. XPS sputter profile (500 eV) of oxygen (up-triangle) and chlorine atoms present in ClO_4 (peak around 208 eV in the Cl_{2p} region, squares) and in C-Cl and/or Cl^- (peak around 200 eV in the Cl_{2p} region, circles) in a HP-PPT layer (100 W, 10 pulses of 10 s on; 10 s off, 0.3 mbar) doped with $ThClO_4$ for 7 days.

ESR was used to investigate the number of spins on the charge carriers (Figure 8.5). The small difference between the glass substrate and the PPT layers shows that most of the ESR signal originates from the glass substrate. For the $ThClO_4$ doped PPT layers (HP-PPT layers not shown) a small deflection appears around G = 3355, which is indicative of a small amount of thiantrenium radical cations.[33,34] The effect of $ThClO_4$ doping on the amplitude of the signal is due to the superposition of the signals from glass and the PPT layer and thiantrenium radical cations, respectively and is too small to be used for quantitative analysis. Upon iodine doping no change in the ESR signal is observed (data not shown). Apparently, the charge carriers are not spin carrying (i.e., bipolarons). It is known that upon doping bipolarons are formed in polythiophenes at high doping levels,[23,35-37] which may explain these results.

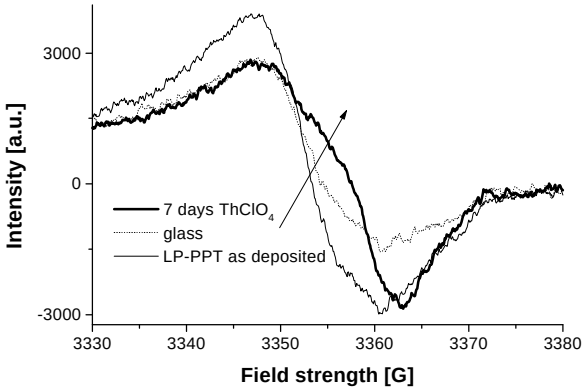

Figure 8.5. ESR signal as a function of field strength for the glass substrate (dotted line, plasma cleaned as mentioned in the experimental section), and a LP-PPT layer (100 W, 5 pulses of 10 s on, 10 s off, 0.06 mbar) as deposited on a glass substrate and after doping with $ThClO_4$ for 7 days. Spectra are arranged in the direction of the arrow.

Transparency. The transparency of doped PPT layers (normalised to 100 nm thick layers) is given in Figure 8.6 for different doping times. For all dopants the transparency decreases upon doping in the order I_2 >> $ThClO_4$ ≈ $NOPF_6$, with a stronger decrease with decreasing wavelength.

The strong decrease in transparency below 500 nm for the iodine doped PPT layers (Figure 8.6) can be ascribed to I_3^-, I_5^-, and I_2 species that have their absorption maxima at 365, 450, and 502 nm, respectively.[38] Earlier we have shown that absorbed iodine is in equilibrium with charge transfer (CT) complexes (PPT^+ with I_3^- and/or I_5^-) that generate charge carriers that govern the conductivity.[12] For the other dopants, the transparency decreases gradually over the whole visible range, which is probably due to charge carriers generated on the PPT chains.[27,36,39] For the $ThClO_4$ doped PPT layers, an additional small decrease in transparency is observed around 500-700 nm. This is probably due to residual thiantrenium radical cations (absorb at 540 nm)[23,33] as was also observed with ESR.

The decrease in transparency over the whole visible range (350-800 nm) is calculated from the differences in area under the curves of undoped and doped PPT layers (Figure 8.6) and is given in Figure 8.7.

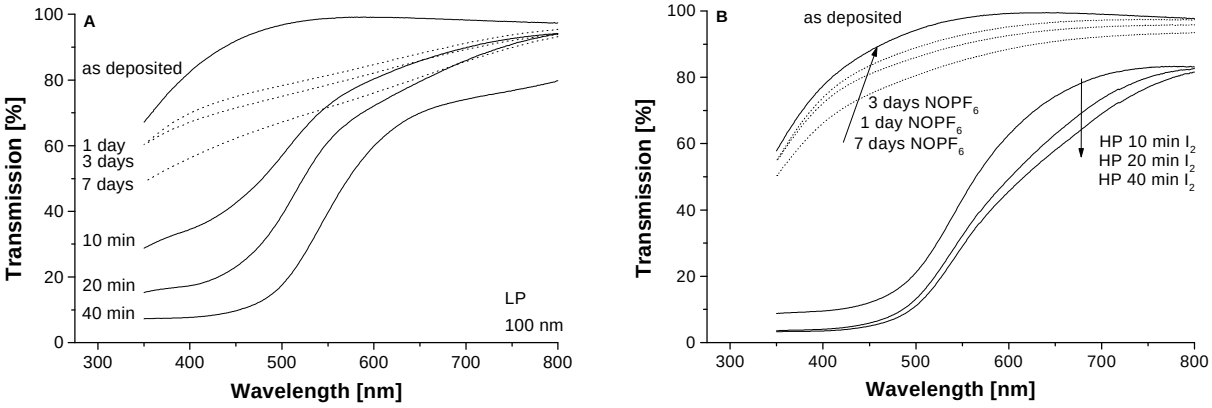

Figure 8.6. A. Transmission of LP-PPT layers (100 W, 10 s on, 10 s off, 0.06 mbar) as a function of wavelength just after deposition (top) and after doping with iodine (solid lines) and $ThClO_4$ doping (dotted lines) for different times. B. Transparency of LP-PPT layers (100 W, 10 s on, 10 s off, 0.06 mbar) as a function of wavelength just after deposition (top), and $NOPF_6$ doping (dotted lines) and of HP-PPT layers (100 W, 10 s on, 10 s off, 0.3 mbar) after doping with iodine (solid lines) for different times. Spectra are normalised to a thickness of 100 nm and arranged in the direction of the arrow.

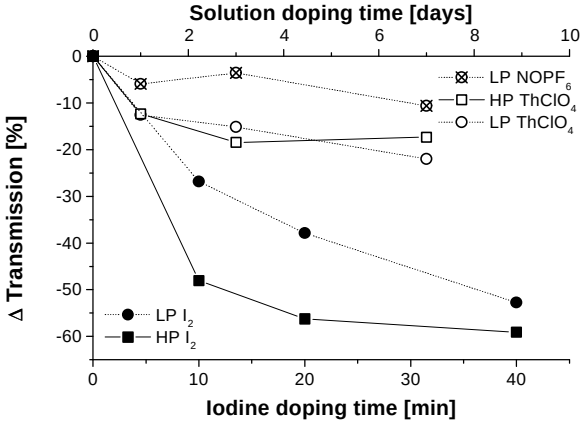

Figure 8.7. Decrease in transmission in the visible range (in %, calculated from the difference in area under the curves from the undoped and the doped PPT layer in Figure 8.6) of PPT layers (100 W, 10 s on, 10 s off) deposited at 0.06 mbar (LP, circles, dotted lines) and 0.3 mbar (HP, squares, solid lines) upon doping with iodine (solid symbols), $ThClO_4$ (open symbols), and $NOPF_6$ (crosses) as a function of doping time.

The loss of transparency decreases in the order I_2 >> $ThClO_4$ > $NOPF_6$. At maximum conductivity (cf. Figure 8.2) the loss in transparency after doping with $NOPF_6$ and $ThClO_4$ is only 6 and 12 %, respectively, whereas for doping with iodine the transparency is reduced with 40-50%, showing the strong effect of the dopant on the transparency. Furthermore, the absorption increases with increasing doping time, whereas the conductivity does not change (Figure 8.6 and Figure 8.2). The differences in transparency between the HP- and the LP-PPT layers are small, except for the iodine-doped samples, which is consistent with the conductivity results.

Post-doping exposure to air. In the following section, the effect of post-doping exposure time to air on the conductivity and the transparency of doped HP- and LP-PPT layers will be discussed in detail for each dopant.

Conductivity. The conductivity of the doped PPT layers is followed as a function of exposure time to atmospheric conditions (Figure 8.8). The decrease in conductivity of the solution doped PPT layers is less than of the iodine doped PPT layers. As the stability of the dopants used for the solution doping at atmospheric conditions is less than 1 day,[27,40] residual dopant can be excluded as conducting species, implying that the PPT layers are truly conducting.

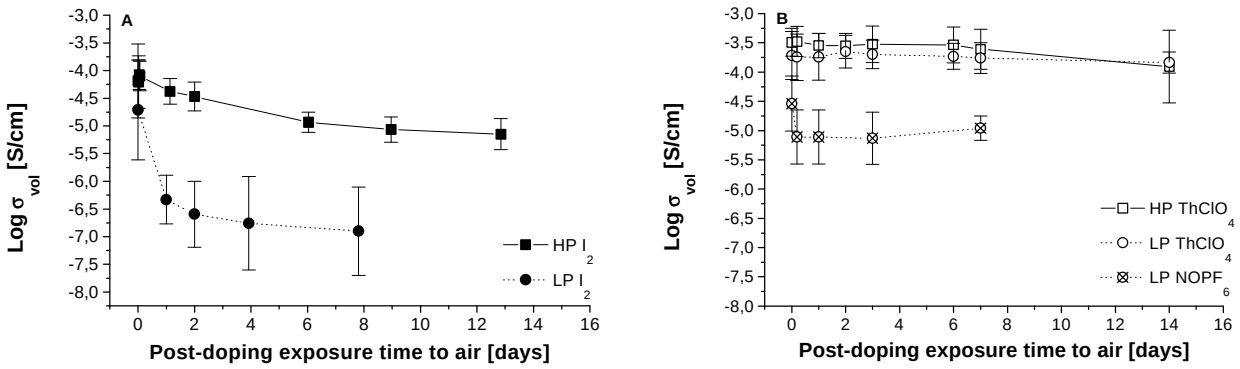

Figure 8.8. Logarithm of the volume conductivity (S/cm, n = 3 ± sd) of (A) iodine (40 min, solid symbols), and (B) $ThClO_4$ (7 days, open symbols), and $NOPF_6$ (7 days, crosses) doped PPT layers (100 W, 10 s on, 10 s off) deposited at 0.06 mbar (LP, 5 pulses, circles, dotted lines) and 0.3 mbar (HP, 10 pulses, squares, solid lines) as a function of post-doping exposure time to air.

The decrease in conductivity of the iodine doped samples is due to the diffusion of absorbed iodine from the samples upon exposure to air that is in equilibrium with the CT complexes, which govern the conductivity.[12] Figure 8.8 shows that the rate and/or effect of this process on the conductivity is higher, respectively, stronger for the LP-PPT layers than for the HP-PPT layers. The higher stability of the solution doped LP-PPT layers is probably because the counter-ions cannot diffuse out of the PPT layers in these cases. Apparently, reactions that result in a decrease in the number of charge carriers (e.g., oxygen radicals) do not occur to such an extent that the conductivity is affected.

Transparency. In Figure 8.9 the transparency of doped LP-PPT layers (HP-PPT layers gave comparable spectra) upon exposure to atmospheric conditions is followed in time. For the iodine-doped samples, a large increase in transparency below 500 nm is observed within the first day, after which the increase is much less. This is in good agreement with the conductivity results, and confirms the important role of iodine species (I_3^-, I_5^-, and absorbed I_2) for the conductivity. The results from an earlier study are consistent with this.[12]

The additional decrease in transparency around 500-700 nm of the $ThClO_4$ doped samples (cf. Figure 8.6.A) disappears within 1 day, after which the transparency almost does not change. This confirms that this band originates from residual thiantrenium radical cations that react upon exposure to air. Together with the conductivity results, this again shows that the conductivity is not due to the presence of residual thiantrenium radical cations. For the $NOPF_6$ doped LP-PPT layers no change in transparency upon exposure to air is observed (data not shown), which is also consistent with the conductivity results.

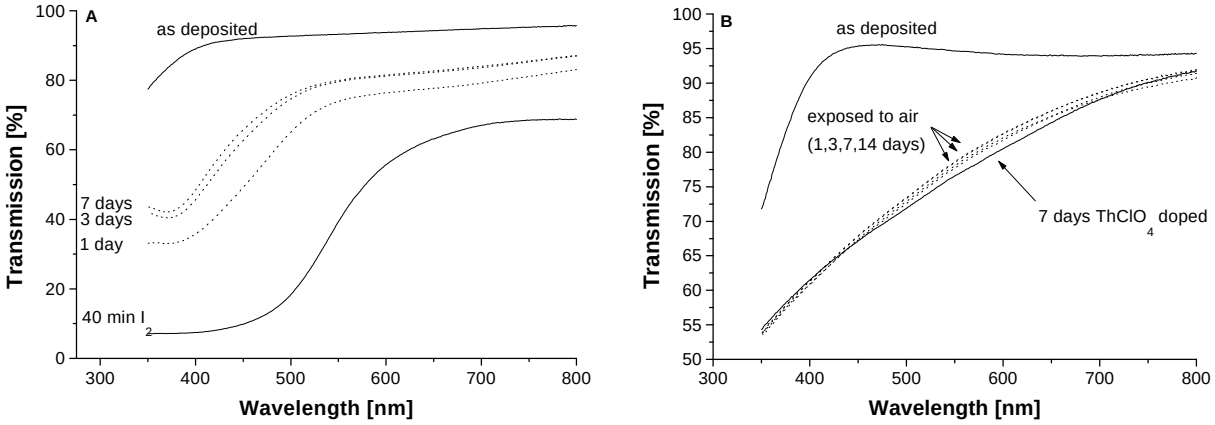

Figure 8.9. Transmission of a HP-PPT layer (100 W, 10 s on, 10 s off, 0.3 mbar) as a function of wavelength just after deposition (top), after doping (bottom, solid lines) with iodine (A, 40 min) and $ThClO_4$ (B, 7 days) and after post-doping exposure to air for different times (dotted lines). Spectra are normalised for a thickness of 100 nm.

Conclusions

Dopants have a strong effect on the transparency and conductivity of PPT layers and the stability thereof. A high and stable conductivity can be obtained when strong oxidators are used in combination with counter-ions that delocalise charge to a high extent. To retain a high transparency, the combination of the reduced oxidator, the oxidised conductive polymer and the counter-ion should be transparent. Given an optimal doping procedure, the maximal conductivity is determined by the PPT layer via the number and mobility of generated charge carriers. Iodine is not a suitable dopant for PPT layers that are to be used in applications requiring a high transparency and a stable conductivity. In contrast, highly transparent and stable conductive PPT layers can be obtained when $ThClO_4$ or $NOPF_6$ are used as dopants.

Acknowledgements

The authors thank VG Scientific (East-Grinstead, UK) for the unrestricted use of the Escalab 250. Martin Struijk and Rene Janssen from Technical University Eindhoven (Eindhoven, the Netherlands) are kindly acknowledged for supplying the $ThClO_4$ dopant and performing the ESR measurements, respectively.

References

[1] Pekker, S.; Janossy, A. In *Handbook of conducting polymers*; Skotheim, T. A., Ed.; Marcel Dekker: New York, **1986**; Vol. 1, pp 45-79.

[2] Chance, R. R.; Boudreaux, D. S.; Bredas, J. L.; Silbey, R. In *Handbook of conducting polymers*; Skotheim, T. A., Ed.; Marcel Dekker: New York, **1986**; Vol. 2, pp 825-857.

[3] Brédas, J. In *Handbook of conducting polymers*; Skotheim, T. A., Ed.; Marcel Dekker Inc.: New York, **1986**; Vol. 2, pp 859-914.

[4] Sadhir, R. K.; K.F. Schoch, J. *Polym. Prepr.* **1992**, *33*, 412-413.

[5] Sadhir, R.; K.F. Schoch, J. *Thin Solid Films* **1993**, *223*, 154-160.

[6] Sadhir, R.; K.F. Schoch, J. *Polym. Prepr.* **1995**, *34*, 679-680.

[7] Tanaka, K.; Yoshizawa, K.; Takeuchi, T.; Yamabe, T.; Yamauchi, J. *Synth. Met.* **1990**, *38*, 107-116.

[8] Tanaka, K.; Yamabe, T.; Takeuchi, T.; Yoshizawa, K.; Nishio, S. *J. Appl. Phys.* **1991**, *70*, 5653-5660.

[9] Tanaka, K.; Okazaki, S.; Inomata, T.; Kogoma, M. *8th Symp. Plasma Sci. Mater.* **1995**, pp 33-37.

[10] Giungato, P.; Ferrara, M. C.; Musio, F.; d'Agostino, R. *Plasmas Polym.* **1996**, *1*, 283-297.

[11] Groenewoud, L. M. H.; Engbers, G. H. M.; Terlingen, J. G. A.; Wormeester, H.; Feijen, J. *Langmuir* **2000**, *16*, 6278-6286.

[12] Groenewoud, L. M. H.; Engbers, G. H. M.; White, R.; Feijen, J. *Synth. Met., submitted*.

[13] Bott, D. C. In *Handbook of conducting polymers*; Skotheim, T. A., Ed.; Marcel Dekker: New York, **1986**, pp 1191-1232.

[14] Pross, A. *Acc. Chem. Res.* **1985**, *18*, 212-219.

[15] Leeuw, D. M. d.; Simenon, M. M. J.; Brown, A. R.; Einerhand, R. E. F. *Synth. Met.* **1997**, *87*, 53-59.

[16] *Handbook of conducting polymers*; Skotheim, T. A., Ed.; Marcel Dekker: New York, **1986**; Vol. 1 and 2.

[17] Koβmehl; Chatzitheodorou, G. *Macrmol. Chem., Rapid Commun.* **1983**, *4*, 639-643.

[18] Tourillon, G.; Garnier, F. *J. Electroanal. Chem.* **1982**, *135*, 173-178.

[19] Wellinghoff, S. T.; Deng, Z.; Reed, J.; Racchini, J. *Polym. Prepr.* **1984**, *25*, 238-239.

[20] Gagnon, D. R.; Capistran, J. D.; Karasz, F. E.; Lenz, R. W. *Polym. Prepr.* **1984**, *25*, 284-285.

[21] Friend, R. H.; Giles, J. R. M. *J. Chem. Soc., Chem. Comm.* **1984**, 1101-1103.

[22] Djellab, H.; Armand, M.; Delabouglise, D. *Synth. Met.* **1995**, *74*, 223-226.

[23] v. Haare, J. A. E. H. *Redox states of p-conjugated oligomers and polymers*; Eindhoven Technical University: Eindhoven, **1997**.

[24] v. Haare, J. A. E. H.; Groenendaal, L.; Havinga, E. E.; Meijer, E. W.; Janssen, R. A. J. *Synth. Met.* **1997**, *85*, 1091-1092.

[25] Nowak, M. J.; Spiegel, D.; Hotta, S.; Heeger, A. J.; Pincus, P. A. *Macromolecules* **1989**, *22*, 2917-2926.

[26] Jen, K. Y.; Miller, G. G.; Eisenbaumer, R. L. *J. Chem. Soc., Chem. Comm.* **1986**, 1346-1347.

[27] Murata, Y.; Shine, H. J. *J. Org. Chem.* **1969**, *34*, 3368-3372.

[28] Rundel, W.; Scheffler, K. *Tetrahedron Letters* **1963**, *15*, 993-995.

[29] Armarego, W.L.F.; Perrin, D.D. *Purification of laboratory chemicals*; 4th ed.; Butterworth-Heinemann: Oxford, **1996**.

[30] Jellison jr., G. E. *Thin Solid Films* **1998**, *33*, 313-314.

[31] Boduszek, B.; H.J.Shine *J. Org. Chem.* **1988**, *53*, 5142-5143.

[32] Morea, G.; Sabbatini, L.; Zambonin, P. G.; Swift, A. J.; West, R. H.; Vickerman, J. C. *Macromolecules* **1991**, *24*, 3630-3637.

[33] Folgado, J. V.; Garcia, H.; Marti, V.; Espla, M. *Tetrahedron* **1997**, *53*, 4947-4956.

[34] Shine, H. J.; Dais, C. F.; Small, R. J. *J. Org. Chem.* **1964**, *29*, 21-25.

[35] Harima, Y.; Kunugi, Y.; Yamashita, K.; Shiotani, M. *Chem. Phys. Letters* **2000**, *317*, 310-314.

[36] Fichou, D.; Horowitz, G.; Garnier, F. *Synth. Met.* **1990**, *39*, 125-131.

[37] Fichou, D.; Xu, B.; Horowitz, G.; Garnier, F. *Synth. Met.* **1991**, *41-43*, 463-469.

[38] Petit, M. A.; Soum, A. H. *J. Polym. Sci. B* **1987**, *25*, 423-433.

[39] Tourillon, G.; GArnier, F. *J. Phys. Chem.* **1983**, *87*, 2289-2292.

[40] Struijk, M., personal communication.

Summary

Polymers are widely used in a great number of applications because of their general properties such as low density, low cost, and processability. If these properties could be combined with electrical conductivity, this would open up the way to desirable applications such as flexible LCD's and polymer electronics (cheap, lightweight, etc.). For applications requiring electrical conductivity, the choice of a suitable polymer is limited to polymers with a conjugated chemical structure such as polythiophene. Along the conjugated structures charge (i.e., electricity) is transported by charge carriers. However, the conjugated structure of conductive polymers inherently results in a non-transparent, intractable polymer, which makes them unsuitable for applications requiring transparency and conductivity (e.g., antistatic coatings on photographic films). These disadvantages can be overcome when a thin conductive polymer layer is applied on a polymer that has all desired properties for a specific application, but only lacks conductivity. A very attractive way to do this is by using the plasma technique. With this technique it is possible to modify the surface properties of a substrate, while retaining the transparency and bulk properties of the substrate material. Furthermore, it is a solvent-free, fast and versatile process. Plasma can be used to actually modify the surface top-layer (plasma treatment) of or to deposit a thin conductive layer (plasma polymerisation (PP)) on a transparent substrate.

In the present study the plasma technique is used to obtain transparent and conductive polymer systems. A literature survey on conductive polymers and the plasma technique is given in **Chapter 2**. For plasma treatment, the transparent substrate material should be chosen such that upon plasma treatment conjugated structures are created in the surface layer. The preferential removal of pendant groups from vinyl polymers seems a promising way to introduce unsaturated bonds in the surface layer that can be used for the transport of electricity. Plasma polymerisation is a more versatile method than plasma treatment as it is not dependent on the chemical structure of the substrate material. On the other hand, complicated relations between gas composition, plasma conditions and the characteristics of the resulting surface exist, which makes detailed investigation necessary.

In **Chapter 3**, polyacrylic acid (PAAc) and polyvinylchloride (PVC) are treated with an argon plasma in order to selectively remove the pendant group, thereby creating unsaturated bonds in the surface layer. By use of X-ray induced photoelectron spectroscopy (XPS) and Fourier transform infrared (FTIR) measurements, it was shown that the pendant groups of

these polymers are removed by UV light emitted by the argon plasma. Due to the decarboxylation of PAAc induced by the argon plasma treatment, the argon plasma became more oxidative in character, which resulted in reoxidation and eventually ablation of the modified layer. The removal of chlorine from PVC was found to be preferential and a highly cross-linked layer, containing at least 15% unsaturated bonds (determined with solid-state nuclear magnetic resonance (SSNMR) measurements) was obtained.

In **Chapter 4-6** attention was focussed on the plasma polymerisation process. The plasma phase was characterised with optical emission spectroscopy (OES) and mass spectroscopy (MS), while for the characterisation of the resulting PP layers several techniques such as XPS, FTIR, NMR, ellipsometry, and conductivity measurements were used.

Chapter 4 deals with the plasma polymerisation of thiophene. The influence of power, pressure, pulse time, duty cycle, and position in the reactor on the characteristics of the plasma and the resulting PP thiophene (PPT) layer (e.g., chemical structure, transparency, and conductivity) has been evaluated. It appeared that, in the used ranges, only pressure had a significant effect on the conductivity of the deposited layer. By use of OES, MS, and FTIR this could be correlated to the effect of the deposition parameters on the fragmentation of the thiophene monomer during deposition. At high pressure (HP) there was less fragmentation of thiophene than at low pressure (LP), resulting in a higher conductivity of the PPT layer after iodine doping. It was concluded that the use of a pulsed plasma as a means to minimise fragmentation is most efficient when the off time is chosen such that the reactor is replenished with new monomer during the off period. With ellipsometry and conductivity measurements it was shown that highly transparent (> 80%) and conductive layers (10^{-6} S/cm) can be obtained by pulsed plasma polymerisation of thiophene.

Next to the process parameters, the monomer structure may also be used to gain better control over the chemistry of the deposition process. Therefore, the effect of substituent(s) on thiophene (methyl, chlorine, and bromine) on the fragmentation during deposition (**Chapter 5**) and the chemistry of the deposition process (**Chapter 6**) has been studied.

It was found that deposition most probably proceeds via a mechanism involving radicals, which are generated via the most favourable energy dissipation path. For mono-halogenated thiophenes this is the dissociation of C-H bonds from positions adjacent to the substituent. The dissociation of the C-halogen bond in dihalogenated thiophenes is energetically more favourable than in mono-halogenated thiophenes due to the presence of a second halogen. The ease of radical formation increases with increasing electron affinity of the substituent.

Therefore, fragmentation during deposition increases with increasing electron affinity of the substituent (i.e., Me < H < Br < Cl). It appeared that radicals formed on carbon atoms also attached to sulphur result in more fragmentation of the thiophene ring than radicals on other carbon atoms. Consequently, for a specific substituent, fragmentation was less for thiophene derivatives with substitution on the 2-position than on the 3-position. The deposition of methylated thiophenes was found to proceed mainly via C-H bond dissociation in the CH_3 substituent. As a result, the thiophene ring is preserved to a high extent and consequently, a higher conductivity was measured for these PP layers after iodine doping.

In the last two chapters the doping process of PPT layers is addressed. To make a fair comparison of the conductive properties of PPT layers deposited under different conditions, optimal doping procedures should be applied. The iodine doping process of HP- and LP-PPT layers has been studied in detail in **Chapter 7**. The effect of doping time, thickness and chemical structure of the PP layer, and time (and conditions) until and after doping on the conductivity and chemical structure of PPT layers has been evaluated. Using XPS, FTIR, and conductivity measurements it was shown that iodine doping generates charge carriers by the formation of charge transfer (CT) complexes, which are in equilibrium with absorbed iodine. Absorbed iodine slowly diffuses out of the PPT layers upon exposure to air, resulting in a decrease in conductivity. Upon exposure to air before doping, LP-PPT layers loose their capability to form CT complexes and consequently, the conductivity for LP-PPT layers exposed to air before doping decreases with exposure time.

Considering the rapidly decaying conductivity upon exposure to air and the absorption of light by iodine species that are present in the doped PPT layer, iodine is obviously not a suitable dopant for applications requiring a high transparency and a stable conductivity. Therefore, two alternative solution dopant systems ($ThClO_4$ and $NOPF_6$ in CH_2Cl_2) have been used in **Chapter 8**. It appeared that the conductivity is determined by the chemical structure of the PPT layer, whereas the transparency of the conductive PPT layer is strongly influenced by the dopant used. Iodine doping resulted in conductive PPT layers that had lost about 50% of their transparency. Furthermore, the stability of the conductivity was low (2 orders of magnitude within 2 weeks). With both alternatives, highly transparent (> 90% over the whole visible range) PPT layers were obtained of which the conductivity (10^{-4} S/cm) was stable during the period of evaluation (2 weeks).

Samenvatting

Polymeren (plastics) worden toegepast op vele terreinen omdat ze een lage dichtheid hebben, goedkoop zijn en omdat ze goed verwerkbaar zijn. Wanneer polymeren electrisch geleidend zouden zijn, zouden enkele gewilde toepassingen zoals flexibele LCD's en plastic electronica tot de mogelijkheden behoren. Om een polymeer geleidend te laten zijn is een geconjugeerde structuur zoals in polythiopheen vereist . Langs deze geconjugeerde structuur wordt de lading getransporteerd. Helaas zijn geleidende polymeren door hun geconjugeerde structuur niet transparant, bros en slecht verwerkbaar (niet smeltbaar) zodat ze niet toegepast kunnen worden in applicaties die zowel geleiding als transparantie vereisen (bijvoorbeeld antistatische lagen op fotofilms). Omdat dit een intrinsiek probleem is kan dit alleen worden opgelost door verdunning van de geleidende fase met een transparante fase. Een voorbeeld hiervan is het aanbrengen van een dunne geleidende laag op een tranparant substraat dat alle gewenste eigenschappen voor een bepaalde toepassing bezit, maar geleiding mist. De plasmatechniek is een veel belovende techniek om dit te bewerkstelligen. Met deze techniek is het mogelijk om alleen de oppervlakteeigenschappen van het substraat te veranderen. De bulkeigenschappen zoals transparantie en flexibiliteit worden niet aangetast. Daarnaast is het een snelle en oplosmiddelvrije techniek. Met een plasma kan óf de toplaag van een transparant substraat gemodificeerd worden (plasmabehandeling) óf er kan een dunne laag op gedeponeerd worden (plasmadepositie).

In dit proefschrift is de plasmatechniek gebruikt om transparante en geleidende polymeersystemen te verkrijgen. In **Hoofdstuk 2** wordt een overzicht van de literatuur over geleidende polymeren en de plasmatechniek gegeven. In het geval van plasmabehandeling moet het substraat zo gekozen worden dat door de plasmabehandeling een geconjugeerde structuur ontstaat in de toplaag. Het selectief verwijderen van zijgroepen van vinylpolymeren zou kunnen resulteren in vorming van onverzadiging in de toplaag, welke gebruikt zou kunnen worden voor het transporteren van electriciteit. Plasmadepositie heeft een breder toepassingsgebied omdat de keuze van het substraat niet afhangt van de chemische structuur ervan. Anderzijds bestaan er gecompliceerde relaties tussen de gas compositie, de plasma condities en de karakteristieken van de resulterende laag. Dit maakt gedetailleerd onderzoek noodzakelijk.

In **Hoofdstuk 3** zijn polyacryl zuur (PAAc) en polyvinyl chloride (PVC) behandeld met een argon plasma om zo de zijgroepen selectief te verwijderen. Door middel van

röntgen geïnduceerde photoelectron spectroscopie (XPS) en Fourier getransformeerde infrarood metingen (FTIR) is aangetoond dat de zijgroepen van deze polymeren verwijderd worden door het UV licht dat het argon plasma uitzendt. Omdat PAAc decarboxyleert onder invloed van de argon plasma behandeling wordt het plasma meer oxidatief van karakter. Dit veroorzaakt re-oxidatie van het gemodificeerde oppervlak, wat uiteindelijk resulteert in verwijdering van deze laag. De verwijdering van chloor is wel preferentieel en een gecrosslinkte laag werd verkregen. Met vast stof nucleair magnetische resonantie (SSNMR) werd vastgesteld dat deze laag minstens 15% onverzadiging bevat.

In **Hoofdstuk 4 tot en met 6** is de plasmatechniek gebruikt om een geleidende laag te deponeren. De plasma fase zelf werd gekarakteriseerd door middel van optische emissie spectroscopie (OES) en massa spectroscopie (MS). Voor de karakterisering van de gedeponeerde lagen werden verschillende technieken gebruikt zoals XPS, FTIR, NMR, ellipsometrie en geleidingsmetingen.

De plasmadepositie van thiopheen word behandelt in **Hoofdstuk 4**. Het effect van vermogen, druk, puls tijd, de verhouding plasma “aan/uit” tijd en de substraat positie in de reactor op het plasma en de resulterende plasma gepolymeriseerde thiopheen (PPT) lagen is onderzocht. Het bleek dat, in de gebruikte range van instellingen, druk de enige parameter was met een significant effect op de geleiding van de PPT lagen. Met behulp van OES, MS en FTIR kon dit worden gerelateerd aan het effect van de depositie parameters op de fragmentatie tijdens depositie. Er trad minder fragmentatie op tijdens depositie bij hoge druk (HP) dan bij lage druk (LP), waardoor de geleiding van de HP-PPT lagen hoger was. Er kon worden geconcludeerd dat een gepulseerd plasma het meest effectief is in het verlagen van de fragmentatie wanneer de plasma “uit” tijd zodanig gekozen wordt dat tijdens deze periode de reactor ververst wordt met monomeer. Ellipsometrie en geleidingsmetingen lieten zien dat PPT lagen met een transparantie van 80% en een geleiding van 10^{-6} S/cm tot de mogelijkheden behoren.

Naast de procesparameters zou de monomeerstructuur ook gebruikt kunnen worden om een betere controle te verkrijgen over de chemie die plaatsvindt tijdens depositie. Om dit te verifiëren is het effect van substituenten (methyl, chloor en broom) op de thiopheen ring op de fragmentatie (**Hoofdstuk 5**) en de chemie van het depositie proces (**Hoofdstuk 6**) onderzocht.

Er is geconstateerd dat deposite waarschijnlijk via een radicalair mechanisme verloopt, welke gevormd worden via het energetisch meest gunstige reactiepad. Voor de

mono-gehalogeneerde thiophenen is dit de dissociatie van de C-H binding naast de substituent. In het geval van di-gehalogeneerde thiophenen is de breking van de C-Halogeen binding gunstiger dan voor de mono-gehalogeneerde thiophenen door de aanwezigheid van een tweede electronegatieve groep. Het gemak waarmee radicalen gevormd worden neemt toe bij toenemende electron affiniteit van de substituent (i.e., Me < H < Br < Cl) wat resulteert in een toename van de fragmentatie. Het bleek dat radicalen die gevormd worden op koolstof atomen die ook aan zwavel gebonden zijn meer fragmentatie veroorzaken dan wanneer ze op andere koolstof atomen gegenereerd worden. Als gevolg hiervan is de fragmentatie minder voor monomeren met substitutie op de 2 plaats in vergelijking met die met substitutie op de 3 plaats. De deposite van methyl gesubstitueerde thiophenen verloopt voornamelijk onder afspliting van een waterstof atoom van de methyl groep. Hierdoor wordt de thiopheen zonder veel fragmentatie ingebouwd wat resulteert in een hoge geleiding voor deze lagen na jood doping.

De laatste twee hoofdstukken behandelen het doping proces van PPT lagen. Om een eerlijke vergelijking te maken van de geleiding van PPT lagen welke gedeponeerd zijn onder verschillende condities moeten optimale doping procedures gebruikt worden. In **Hoofdstuk 7** wordt het jood doping proces van HP- en LP-PPT lagen beschreven. Het effect van doping tijd, dikte en chemische structuur van de PPT lagen, en de tijd en condities voor en na doping op de geleiding en de chemische structuur van de PPT lagen is uitgebreid onderzocht. Met behulp van XPS, FTIR en geleidingsmetingen kon worden aangetoond dat er ladingsdragers gegenereerd worden door ladingsoverdrachtscomplexen (CT complexen), welke in evenwicht zijn met geabsorbeerd jood. Dit geabsorbeerde jood diffundeert langzaam uit de matrix wanneer deze na dopen wordt blootgesteld aan de lucht, wat een daling in geleiding tot gevolg heeft. Wanneer de LP-PPT lagen voor het dopen aan de lucht blootgesteld worden verliezen ze hun vermogen om CT complexen te vormen. Dientengevolge neemt de geleiding af met de blootstellingstijd voor dopen.

Gezien de snelle afname van de geleiding in de tijd en de absorptie van licht door de jood soorten (I_3^-, I_5^- en I_2) moge het duidelijk zijn dat jood geen geschikte dopant is voor toepassingen waarin zowel een stabiele geleiding als transparantie vereist zijn. Twee alternatieve doping systemen ($ThClO_4$ en $NOPF_6$ in CH_2Cl_2) zijn gebruikt in **Hoofdstuk 8**. Het bleek dat de geleiding wordt bepaald door de chemische structuur van de PPT laag terwijl de transparantie van de gedoopte PPT sterk afhangt van de gebruikte dopant. Jood

doping resulteerde in geleidende PPT lagen die ongeveer 50% van hun transparantie verloren hadden. Daarnaast was de stabiliteit van de geleiding slecht (daling van 2 ordes in 2 weken). Met beide alternatieven konden transparante (> 90% over het gehele zichtbare gebied) PPT lagen verkregen worden waarvan de geleiding (10^{-4} S/cm) stabiel was over de gehele periode dat ze bestudeerd zijn (2 weken).

Curriculum Vitae

Luuk Groenewoud zag het licht op 20 april 1972 in het dorpje Heeten. Na fluitend de lagere school in Heeten, het VWO op het Florens Radewijn College in Raalte, en de studie Chemische Technologie aan de Universiteit Twente te hebben doorlopen, begon hij in maart 1996 aan zijn promotieonderzoek in de vakgroep Polymeer Chemie en Biomaterialen van prof.dr. J. Feijen, eveneens aan de Universiteit Twente. Het produkt hiervan ziet u op dit moment voor u en hij hoopt daarop op 10 november te promoveren. Op 1 november trad hij in dienst van het fluitend jonge bedrijf Holland Biomaterials Group te Enschede.